Symbiotic systems between Hydra and green algae and their evolutionary processes

御代川, 涼

出版情報：九州大学, 2021, 博士（理学）, 課程博士
バージョン：
権利関係：

Symbiotic systems between *Hydra* and green algae and their evolutionary processes

（ヒドラと緑藻の共生システムとその進化の過程）

Graduate School of Integrated Sciences for Global Society

Kyushu University

Ryo Miyokawa

2022

CONTENTS

List of Tables

List of Figures

Abstract

Symbiosis is the sympatric living of multiple organisms and generally benefits both host and symbiont. Photosymbiosis is broadly observed between various animals and algae which are hosts and symbionts, respectively. The host is provided with the photosynthetic products by the symbiont, and the symbiont receives from the host the supply of inorganic substances necessary for photosynthesis and protection from external enemies. Some species of *Hydra*, which belongs to Cnidaria, have endosymbiotic relationships with green algae. *Hydra* is a suitable organism for studying symbiosis because information of *Hydra* as a model organism has been accumulated due to rapid asexual proliferation by budding and because *Hydra* has independently established two types of symbiotic systems. A symbiotic hydra, *Hydra viridissima*, has a stable symbiotic relationship with a green alga, chlorella. On the other hand, the other symbiotic hydra, some strains of *H. vulgaris* (J7, J10), has a symbiotic relationship with the green alga, chlorococcum, but the *H. vulgaris* seems to have newly established symbiosis and has been in an incipient evolutionary stage. I provided an overview of the symbiotic mechanism in the two symbiotic systems and aimed to elucidate the evolutionary mechanism of symbiosis by examining the intracellular processes in the hosts during symbiosis with transcriptomic analyses.

Non-symbiotic *H. vulgaris* 105 can acquire the symbiotic chlorococcum by horizontal transmission from the native symbiotic strains. The newly established symbiotic hydra (105G) has shortened its interval of budding, which led to an increase in the proliferation rate and a decrease in the polyp size. I confirmed the identity of symbiotic chlorococcum in 105G with the algae in the surrounding water by DNA sequencing, then reconstructed the phylogenetic tree of the green algae to determine the phylogenetic position of the symbiotic chlorococcum. Next, I conducted a gene expression analysis of the newly established symbiotic polyps (105G) and their non-symbiotic polyps to examine what changes would occur at the early stage of the evolution of symbiosis. I found that both 105G and native symbiotic strain J7 showed comparable expression patterns, exhibiting upregulation of lysosomal enzymes and

downregulation of genes related to nematocyte development and function. Meanwhile, genes involved in translation, transcription factors belonging to homeobox genes and ones in the Wnt signaling pathway, and genes involved in the respiratory chain were upregulated only in 105G. Furthermore, genes in the TOR pathway, which regulates these cellular processes based on the nutrient condition, were upregulated. I examined the effect of the expression change in translation and electron transport chain by rapamycin treatment, which inhibits the TOR pathway. Rapamycin stopped the budding of hydras and caused the symbiotic polyps (105G, J7) to degenerate. The results suggested that evolving the ability to balance the cellular metabolism between the host and the symbiont is a key requirement for adapting to endosymbiosis with chlorococcum.

H. viridissima has been considered to co-speciate with the symbiotic alga *Chlorella*, and there are unique combinations between the host hydras and the symbiotic algae. I attempted to elucidate the mechanism of the specificity between host and symbiotic algae by removing and replacing the symbiont from host hydras and examining the gene expression changes in these hydras. In *H. viridissima* K10, symbiont removal and symbiont replacement showed similar gene expression changes. The GO enrichment analysis showed that genes related to the electron transport system were downregulated and that genes related to translation were upregulated both for symbiont removal and symbiont replacement. On the other hand, *H. viridissima* M9 did not show such a gene expression pattern, suggesting that the regulation of energy balance in the symbiotic hydras was different between the strains. In addition, I found similar changes in expression patterns of genes such as glutamine synthetase and ammonium transporter, which act in the metabolic process to supply glutamine to the symbiont as a nitrogen source, during symbiont removal and symbiont replacement in K10, but these patterns were not observed in M9. The differences in the gene expression changes between these strains would reflect the differences in symbiotic mechanisms between the strains.

These results and the comparison of the gene expression changes between the two symbiotic systems of *Hydra* allowed you to clarify the symbiotic mechanism in the early stage of symbiosis and the mechanism of host-symbiont specificity.

CHAPTER 1

General introduction

1.1 Backgrounds

1.1.1 Diversity of photosymbiotic systems and symbiosis in Cnidaria

Symbiosis is originally defined as living together of dissimilarly named organisms (de Bary, 1879). Since then, many researches have shown that symbiosis enables organisms to fill various niches by helping to adapt environment (Moran, 2007; Lengyel et al., 2009; Joy, 2013). Photosymbiosis is one of the most studied symbioses. Animals in various phyla are hosts of photosymbiosis, Porifera, Cnidaria, Acoela, Mollusca, and Chordate, and algae in different kinds of taxa, green algae, diatom, dinoflagellate, and cyanobacteria, become endosymbionts by being incorporated into host cells (Melo Clavijo et al., 2018). Host and symbiont usually derive mutual benefits from photosymbiosis. Symbiont provides nutrients produced by photosynthesis for the host, and the nutrient supply allows the host to live in water with low nutrient concentration and low prey density (Yellowlees et al., 2008). On the other hand, the host provides the symbiont with inorganic compounds for photosynthesis and shelter, which protects the symbiotic algae against predators, pathogens, in endosymbiosis (Melo Clavijo et al., 2018). Photosymbiosis does not only benefit organisms constituting the symbiotic system but also creates a diverse and productive ecosystem. As a major example, coral-*Symbiodinium* symbiosis preserves the ecosystem in a coral reef by converting sunlight and carbon dioxide to organic carbon and oxygen (Muscatine and Porter, 1977; Roth, 2014). In addition, the coral-*Symbiodinium* symbiotic system circulates organic nitrogen in a coral reef under a nitrogen-limited environment (Tanaka et al., 2018). However, disruption of the balance between host and symbiont needs causes a breakdown of the symbiosis. The symbiont produces reactive oxygen species (ROS) in photosynthesis, and ROS damages host cells under conditions with increased temperature and light (Weis, 2008; Plass-Johnson et al., 2015). High temperature also promotes proliferation of the symbiont, but the symbiont does not increase nutrient supplies to

the host (Baker et al., 2018). These indicate a shift from a symbiotic to a parasitic relationship depending on the conditions. Therefore, climate change influences the photosymbiotic relationship in microscale and the ecosystem in macroscale (Hoegh-Guldberg, 2011).

Some other cnidarians also have a symbiotic relationship with algae. Sea anemones (e.g., *Aiptasia*, *Anthopleura*) and jellyfishes (*Cassiopea*, *Mastigias papua*) possess zooxanthellae as symbiotic algae (Trench, 1971; Cates and McLaughlin, 1976; Muscatine and Marian, 1982; Cook et al., 1988). In addition, some species in *Anthopleura* and *Hydra* have symbiotic green algae in their cells (Muscatine and Lenhoff, 1963; Muscatine 1971). These cellular mechanisms in symbiosis have been studied due to impacts on the ecosystems. Recently, the development of genomics and transcriptomics has made it possible to understand cellular mechanisms through genome sequence and gene expression analyses, and the mechanisms of symbiosis in these symbiotic systems have been clarified (Hamada et al., 2018; Cui et al., 2019). However, the evolutionary process of photosymbiosis and the causes of host-symbiont specificity are still not well elucidated.

1.1.2 Two types of symbiotic systems in *Hydra*

Hydra is a freshwater cnidarian distributed almost all over the world (Jankowski et al., 2008). *Hydra* captures plankton such as *Artemia* by detecting movement of the prey through a mechanosensory cilium and discharging nematocysts in its tentacles and causes a feeding response by detecting reduced glutathione released from the prey (Loomis, 1955). Since the experiment by Trembley (Mémoires pour servir à l'histoire d'un genre de polypes d'eau douce, 1744), *Hydra* has been used as an important model system in various study areas: developmental biology, neurogenesis, environmental study, etc (Galliot, 2012). For example, in developmental biology, *Hydra* has brought a lot of insights into axis pattern formation in the Metazoa through Wnt/β-catenin signaling (Hobmayer et al., 2000; Reddy et al., 2019). From the morphology and the molecular data, *Hydra* is divided into four groups: *viridissima* group, *braueri* group, *oligactis* group, and *vulgaris* group (Campbell, 1987a; Hemmrich et al., 2007;

Kawaida et al., 2010).

Hydra is a suitable model organism to study symbiosis because of rapid reproduction by budding and accumulation of research on both hydra and symbiotic algae (Kovacevic, 2012). There are two types of endosymbiosis with green algae in the genus *Hydra*. *Hydra viridissima* (green hydra) has a symbiotic relationship with *Chlorella*, while some strains of *H. vulgaris* (brown hydra) also have a symbiotic relationship with *Chlorococcum* (Rahat and Reich, 1985a; Dunn 1987). *H. viridissima* and *H. vulgaris* belong to the *viridissima* group and the *vulgaris* group respectively, and so the symbiotic hydra species have independently established symbiotic relationships with their green algae (Kawaida et al., 2013; Ishikawa et al., 2016a). All the green hydra has the symbiotic chlorella, and it is estimated that the lineage of the green hydra diverged from the other group hydras 61–45 million (Martínez et al., 2010) or 149–241 million years ago (Schwentner and Bosch, 2015). It suggests that the green hydra has established a stable symbiotic relationship with *Chlorella* for a long time. On the other hand, only some strains of the brown hydra can establish the symbiotic relationship with *Chlorococcum*, and the brown hydra acquired the ability to establish the symbiosis with the alga more recently than the green hydra did (Kawaida et al., 2013; Ishikawa et al., 2016a).

Both symbiotic hydras can harbor non-native symbiotic algae acquired by the artificial introduction (Huss et al., 1994; Kawaida et al., 2013; Ishikawa et al., 2016a). So, experiments of removing and introducing the non-native symbionts can provide information on the specificity of the combination between host hydras and symbiotic algae. The genomes of the two symbiotic hydra species were sequenced (Chapman et al., 2010; Hamada et al., 2020). It provides a tool kit for analyzing the mechanism of symbiosis. Therefore, the symbiotic hydras are suited to study the evolutionary process of endosymbiosis and the host-symbiont specificity.

1.2 Description of *Hydra* species used in this study

1.2.1 The brown hydra symbiosis with the chlorococcum

H. vulgaris (brown hydra) inhabits fresh water in the Eurasian continent, and hydras from other continents, which have been considered *H. vulgaris* (e.g. AEP strain), are classified as other biological species (Martínez et al., 2010; Schwentner and Bosch, 2015). Three species of hydras in the *vulgaris* group, *H. maganipapillata, H. japonica,* and *H, paludicola*, were described in Japan (Ito, 1947a,b), but Kawaida et al. (2010) classify these three species into *H. vulgaris* with molecular phylogenetic analyses. The existence of symbiotic polyps is mentioned in the description of one of these species, *H. magnipapillata*: "greenish brown and green from the symbiotic algae" in Ito (1947a). Rahat and Reich (1985a) reported the symbiosis between *H. vulgaris* and *Chlorococcum* based on the symbiotic *H. vulgaris* collected in Aomori and Ishikawa prefectures by Sugiyama. The two symbiotic strains (J7, J10) have been stored in the National Institute of Genetics (NIG; Mishima, Japan). The symbiotic chlorococcum is described as "*Symbiococcum hydrae*" (Rahat and Reich, 1989), and a recent phylogenetic analysis of the symbiotic chlorococcum shows that the symbiotic chlorococcum is closely related to other *Chlorococcum* algae (Ishikawa et al., 2016a). However, the phylogenetic position remains unclear because the taxonomy of *Chlorococcum* has not been well organized (Pröschold et al., 2011; Kawasaki et al., 2015).

The symbiotic chlorococcum can be transmitted to non-symbiotic hydras by artificial transmission. Rahat and Reich (1986) fed isolated symbiotic algae to *Artemia* larvae, and then the larvae were fed to non-symbiotic hydras. Rahat and Sugiyama (1993) fed freshly hatched *Artemia* larvae to non-symbiotic hydras, and then immediately gave the feeding polyps concentrated suspensions of isolated symbiotic algae for the artificial transmission. Ishikawa et al. (2016a) introduced isolated symbiotic algae into a gastric cavity of a hydra polyp using a glass micro-capillary and also grafted an upper half of non-symbiotic polyp onto a symbiotic polyp. These artificial transmissions reveal that some non-symbiotic hydra strains, but not all,

have the potential of endosymbiosis with the symbiotic chlorococcum. Ishikawa et al. (2016a) show that *H. vulgaris* in three of four clades surveyed in the study can establish endosymbiosis with the chlorococcum and that the native symbiotic strains J7 and J10 belong to different clades (Fig. 1.1). In addition, hydras in groups other than the *vulgaris* group (*H. oligactis*, *H. viridissima*) are also able to incorporate the chlorococcum in their cells, but the symbiotic chlorococcum is transmitted to the next generation by budding only in *H. vulgaris* (Rahat and Reich, 1986). These studies suggest that only *H. vulgaris* has sufficient potential for endosymbiosis with the symbiotic chlorococcum. Miyokawa et al. (2018) found that the symbiotic chlorococcum can be transmitted to a non-symbiotic polyp by horizontal transmission through the culture solution without any artificial procedures. It reports that the co-culture of a symbiotic polyp and a non-symbiotic polyp causes horizontal transmission from the symbiotic polyp to the non-symbiotic polyp and that the chlorococcum is also transmitted to hydras other than *H. vulgaris* by the horizontal transmission. These findings suggest that the transmission of the symbiotic chlorococcum can happen in nature. However, *H. vulgaris* having the symbiotic chlorococcum is extremely rare in nature constituting not more than 2% of the population (Slobodkin et al. 1991).

The other symbiotic hydra, *H. viridissima*, which has the symbiotic relationship with chlorellae, proliferates faster than the aposymbiotic (symbiont-removed) hydra by budding, but the proliferation rate of the symbiotic *H. vulgaris* is not significantly different from that of the aposymbiotic hydra (Ishikawa et al., 2016b). The symbiotic *H. viridissima* survives longer days under starvation than the aposymbiotic hydra, while the symbiotic *H. vulgaris* survives shorter days under starvation than the aposymbiotic hydra (Ishikawa et al., 2016b). *H. vulgaris* acquired the ability of endosymbiosis more recently than *H. viridissima* (Ishikawa et al., 2016a). Therefore, Ishikawa et al. (2016b) conclude that the symbiosis between the *H. vulgaris* and the chlorococcum is not yet well established, and that lacks the mechanisms for stable endosymbiosis. The symbiotic hydra acquired the chlorococcum by the horizontal transmission proliferates faster than the non-symbiotic hydra, but the polyp size of the symbiotic hydra is

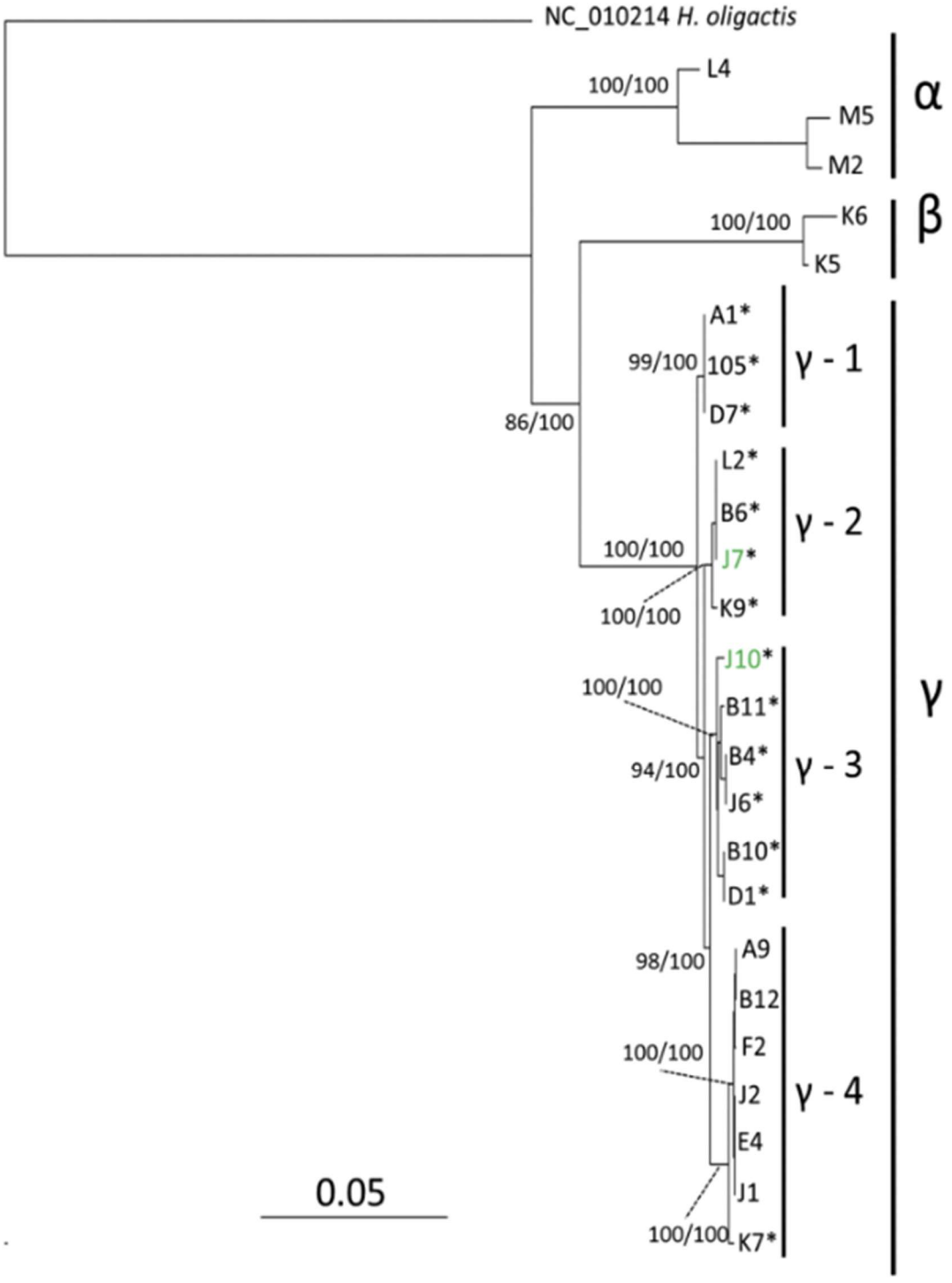

Figure 1.1 Maximum likelihood (ML) tree inferred from nucleotide sequences of the mitochondrial genomes of the *vulgaris* group strains (reprinted from Ishikawa et al. 2016a, Fig 5). The γ cluster is equivalent to *H. vulgaris*, and γ - 1−4 are equivalent to clades in *H. vulgaris*. The numbers along branches indicate the bootstrap values for ML (left) and the Bayesian posterior probabilities for Bayesian inference (right). Strains which can establish endosymbiosis with artificially introduced algae are indicated by asterisks.

shortened (Miyokawa et al., 2018). It is considered that the cellular process during the symbiosis is different from the native symbiotic hydra and the symbiotic hydra by the horizontal transmission.

1.2.2 The green hydra symbiosis with the chlorella

Hydra viridissima (green hydra) has long been studied for the symbiosis with green algae due to its green polyp (Whitney, 1907; Muscatine and Lenhoff, 1965). *Hydra viridissima* has been identified as one species because of its symbiotic association with chlorella, but it contains genetically diverse lineages (Martínez et al., 2010; Schwentner and Bosch, 2015). In these lineages, the topology of the host hydra phylogeny corresponds to that of the symbiotic chlorella phylogeny (Kawaida et al., 2013). The authors consider that the green hydra and the chlorella evolved the symbiosis only once and that the free-living state has been restored in parts of symbiotic chlorellae. However, Rajević et al. (2015) found that symbiotic algae of the green hydra belong to various taxa of green algae and proposed multiple origins of the symbiosis between the green hydra and the algae.

The green hydra vertically transmits the symbiotic chlorella to buds and eggs (Habetha and Bosch, 2005; Kawaida et al., 2013). On the other hand, it is difficult to culture the symbiotic chlorellae for a long time, and the horizontal transmission has not been observed (Muscatine, 1965; Park et al., 1967). The symbiotic chlorella is inside a host endodermal epithelial cell within a perialgal vacuole called symbiosome (Muscatine, 1965; Neckelmann and Muscatine, 1983; Rahat and Reich 1985b). The number of the symbiotic chlorellae in each cell is regulated to a certain level (Douglas and Smith, 1984; Dunn, 1987). The regulation of the symbionts requires release to the gastric cavity or digestion in lysosomes (Neckelmann and Muscatine, 1983; Fishman et al., 2008). In the symbiosome, there is a mutualistic interaction between the host and the symbiotic algae in the exchange of nitrogen sources and photosynthetic products. The green hydra provides glutamine to the symbiotic chlorella as a nitrogen source, and the symbiont provides maltose produced by photosynthesis to the host (McAuley, 1995; Muscatine,

1965; Mews and Smith, 1982; Hamada et al., 2018). The symbiotic chlorella within the green hydra cannot utilize ammonium and nitrate, and so the host hydra needs to synthesize glutamine, which the symbiont can utilize as a nitrogen source (Hamada et al., 2018).

Experiments introducing various strains of chlorella into aposymbiotic green hydras were conducted by injection of the chlorellae into the gastric cavity (Jolley and Smith 1980; McAuley and Smith, 1982; Rahat and Reich, 1985b). In these experiments, the green hydra can establish the symbiotic relationship with non-native symbiotic chlorellae and some free-living chlorellae, and the chlorellae which can establish the symbiotic relationship is tolerant to low pH and proliferate in eutrophic culture medium. Kawaida et al. (2013) grafted an aposymbiotic polyp onto a symbiotic polyp. In the experiment, the symbiont in the symbiotic polyp moved to the aposymbiotic polyp and established the symbiotic relationship with the aposymbiotic polyp. Traits of the chlorella introduced into the green hydra will affect host fitness. Introduction of the symbiotic chlorellae to aposymbiotic hydras alters tolerance to a high temperature (Ye et al., 2019). Hamada et al. (2018) introduced the symbiotic chlorella of *Paramecium bursaria* into aposymbiotic green hydras, and the proliferation rate of the introduced hydra was decreased. Hanada (2020) conducted experiments removing and reciprocally replacing the symbiont in two green hydra strains, K10 and M9. Both the aposymbiotic strains are decreased in the proliferation rates by budding, but changes in the proliferation rates of the hydras introduced with the non-native symbionts are altered by strain; K10 strain is decreased in the proliferation rate, while M9 strain does not change. These results support the existence of the specificity between the host and the symbiont.

1.3 Objectives in this study

The following contents in this thesis consist of three parts: In chapter 2, I compared gene expression patterns in the native symbiotic hydra and the hydra acquiring the symbiont by horizontal transmission to reveal the differences in symbiotic mechanisms between those *H. vulgaris* strains. In chapter 3, I investigated the symbiotic mechanisms of two *H. viridissima*

strains with gene expression changes in hydras with the symbiont removal and replacement to know what kind of symbiotic mechanisms is responsible for the specificity between hydra and symbionts. In chapter 4, I discussed the symbiotic relationships between the hydras and the symbionts and compared the symbiotic mechanisms in *Hydra* with those in other symbiotic systems to infer evolutionary processes of endosymbiosis based on the findings in chapter 2 and 3.

CHAPTER 2

Symbiotic system between brown hydra and chlorococcum

2.1 Introduction

Symbiotic algae behave as mutualistic, parasitic, or free-living organisms, depending on host and symbiont genotypes and environmental conditions (Douglas, 1998; Lesser et al., 2013). Organisms with algal symbionts are widely distributed among various taxonomic groups. Hosts can acquire photosynthates from symbionts, and the symbionts are supplied with nitrogen and carbon sources from their hosts. Hosts also provide symbiotic algae with the benefit of host shelters, which protect the symbionts from predators and environmental fluctuations (Yellowlees et al., 2008; Melo Clavijo et al., 2018). Such algal endosymbiosis is inferred to have evolved from predator-prey or host-parasite interactions, but the evolutionary processes enabling symbiosis have not been elucidated to date (Weiblen and Treiber, 2015).

Many cnidarian species exhibit symbiotic relationships with algae. For instance, the symbiosis of reef-building corals and sea anemones with zooxanthellae has been intensively studied (Meyer and Weis, 2012). Additionally, some anemones and hydras are known to have symbiotic relationships with green algae (Bates et al., 2010; Kawaida et al., 2013). A stable symbiotic relationship between *Hydra viridissima* (known as green hydra) and *Chlorella* is well-known, and molecular clock analysis has indicated that their symbiotic relationship first appeared more than 77 million years ago (Schwentner and Bosch, 2015). Moreover, several strains of brown hydra (*H. vulgaris*) collected in Japan exhibit *Chloroocccum* sp. as an endosymbiont in their endodermal cells (Rahat and Reich, 1986; e.g., the J10 and J7 strains). Only *Chloroocccum* sp. can establish the symbiotic relationship with brown hydra among algae species in the genus *Chlorococcum* (Rahat and Reich, 1986). Interestingly, many strains of *H. vulgaris* can incorporate the symbiotic algae by the artificial introduction to the gastral cavity (Rahat and Reich, 1989; Ishikawa et al., 2016a), despite the rarity of symbiotic *H. vulgaris* strains in the wild. However, most of the artificially introduced symbionts are not stable, and

the tolerance to starvation of the host polyp is decreased in the symbiotic strains of *H. vulgaris* compared with the non-symbiotic strains (Rahat and Reich, 1989; Ishikawa et al., 2016b). This finding suggests that the symbiosis between *H. vulgaris* and *Chloroocccum* is less stable than that between *H. viridissima* and *Chlorella*. Ishikawa et al. (2016a) suggested the "two-step evolution" of endosymbiosis: the common ancestor had previously obtained endosymbiotic potential with *Chlorococcum*, and the native symbiotic strains obtained symbiotic chlorococci recently. The authors interpreted that the non-symbiotic strains with endosymbiotic potential had not been fully adapted to the symbiosis. In this respect, the hydra-chlorococcum interaction is considered to be a suitable system for elucidating the evolution of symbiosis at an early stage. Miyokawa et al. (2018) showed that non-symbiotic hydras can acquire the symbiotic chlorococci by horizontal transmission without artificial introduction. The symbiotic hydra strain established by horizontal transmission exhibited notable changes, displaying decreased polyp size, decreased number of cells per polyp, and elevated proliferation rate by budding. These changes indicate that the reduction in the size of the symbiotic hydras is not due to a change in cell size, but due to an increase in the frequency of budding.

In this study, I confirmed the identity of the symbiotic chlorococcum in the hydra cell and the algae in the surrounding water and decided the phylogenetic position of the symbiotic chlorococcum. Next, I analyzed the gene expression changes between the newly established symbiotic polyps through horizontal transmission and the original non-symbiotic ones using RNA-seq. I aimed to investigate the mechanisms of hydra-chlorococcum symbiosis, which is still in progress, based on the gene expression observed in the acquired symbiotic strain. To elucidate the mechanism of the hydra for adaptation to symbiosis in the wild, I compared gene expression changes by symbiosis with the symbiotic chlorococcum between the acquired symbiotic strain and the native symbiotic strain. I also observed the effects of interference in cellular metabolism between the non-symbiotic strain and the symbiotic strains. These results may help to characterize the early steps of symbiosis evolution.

2.2 Materials and Methods

2.2.1 Materials

I employed four strains of *H. vulgaris* (formally described as *H. magnipapillata*): 105, 105G, J7, and J7apo. Strain J7 is a native symbiotic strain, and strain J7apo is an aposymbiotic strain whose symbiont was eliminated by keeping the polyp in a dark place (Ishikawa et al., 2016b). Strain 105, J7, and J7apo were stored at the National Institute of Genetics (NIG; Mishima, Japan). Strain 105G is a symbiotic strain that originated from strain 105, and strain 105G has established a symbiotic relationship with *Chlorococcum* sp. in my laboratory by the horizontal transmission of the symbionts from symbiotic polyps in the same vessel (Miyokawa et al., 2018). The *rbcL* sequence of the symbiont in strain 105G is identical to that of the symbiont in strain J7. All the strains were maintained in hydra culture solution (HCS; 1 mM NaCl, 1 mM $CaCl_2$, 0.1 mM KCl, 0.1 mM $MgSO_4$, 1 mM tris-(hydroxymethyl)-aminomethane; pH 7.4, adjusted with HCl) in glass vessels at 20 °C under 14 h∶10 h light/dark illumination cycles (84 μmol/m^2/s light intensity). Polyps were fed newly hatched *Artemia* nauplii two times a week. The day after feeding, the polyps were transferred into glass vessels with fresh HCS.

2.2.2 Observation of endosymbiotic and floating free-living algae

Two or three symbiotic polyps of strains J10 and 105G were homogenized with a BioMasher II (Nippi, Tokyo) in 100 μL of HCS to extract endosymbiotic algae, and the homogenates were centrifuged at 2000 g for a few minutes. The extracted algae were precipitated at the bottom of 1.5-mL microtubes. The precipitates were re-suspended in 500 μL of HCS and were centrifuged at 2000 g for a few minutes to wash the algae. After three washes, the precipitated algae were re-suspended in 50μL of HCS and mounted on a glass slide, and I observed them with a Nomarski differential interference microscope (Nikon). To correct for the free-swimming algae from HCS that contained symbiotic hydras, J10 and 105G, 20–30 mL of HCS was centrifuged at 2000 g for a few minutes. A small amount of precipitate was formed. I re-suspended it and observed the algae with the microscope. The free-living algae were cultured in BBM+ medium

(BBM medium with 0.5 % glucose, 0.5 % peptone, 0.1 % yeast extract, 0.01 % liver infusion; Rahat and Reich, 1985b) with 5mg/L gentamycin and 50mg/L ampicillin.

2.2.3 Nucleotide sequences of the symbiotic chlorococcum and algae in surrounding water

I determined the nucleotide sequences of the partial chloroplast genome-encoded gene, ribulose-1, 5-bisphosphate carboxylase/oxygenase large subunit (*rbcL*), and the 18S ribosomal RNA gene (18S rDNA). The polyps were homogenized with a BioMasher II (Nippi) in a 50 μL buffer (50 mM KCl, 10 mM tris-(hydroxymethyl)-aminomethane HCl; pH 8.3, 0.1 % NP-40) and incubated with proteinase K (2mL of 20 mg/mL proteinase K stock solution; Takara Bio, Shiga, Japan) at 55 °C for 15–60 min until the polyps lost their shapes. Then, I used the solution as a DNA template for PCR. I also obtained algal DNA from the precipitated free-living algae collected from the HCS of the symbiotic polyps. DNA was extracted with a DNeasy Plant Mini Kit (Qiagen, Hilden, Germany), following the manufacturer's instructions. The PCR amplification of the 18S rDNA of symbiotic chlorococcum was performed with a primer pair 5'-GAGGATTGACAGATTGAGAGC-3' and 5'-GAACACTTCACCAGCACACC-3'. For the chloroplast rbcL gene, I used a primer pair 5'-AGGTCCTCCACACGGTATTCA-3' and 5'-TCAATAACAGCGTGCATAGC-3'. The PCR conditions were as follows: an initial denaturation step at 94 °C for 1 min, followed by 35 cycles of 30 s at 94°C, 1 min annealing at 50 °C, and 1 min elongation at 72 °C; and a final elongation step of 5 min at 72 °C. The PCR products were directly sequenced using an ABI3730 DNA Analyzer and BigDye Terminator v3.1 Cycle Sequencing Kits (Thermo Fisher Scientific, Waltham, MA). To reconstruct the phylogenetic tree, I collected algal sequences from National Center for Biotechnology Information (NCBI) database (Table 2.1). These sequences were aligned using clustalW (Thompson et al., 1994). Phylogenetic trees were reconstructed using MEGA11 (Tamura et al., 2021) adopting the maximum-likelihood method with Tamura-Nei model + gamma distribution.

Table 2.1 NCBI accession numbers of 18S rDNA sequences of algal strains used in the phylogenetic tree construction

Species	Strain	NCBI accession number
Chlamydomonad sp.	Pic 9/21 P-2w	AY220092
Chlamydomonas acidophila	CCAP 11/137	AJ852427
Chlamydomonas moewusii	CGC CC-1419	U41174
Chlamydomonas reinhardtii	SAG 11-32a	AB511835
Chlorella sorokiniana	SM12-4	KX495086
Chlorella variabilis	NC64A	AY876294
Chlorella vulgaris	SB44-3	KX495067
Chlorococcum aquaticum	UTEX2222	AB983622
Chlorococcum ellipsoideum	UTEX 972	CEU70586
Chlorococcum littorale	MBIC10280	AB058336
Chlorococcum minutum	SAG 213-7	KM020099
Chlorococcum nivale	UTEX2225	AB983623
Chlorococcum oleofaciens	SAG 30.93	AB983614
Chlorococcum sp.	51.3	KU521558
Chlorococcum sp.	RK261	AB490286
Chlorococcum sp.*	J7	AB713407
Chlorogonium capillatum	SAG 12-2a	AJ410441
Chloromonas reticulata	SAG 32.86	JN904006
Dunaliella parva	FACHB-815	KT355034
Dunaliella viridis	CONC002	DQ009776
Ettlia oleoabundans	UTEX 1185	KM068042
Macrochloris radiosa	SAG 213-2a	KM020104
Micractinium pusillum	SAG 7.93	AF499921
Oophila sp.	LA2008	KJ635658
Oophila amblystomatis	Suddent Tract	KY091670

* The symbiotic chlorococcum with *H. vulgaris*.

Library preparation and sequencing of the cultured free-living algae were performed by Bioengineering Lab. Co., Ltd. The libraries of the algae were prepared using MGIEasy FS DNA Library Prep Set and MGISP960, and DNA nanoballs were prepared using MGIEasy Circularization Kit and DNBSEQ-G400RS High-throughput Sequencing Kit. The sequencing of the 200 bp paired-end reads was performed on DNBSEQ-G400.

2.2.4 RNA extraction from *Hydra* and transcriptome sequencing

Hydra polyps, after being starved for three days, were used for RNA-seq analysis to remove the effect of nutrient factors on the gene expression from the prey. Total RNA was extracted from intact polyps (30 polyps of strain 105, 50 polyps of strain 105G) using the acid guanidinium thiocyanate-phenol-chloroform (AGPC) method (Chomczynski and Sacchi, 1987). Three biological replicates were prepared for both strains. Total RNA was treated with DNase I (Roche, Mannheim, Germany) to remove genomic DNA. The total RNA samples were sent to Novogene Co., Ltd. (Beijing, China), and cDNA library preparation and sequencing of 150 bp paired-end reads on Illumina HiSeq 4000 were performed by Novogene.

2.2.5 Mapping and differential gene expression analysis

Quality trimming of reads was performed using cutadapt (Martin, 2011). Low-quality ends (QV < 30) and adapter sequences were trimmed, and short reads (< 20 bp) were discarded, for quality control. The trimmed reads were aligned to the *Hydra* genome reference (GCA_000004095.1, Chapman et al., 2010) using TopHat2 version 2.1.1 (Kim et al., 2013). I estimated gene expression levels based on fragments per kilobase of exon per million mapped reads (FPKM) using the Cufflinks (version 2.2.1) pipeline (Trapnell et al., 2012). All transcriptome samples were merged into contigs using Cuffmerge, and then Cuffdiff was used to normalize the read counts of each sample and to analyze differential gene expression between strains 105 and 105G. The contigs were considered differentially expressed if they showed a false discovery rate (FDR) < 0.05. To compare strain 105G with native symbiotic strain J7, I used RNA-seq data of strain J7 and J7apo (symbionts eliminated strain J7) analyzed

by Ishikawa et al. (2016b). I obtained raw sequence data of J7 and J7apo strains (PRJDB4331) and carried out quality trimming for these data using the same criteria as for strains 105 and 105G described above. The trimmed reads were mapped to the *Hydra* genome reference in the same way as those of 105 and 105G. I also performed differential gene expression analyses of each strain with the -b/--frag-bias-correct Cuffdiff command-line option for comparison of changes in expression patterns between 105G/105 and J7/J7apo to normalize read counts. The -b/--frag-bias-correct command-line option is expected to improve the accuracy of expression estimates across RNA-seq libraries (Roberts et al., 2011).

2.2.6 Gene Ontology (GO) enrichment analysis

The contigs were subjected to a similarity search against the UniProtKB Swiss-Prot and *H. vulgaris* proteins in the UniProtKB TrEMBL using BLASTX with an e-value cutoff of 1e-5. GO enrichment analysis was performed using the DAVID Functional Annotation tool (Huang et al., 2009). UniProt accessions annotated to the contigs were entered into DAVID as queries. I used GO Direct as GO categories in DAVID. GO terms were considered to be significantly enriched if they showed adjusted P (Benjamini) < 0.05 by Fisher's exact test. GOCircle plots, which show expression levels and z-scores of the differentially expressed genes (DEGs) in enriched GO terms, were drawn using the R package GOplot (Walter et al., 2015). The R package pathview (Luo and Brouwer, 2013) was used to conduct a pathway analysis for several KEGG pathways (https://www.genome.jp/kegg/pathway.html), including the DEGs.

2.2.7 Rapamycin treatment

Rapamycin (LC Laboratories, Woburn, MA) was dissolved in dimethyl sulfoxide (DMSO) to 1 mM or 3 mM as a stock solution. Next, each rapamycin stock solution was dissolved in 6 mL HCS to make 1 μM or 3 μM solutions. For the control condition, 0.1% DMSO in HCS was used. Ten budless polyps for each condition were used at the start of the experiments and cultured in plastic containers filled with rapamycin solutions at 20 °C under 14 h∶10 h light/dark illumination cycles (15 μmol/m^2/s light intensity) for two weeks. The numbers of

live polyps under each condition were counted per day. The polyps were fed *Artemia* nauplii on days 0, 4, 7, and 11. The polyps were observed with a stereomicroscope (MZ75, Leica, Wetzlar, Germany) and photographed with a digital camera (Digital Sight DS-L1, Nikon, Tokyo). The number of polyps in each condition or strain was tested by Tukey's test.

2.3 Results

2.3.1 Morphology and phylogeny of the symbiotic chlorococcum

To confirm the identity between the green algae in the symbiotic polyps which acquired the algae by horizontal transmission and the ones in the native symbiotic strain J10 polyps, I compared the partial sequences of *rbcL* in the algae. The examined nucleotide sequences (NCBI accession no. LC381699) were identical to those of the symbiotic *Chlorococcum* sp., whose partial *rbcL* sequences are the same between the symbiotic J7 and J10 strains (accession no. AB713414). I observed some algal cells, non-flagellate algae like the chlorococci in hydra cells, slender flagellate zoospores, and large flagellate algae, in the HCS containing strain J10 and 105G polyps (Fig. 2.1a,b,c). The two flagellate algae had a pair of flagella (Fig. 2.1b,c, arrows). The large flagellate algae often contained the chlorococcum-like algae in the cells. I confirmed the identity between the endosymbiotic algae and the algae in the HCS by sequencing the rbcL and 18S rDNA genes (accession no. LC381698, *rbcL*; LC381701, 18SrDNA). These nucleotide sequences were identical to those of the symbiotic chlorococcum. The morphology of the free-swimming zoospores corresponds to the flagellated motile zoospores of the cultured symbiotic chlorococcum reported by Rahat and Reich (1991). However, I cultured the algae in the HCS in the liquid medium, and then only large flagellate algae proliferated. The 18S rDNA sequence of the cultured large flagellate algae was close to *Poterioochromonas malhamensi*s, and their morphology was also similar to *P. malhamensi*s. It indicated that the non-flagellate algae and the flagellate zoospores would be the symbiotic chlorococci, but that the large flagellate algae would not be.

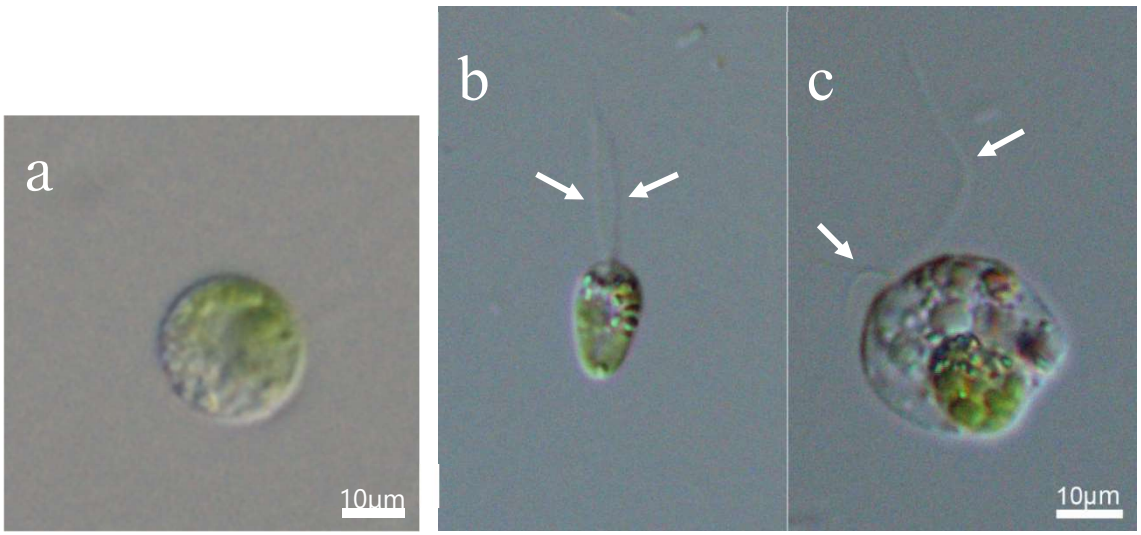

Figure 2.1 Green algae in the HCS which the symbiotic hydra was in. (**a**) a non-flagellate alga like the chlorococcum extracted from endodermal epithelial cell. (**b**) a slender flagellate zoospore. (**c**) a large flagellate alga. (b) and (c) are the same scale.

I conducted a phylogenetic analysis of the symbiotic chlorococcum using the 18S rDNA sequence. Among Chlorophytina, the symbiotic chlorococcum (*Chlorococcum* sp. J7) was close to *Oophila amblystomatis*, which is known as a symbiotic alga of a salamander (Kerney et al., 2011), and *C. oleofaciens* (Fig. 2.2a). Because *C. oleofaciens* belongs to Stephanosphaerinia (Kawasaki et al., 2015), I reconstructed a phylogenetic tree only for the species of Stephanosphaerinia (Fig. 2.2b). *Chlorococcum* sp. J7 was closely related to *C. aquaticum* and *C. minutam*, which are free-living algae living in freshwater and soil, respectively, although its bootstrap support was low (68 %).

2.3.2 Gene expression difference in the symbiotic and non-symbiotic 105G polyps

To analyze the changes in cellular mechanisms that were induced by horizontal transmission in the symbiotic polyps, I compared the gene expression patterns of the symbiotic hydra strain 105G to those of the original non-symbiotic strain 105. I obtained 137 million paired-end sequence reads after quality control was performed. The proportions of mapped reads of strains 105G and 105 were 69.5% and 79.3%, respectively, and GC content of the mapped reads was 35% for both strains. Green algae generally have higher GC content levels (e.g. *Chlorococcum* sp. FFG039: 62%, Maeda et al., 2019), so the equivalent GC content suggested contaminated reads of the chlorococci were correctly filtered from the mapped reads of the 105G samples. Out of the total of 31,725 contigs in the reference, 26,696 contigs and 27,001 contigs were expressed in 105G and 105, respectively, and 27,406 contigs were expressed in either or both of strains. In strain 105G, 2,742 contigs were upregulated, and 2,971 contigs were downregulated, compared to strain 105. In the expressed contigs, 11,467 contigs could be annotated with descriptions of *H. vulgaris* genes in RefSeqGene, excluding uncharacterized genes. In addition, I performed similarity searches using BLASTX to assign functional annotations to the mapped genes. As a result, 6,080 contigs were matched with entries in UniProtKB Swiss-Prot, and 807 contigs were matched with entries for *H. vulgaris* in UniProtKB TrEMBL.

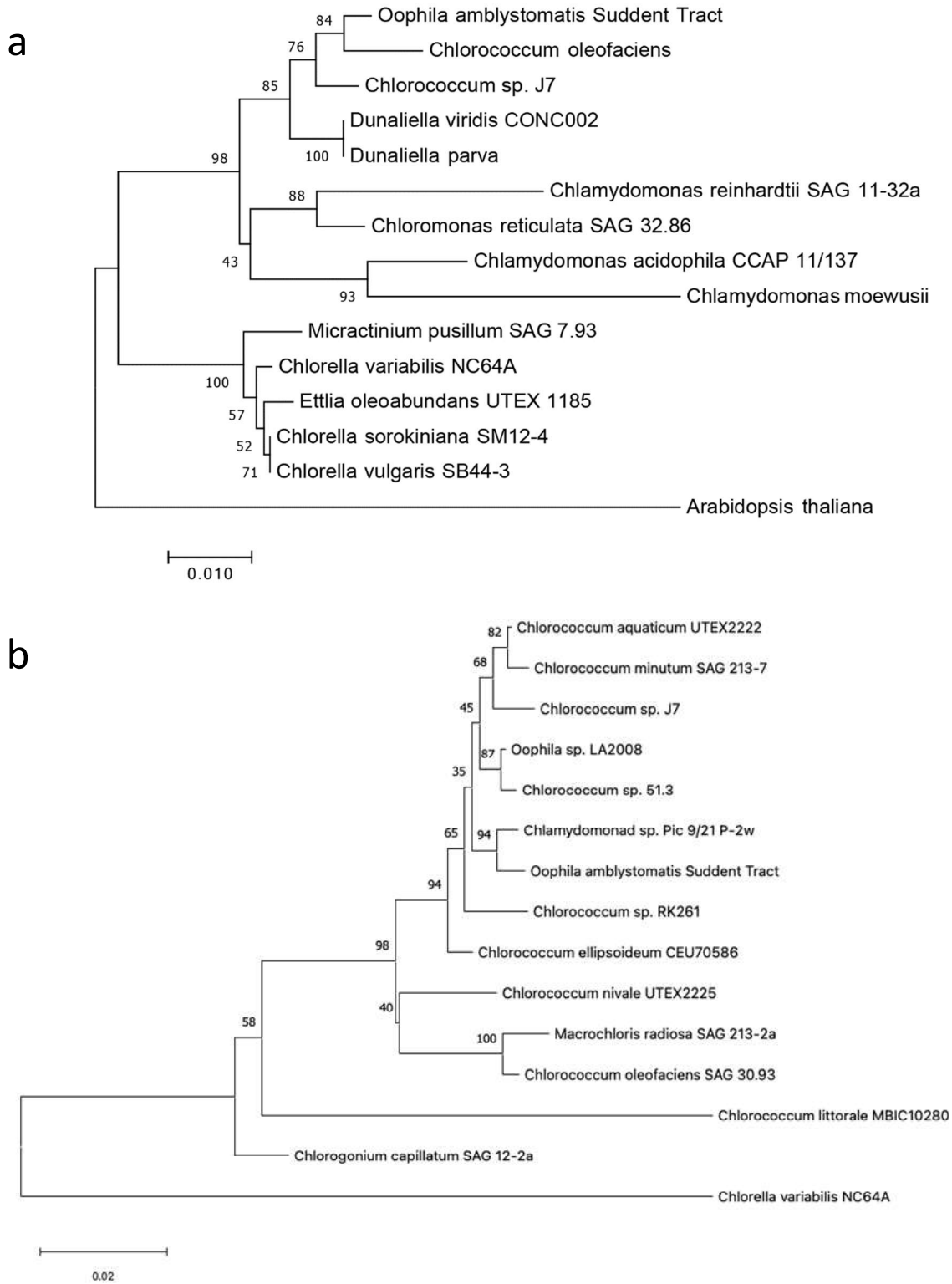

Figure 2.2 Phylogenetic tree of the symbiotic chlorococcum constructed with the maximum likelihood method inferred from the nucleotide sequences of the 18S rDNA of green algae. The numbers along branches indicate the bootstrap value. (a) Phylogenetic position of the symbiotic chlorococcum in Chlorophytina. (b) Phylogenetic position of the symbiotic chlorococcum in *Chlorococcum* and the related algae.

I performed Gene Ontology (GO) enrichment analysis using the DAVID Functional Annotation tool and illustrated enriched Gene Ontology terms as GOCircle plots (Fig. 2.3). Among the upregulated genes, 31 GO terms were significantly enriched, while 8 GO terms were enriched among the downregulated genes (Tables 2.2,3). In the biological process (BP) category, 8 GO terms were significantly enriched in the upregulated genes (Fig. 2.3a). In particular, translation exhibited the highest z-score (Z = 8.20) and the lowest P-value (P = 1.18e-14) among the enriched categories. In cellular component (CC) categories, 22 GO terms were significantly enriched (16 upregulated and 6 downregulated). I present the details for five of the GO terms in the CC category with higher P-values in the upregulated and downregulated genes, respectively, in Fig. 2.3b. Mitochondria had the highest z-score (Z = 10.27) and a lower P-value (P = 2.24e-10). Differentially expressed genes (DEGs) in the GO term mitochondrion, such as respiratory chain complexes, overlapped with DEGs in the GO term oxidation-reduction process.

2.3.3 Comparison of gene expression changes by symbiosis with the chlorococci between the acquired symbiotic strain and the native symbiotic strain

Ishikawa et al. (2016a) postulated that hydras that did not have “endosymbiotic potential” with *Chlorococcum* evolved into native symbiotic hydras in a step-by-step process by first becoming hydras with endosymbiotic potential. Some *Hydra* strains with endosymbiotic potential can acquire symbionts by artificial or spontaneous transmission (Rahat and Reich, 1986; Rahat and Reich, 1989; Ishikawa et al., 2016b). However, it is not clear what kind of step-by-step changes in the cellular mechanisms are required to obtain the endosymbiotic potential. Therefore, I investigated the difference in gene expression patterns between the acquired symbiotic strain 105G and the native symbiotic strain J7 to help elucidate the mechanism governing the establishment of symbiosis.

I obtained RNA-seq data of J7 and J7apo strains sequenced by Ishikawa et al. (2016b). Strain J7apo is a non-symbiotic strain of strain J7 from which the symbiont has been removed.

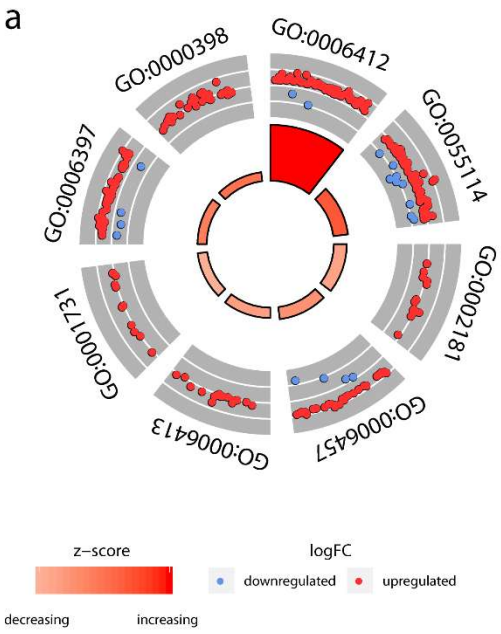

ID	Description
GO:0006412	translation
GO:0055114	oxidation–reduction process
GO:0002181	cytoplasmic translation
GO:0006457	protein folding
GO:0006413	translational initiation
GO:0001731	formation of translation preinitiation complex
GO:0006397	mRNA processing
GO:0000398	mRNA splicing, via spliceosome

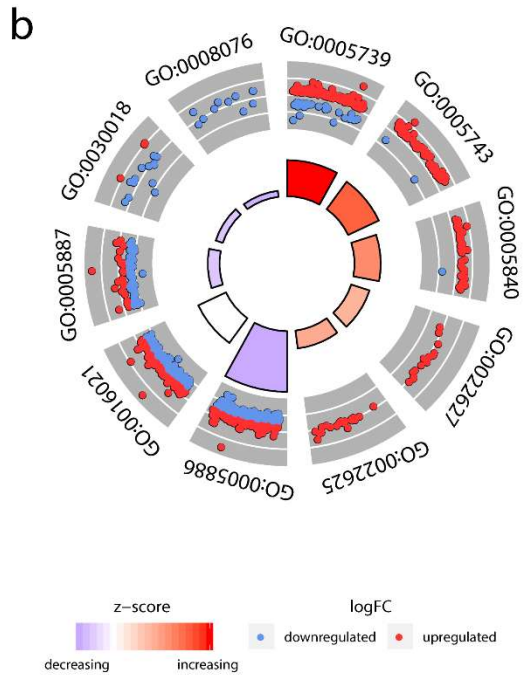

ID	Description
GO:0005739	mitochondrion
GO:0005743	mitochondrial inner membrane
GO:0005840	ribosome
GO:0022627	cytosolic small ribosomal subunit
GO:0022625	cytosolic large ribosomal subunit
GO:0005886	plasma membrane
GO:0016021	integral component of membrane
GO:0005887	integral component of plasma membrane
GO:0030018	Z disc
GO:0008076	voltage–gated potassium channel complex

Figure 2.3 Functionary characterization of differentially expressed genes (DEGs). The outer circle shows scatter plots of the expression levels of DEGs in each enriched GO term. The inner circle represents the z-scores (differences between the number of upregulated DEGs and downregulated DEGs) by color and the adjusted *P*-values by height. (**a**) Top 8 enriched GO terms in the BP category. (**b**) Top 5 enriched GO terms in each upregulated and downregulated gene in the CC category.

Table 2.2 Enriched GO terms in the upregulated genes in strain 105G.

Category	Term	Count	Pop Hits	Fold Enrichment	q-value
MF	structural constituent of ribosome	65	118	2.87	7.56E-15
BP	translation	73	144	2.72	1.18E-14
MF	poly(A) RNA binding	132	383	1.80	1.87E-10
CC	mitochondrion	163	526	1.68	2.24E-10
CC	mitochondrial inner membrane	69	164	2.28	8.86E-10
CC	ribosome	39	77	2.74	1.05E-07
CC	cytosolic small ribosomal subunit	16	20	4.33	7.63E-06
CC	cytosolic large ribosomal subunit	20	31	3.50	1.61E-05
CC	mitochondrial matrix	41	103	2.16	7.63E-05
MF	RNA binding	93	300	1.62	2.09E-04
CC	extracellular exosome	173	691	1.36	3.29E-04
CC	proteasome complex	19	35	2.94	7.00E-04
MF	translation initiation factor activity	23	44	2.72	9.55E-04
BP	oxidation-reduction process	67	202	1.78	0.00107513
CC	myelin sheath	26	61	2.31	0.00203143
BP	cytoplasmic translation	15	22	3.65	0.00344199
BP	protein folding	31	74	2.24	0.00560184
CC	mitochondrial respiratory chain complex I	11	16	3.72	0.00663326
CC	intracellular ribonucleoprotein complex	35	101	1.88	0.00852641
MF	NADH dehydrogenase (ubiquinone) activity	12	17	3.68	0.00990423
CC	eukaryotic translation initiation factor 3 complex	9	12	4.06	0.01480239
CC	eukaryotic 43S preinitiation complex	9	12	4.06	0.01480239
BP	translational initiation	16	28	3.06	0.01717476
MF	translation elongation factor activity	12	18	3.47	0.01748915
BP	formation of translation preinitiation complex	11	15	3.93	0.02471026
CC	catalytic step 2 spliceosome	23	60	2.08	0.02680533
CC	mitochondrial nucleoid	11	19	3.14	0.03149541
BP	mRNA processing	39	113	1.85	0.0330599
BP	mRNA splicing, via spliceosome	33	91	1.94	0.03956714
CC	eukaryotic 48S preinitiation complex	8	11	3.94	0.04296427
MF	oxidoreductase activity	39	116	1.75	0.04455639

Table 2.3 Enriched GO terms in the downregulated genes in strain 105G.

Category	Term	Count	Pop Hits	Fold Enrichment	q-value
CC	plasma membrane	150	912	2.01	6.20E-17
CC	integral component of membrane	185	1489	1.52	7.09E-09
CC	integral component of plasma membrane	51	324	1.92	7.17E-04
MF	calcium ion binding	42	244	2.08	0.00408159
CC	Z disc	13	43	3.69	0.01026727
CC	voltage-gated potassium channel complex	11	35	3.84	0.02461583
CC	membrane	125	1160	1.32	0.02554138
MF	calmodulin binding	18	76	2.86	0.03415116

The sequence data of each sample were analyzed with the frag-bias-correct option for improving the accuracy of expression estimates. According to the bias correction method, there were 7,279 DEGs between 105G and 105 and 1,787 DEGs between J7 and J7apo (Fig. 2.4a). Although there was a significant power difference between the cases of 105G/105 and J7/J7apo (105G and 105 strains: 3 replicates each; J7 and J7apo strains: 2 replicates each), the DEGs exhibited a four-fold difference between the 105G/105 and J7/J7apo pairs. I found 673 overlapping DEGs between the 105G/105 and J7/J7apo (Fig. 2.4a). Among the overlapping DEGs between the 105G/105 and J7/J7apo annotated from RefSeqGene, there were 15 DEGs with log2 fold changes higher than 1 and 2 DEGs with log2 fold changes lower than -1 in both 105G/105 and J7/J7apo (Table 2.4). L-rhamnose-binding lectin CSL3-like showed the highest FC in both strain pairs, and D-galactoside-specific lectin was one of the upregulated genes in both strain pairs. Both lectins belong to the rhamnose-binding lectin (RBL) family according to BLAST searches.

In strain J7, one GO term was enriched in the upregulated genes, namely, lysosome (P = 2.58e-7), and five GO terms were enriched in the downregulated genes (Table 2.5). The GO term lysosome was also enriched in the upregulated genes in the symbiotic strain J7 in Ishikawa et al. (2016b). I found 16 commonly upregulated genes encoding lysosomal enzymes in the symbiotic strains 105G and J7 (Fig. 2.4b). These enzymes encode upregulated genes, except for heparanase and sialate O-acetylesterase, which act as proteases. There were 73 upregulated genes with the GO term translation in the 105G strain, while no genes with the GO term translation were upregulated in strain J7. I compared the fold changes of genes related to translation and respiratory chain complexes in the symbiotic state between the 105G and J7 strains. The upregulated genes in the 105G strain are shown in Fig. 2.4d. All the upregulated genes in strain 105G with the GO term translation did not show significant expression changes in strain J7 (Table 2.6). The plasma membrane exhibited the lowest P-value (P = 6.20e-17) among the GO terms in the CC category (Fig. 2.3b, Table 2.3). Similarly, Ishikawa et al. (2016b) reported that the GO term plasma membrane is enriched in downregulated genes in

a

b

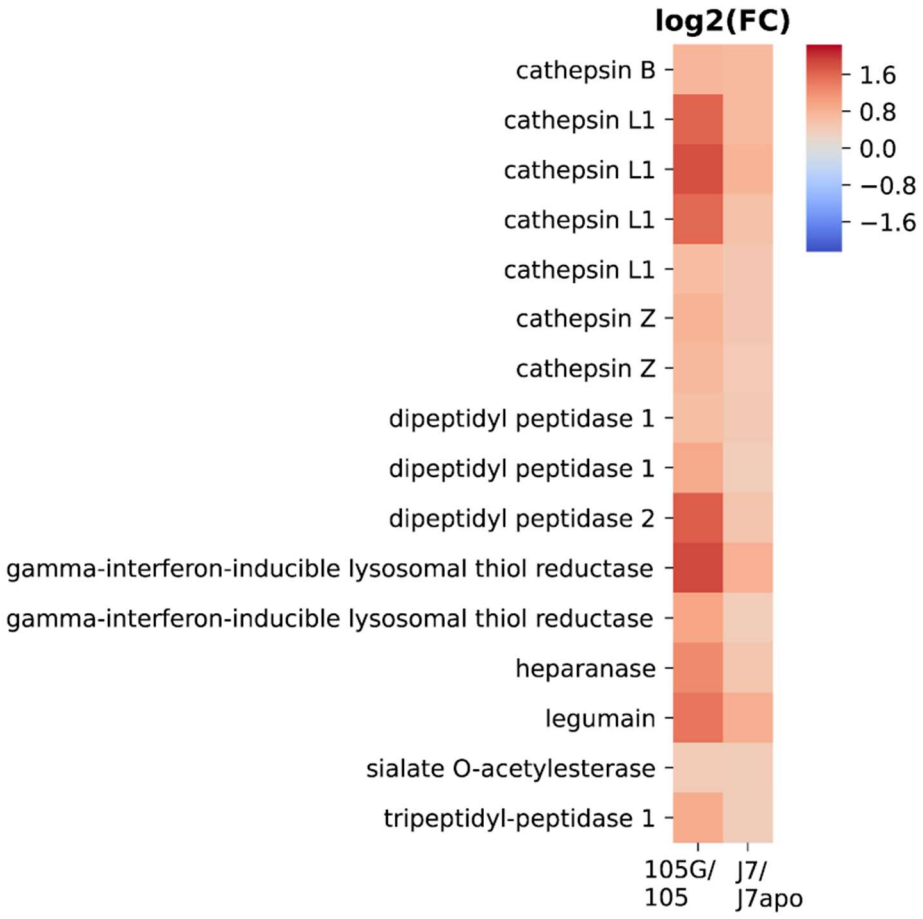

Figure 2.4 Comparison of the gene expression patterns in the 105G/105 and J7/J7apo pairs.

(continued on next page)

(Figure 2.4 continued)

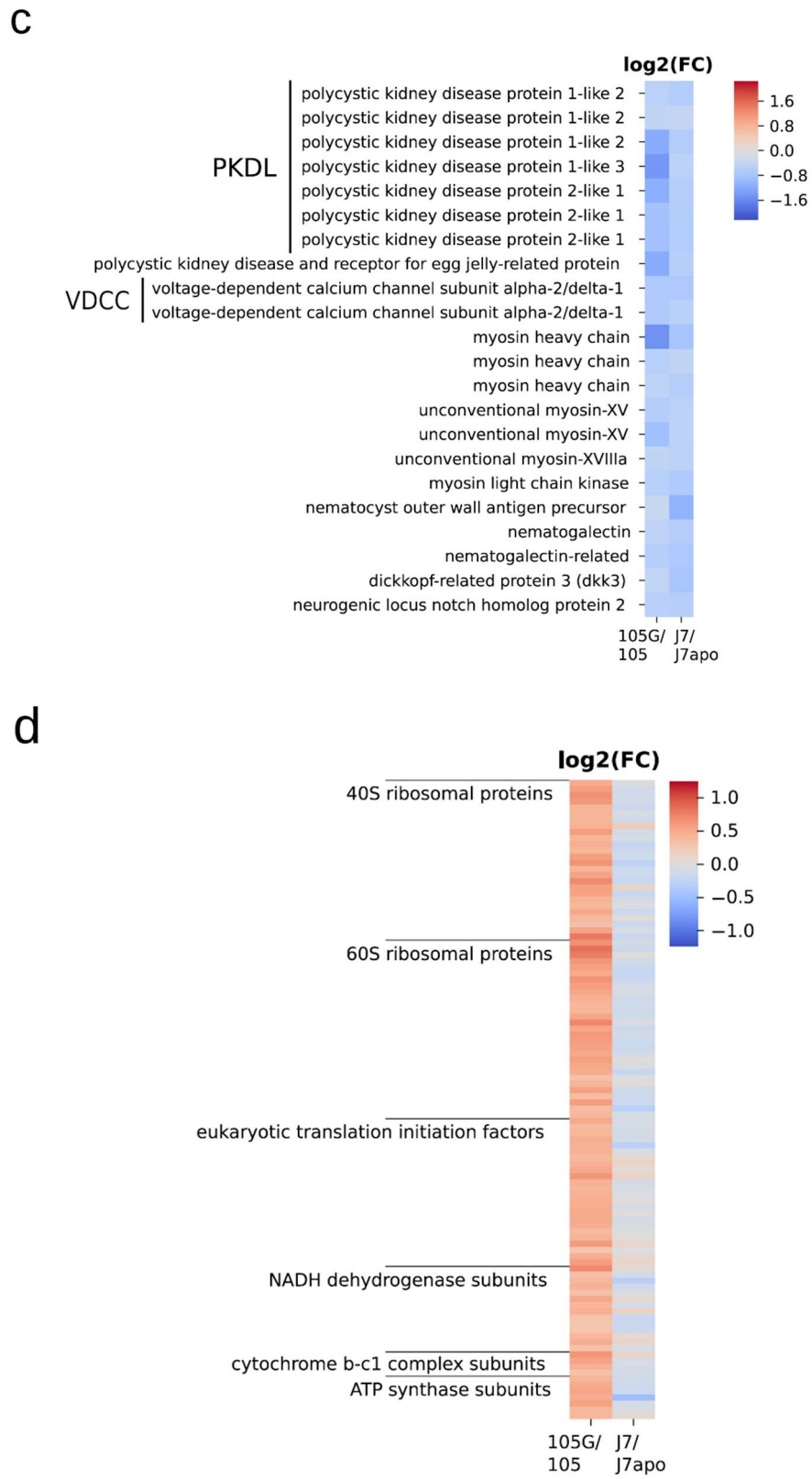

Figure 2.4 Comparison of the gene expression patterns in the 105G/105 and J7/J7apo pairs. (The figure legend is written on the next page.)

Figure 2.4 Comparison of the gene expression patterns in the 105G/105 and J7/J7apo pairs. (**a**) Venn diagram showing the number of differentially expressed genes (DEGs) in both strain pairs with the frag-bias-correct option (FDR < 0.05). The numbers of upregulated genes by symbiosis are indicated in red, and the numbers of downregulated genes by symbiosis are indicated in blue. (**b**) Heat map showing log2 fold change of the FPKMs (fragments per kilobase of exon per million mapped reads) of the upregulated genes coding lysosomal enzymes in both strain pairs. (**c**) Heat map showing log2 fold change of the FPKMs of the downregulated genes expressed in nematocytes or playing a role in nematocyte differentiation in both strain pairs. (**d**) Heat map showing log2 fold change of the FPKMs of the upregulated genes coding the genes related to translation and respiratory chain complex in the 105G/105 strain pair.

Table 2.4 Enriched GO terms in the downregulated genes in strain J7.

Category	Term	Count	Pop Hits	Fold Enrichment	q-value
CC	extracellular region	27	182	3.03	1.35E-04
MF	calcium ion binding	31	227	2.74	2.20E-04
MF	carbohydrate binding	13	60	4.35	0.0058629
CC	integral component of membrane	91	1282	1.45	0.00600012
CC	proteinaceous extracellular matrix	13	74	3.59	0.01747669

Table 2.5 Common remarkably differentially expressed genes (DEGs) in 105G/105 and J7/J7apo pairs.

105G > 105 and J7 > J7Apo

Product	Entrez gene id	FPKM(105G)	FPKM(105)	log2(FC) 105G	FPKM(J7)	FPKM(J7Apo)	log2(FC) J7
L-rhamnose-binding lectin CSL3-like	105848632	7226.29	29.88	7.92	120.56	0.96	6.97
melatonin receptor type 1C-like	105848483	31.23	11.09	1.49	8.88	0.43	4.36
ferric-chelate reductase 1-like	100199865	196.76	27.09	2.86	81.96	11.45	2.84
endochitinase 1-like	100197260	60.53	25.29	1.26	478.37	110.85	2.11
carbonic anhydrase 2-like	101238382	25.87	6.45	2.00	26.13	6.80	1.94
NEDD8-conjugating enzyme ubc12-like	100198375	317.73	83.44	1.93	109.03	31.74	1.78
arrestin domain-containing protein 3-like	100202511	15.57	3.12	2.32	27.16	7.98	1.77
probable G-protein coupled receptor 112	101237689	50.26	22.06	1.19	59.83	17.88	1.74
putative nuclease HARBI1	100200118	293.97	88.66	1.73	24.77	7.62	1.70
G-protein coupled receptor 64-like	101237777	54.59	22.83	1.26	57.20	17.74	1.69
probable caffeoyl-CoA O-methyltransferase 2	100213913	493.92	76.72	2.69	108.20	35.55	1.61
endochitinase 4-like	100199839	42.05	12.79	1.72	27.01	10.35	1.38
gastric triacylglycerol lipase-like	100208269	12.75	5.00	1.35	37.74	15.76	1.26
excitatory amino acid transporter-like	100201274	102.82	28.73	1.84	85.26	36.82	1.21
D-galactoside-specific lectin-like	100209558	757.25	287.99	1.39	639.57	291.22	1.14

105G < 105 and J7 < J7Apo

Product	Entrez gene id	FPKM(105G)	FPKM(105)	log2(FC) 105G	FPKM(J7)	FPKM(J7Apo)	log2(FC) J7
carbonic anhydrase 7-like	100200368	51.65	121.30	-1.23	9.88	27.83	-1.49
fibrocystin-L-like	105847347	4.07	8.32	-1.03	2.66	5.60	-1.07

Table 2.6. The number of the upregulated genes with GO term translation in the symbiotic strains 105G and J7. The numbers of upregulated genes in each strain were shown in UP columns.

Gene group	UP(105G)	UP(J7)	Total
Ribosomal protein	55	0	76
Translation initiation factor	24	0	51
NADH dehydrogenase	14	0	30
Cytochrome b-c1 complex	4	0	5
ATP synthase	7	0	12

the symbiotic state of the native symbiotic strain J7. Calcium ion binding and integral component of membrane appeared in the enriched GO term in the downregulated genes in both 105G and J7 strains (Tables 2.3 and 2.5, respectively).

2.3.4 Effect of translation inhibition with rapamycin treatment

I hypothesized that the upregulations of the genes related to translation and metabolism were necessary to maintain the symbiotic system between strain 105G and the chlorococci. Therefore, I treated polyps with rapamycin to inhibit TORC1 activity (Loewith et al., 2002), which regulates translation and metabolism in host cells based on the nutrient input by symbionts (Voss et al., 2019). Previous studies in *Hydra* reported that short-term exposure to rapamycin (12 h, 10 μM) reduces polyp size (Buzgariu et al., 2008) and that long-term exposure to rapamycin (>30 days, 0.8 μM) delays aging and improves epithelial proliferation in a strain that senesces upon gametogenesis (Tomczyk et al., 2020). I exposed 10 non-symbiotic and symbiotic polyps of the 105, 105G, J7apo, and J7 strains to rapamycin for two weeks with five replicates. Most of the polyps exposed to rapamycin shrank and shortened their tentacles, and some of the polyps totally contracted (Fig. 2.5a). Exposure to rapamycin largely inhibited budding. In particular, budding of the polyps in 3 μM rapamycin was not observed in strains other than J7apo. Fig. 2.5b shows the changes in the number of polyps for each experimental condition two weeks after the start of the treatment, and transitions in the number of polyps for each condition during the treatment are shown in Fig. 2.6. Polyps for each strain in the control condition gradually proliferated by budding (105: 15.4 ± 1.91; 105G: 12.4 ± 0.51; J7apo: 13.2 ± 0.58; J7: 10.4 ± 0.40, means ± SEM). The J7 strain formed buds slowly due to its relatively large polyps. The rapamycin treatment prevented the polyps of the 105 strain from budding (105 [1 μM]: 9.4 ± 0.24; 105 [3 μM]: 9.0 ± 0.45). The polyps of the J7apo strain could generate their buds under the rapamycin treatment, but the increase in the polyps was still suppressed (J7apo [1 μM]: 10.4 ± 0.51; J7apo [3 μM]: 9.8 ± 0.20). On the other hand, the polyps of the 105G strain were severely affected by rapamycin treatment. More than half of the polyps degenerated under both 1 and 3 μM rapamycin (105G [1 μM]: 4.0 ± 0.84; 105G [3 μM]: 3.2 ±

0.86). The polyps of the J7 strain showed an intermediate-severe response to rapamycin treatment, falling between the 105 and 105G strains. Rapamycin at 1 μM impeded budding in the J7 strain, but most of the polyps survived during the treatment, similar to strain 105 (J7 [1 μM]: 8.2 ± 0.73). More than half of the polyps of the J7 strain died, similar to the 105G strain in 3 μM rapamycin (J7 [3 μM]: 4.4 ± 1.17).

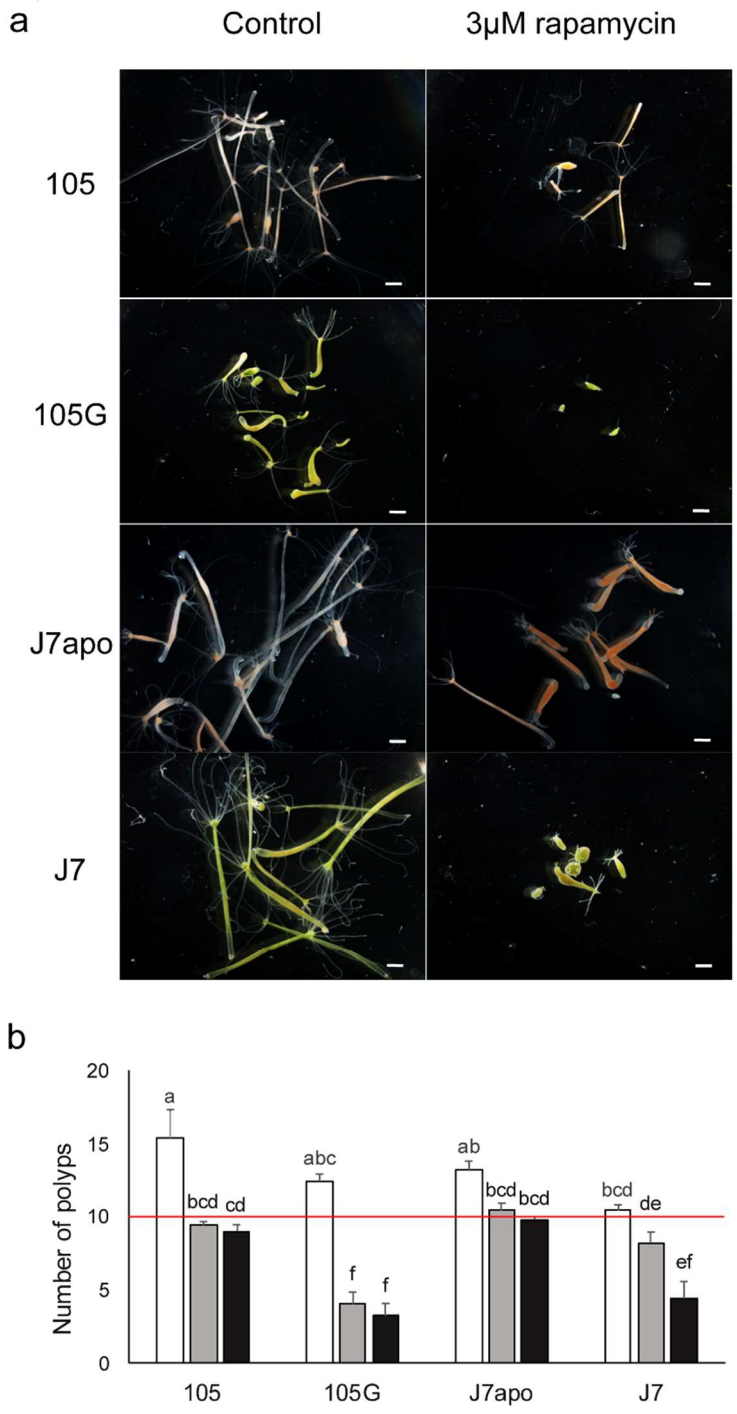

Figure 2.5 Effect of translation inhibition with rapamycin treatment. (**a**) The polyp condition two weeks after the start of rapamycin treatment. The symbiotic polyps (strain 105G, J7) shrank in 3 μM rapamycin. Scale bars: 1 mm. (**b**) The number of polyps two weeks after the start of rapamycin treatment. The error bars show the standard error in each condition. The red line represents the number of polyps (n = 10) at the start of the treatment. The significant differences were calculated by Tukey's test among each condition ($P < 0.05$). The same letters onthe bars represent no significant difference.

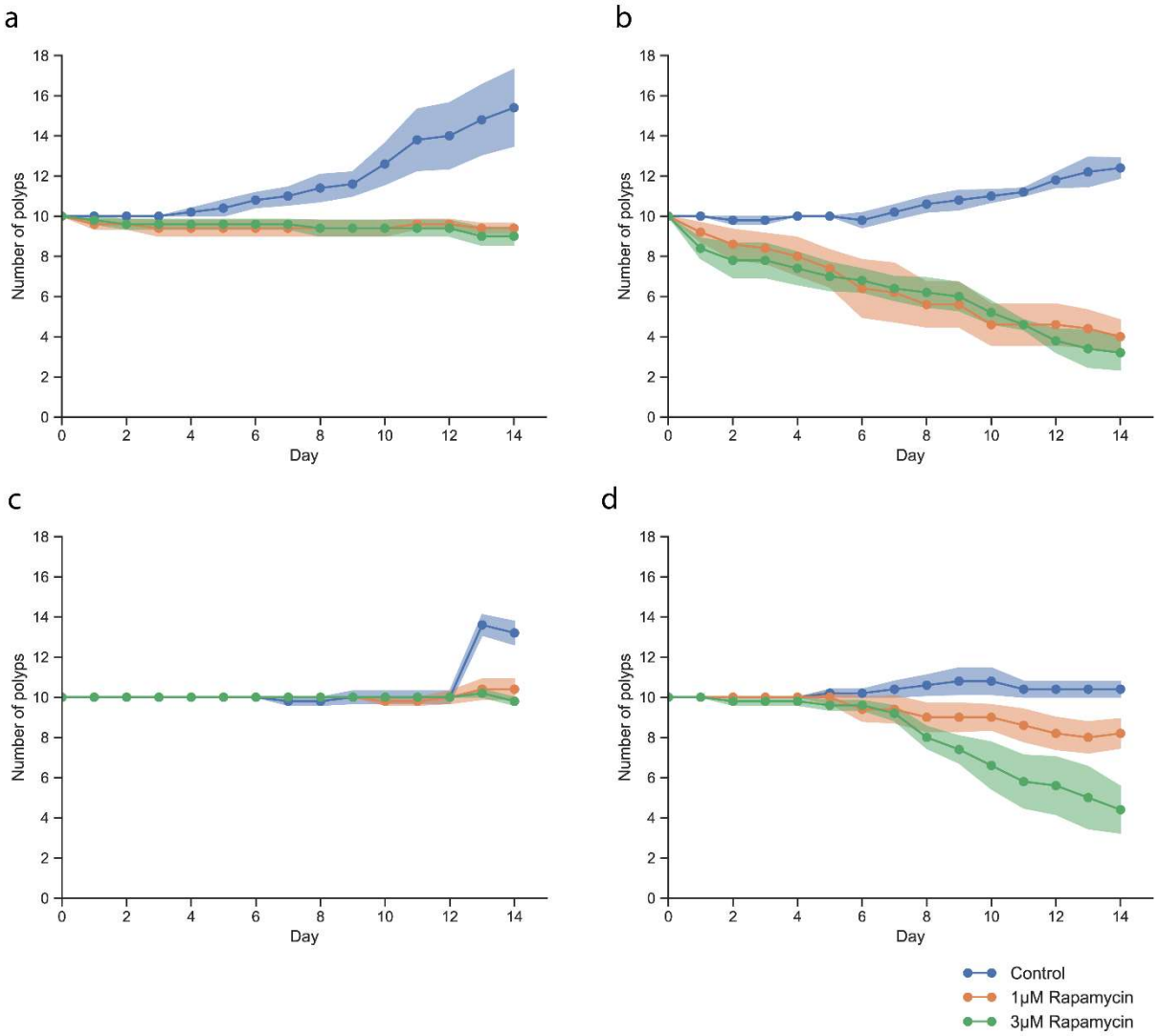

Figure 2.6 Transition in the number of polyps in the rapamycin treatment. Markers represent the average number of polyps, and filled areas represent standard errors. (a) strain 105. (b) strain 105G. (c) strain J7apo. (d) strain J7.

2.4 Discussion

2.4.1 Endosymbiosis of the chlorococcum with the brown hydra

The *rbcL* and 18S rDNA sequences were identical between the endosymbiotic chlorococcum and the alga in the HCS. It indicated that the symbiotic chlorococcum was released from hydra cells to HCS. The chlorococcum may form the zoospores observed in the HCS, and ingestion of the non-flagellated algae or zoospore by a non-symbiotic hydra enables to establish the new symbiotic relationship between the hydra and the chlorococcum. This horizontal transmission was confirmed by the observation that non-symbiotic polyps with co-cultured J10 strain polyps acquired the symbiotic chlorococci (Miyokawa et al., 2018). The large flagellated algae were also found in HCS. Culturing and sequencing these algae revealed that the ones were identical to *P. malhamensi*s. *P. malhamensi*s is a universally distributed mixotrophic golden alga and so the mixotrophic algae are a predator of small algae such as chlorellae (Ma et al., 2018), and so the chlorococcum-like algae in the flagellated algae cells had been eaten by *P. malhamensi*s. In a small ecosystem around hydra in nature, it is suggested that some of the chlorococcum escaped from the host hydra cells are preyed on by predators like *P. malhamensi*s. The endosymbiosis with the hydra can protect the chlorococcum from such a predator. The symbiotic hydra is rarely seen in the wild (Slobodkin et al., 1991). The authors explain that this is because the symbiosis between the brown hydra and the chlorococcum is not stable. However, the finding of the existence of predators raised the probability that the predators may be a factor preventing the horizontal transmission.

My phylogenetic analysis showed that the symbiotic chlorococcum was included in the Stephanosphaerinia clade and that belonged to the same clade as *Oophila* spp., which are symbiotic algae with salamanders. The phylogeny of *Oophila* was consistent with the previous phylogenetic analysis in Nema et al. (2019) and Schultz (2016), and the chlorococcum and *Oophila* spp. did not form a sister group. It suggests that these algae have independently evolved the symbiosis with animals. Symbiotic chlorellae with *H. viridissima* have a common

feature that can tolerate low pH, but the symbioses were evolved independently (Huss et al., 1994; Kawaida et al., 2013). These phylogenetic analyses suggest that green algae which include symbiotic algae in their group are considered to have the potential for symbiosis beforehand. On the other hand, some strains of host *Hydra*, other than *H. vulgaris*, have a potential for harboring the symbiotic chlorococcum (Miyokawa et al., 2018). This paper reports that a part of strains in all four groups of *Hydra* maintained the symbiotic relationship with the chlorococcum for more than two months. The genus *Hydra* also contains *H. viridissima*, mutualistic hydra species with *Chlorella*. *Hydra* seems to widely have the potential for establishing a symbiotic relationship with green algae. Interaction between such hosts and symbionts having the potential for symbiosis might lead to establishing endosymbiosis.

2.4.2 Cellular mechanisms in *Hydra-Chlorococcum* symbiosis

The acquired symbiotic strain, 105G, exhibits a decreased polyp size compared with the original strain, 105 (Miyokawa et al., 2018). A significant difference in the size of endodermal epithelial cells was not observed between strains 105G and 105 (P = 0.789, Table 2.7). Mortzfeld et al. (2019) suggested that the maximum polyp size of *Hydra* is primarily determined by the number of cells, not the size of the cells, in a polyp. The authors showed that Wnt signaling activates TGF-β signaling, that TGF-β signaling initiates budding and that polyp size growth stops when budding begins (Mortzfeld et al., 2019). In strain 105G, several genes in the Wnt pathway were differentially expressed (Fig. 2.7). Downstream of the Wnt pathway, transcription factor 7-like 2 (TCF/LEF) activates transcription by forming a complex that binds to β-catenin (Molenaar et al., 1996). Wnt and TCF/LEF are co-expressed in hydra heads and induce bud initiation and head formation (Hobmayer et al., 2000; Gee et al., 2010). Therefore, an expression change of TCF/LEF can fluctuate the time of bud initiation and the developmental time of a polyp. The serine/threonine-protein kinase NLK inhibits the binding of TCF/LEF to DNA and suppresses transcription activation by TCF/LEF (Ishitani et al., 1999). In the acquired symbiotic strain 105G, TCF/LEF was upregulated, and NLK was downregulated (Fig. 2.7). This result indicates that transcription stimulated by TCF/LEF is

Table 2.7 Sizes of endodermal epithelial cells in strains 105G and 105. Five polyps were measured for both strains, and 100 cells were measured for each polyp. Cell sizes between the strains were tested by Welch's t-test.

	105		105G	
Polyp	Mean	S.E.	Mean	S.E.
1	60.56	1.16	57.22	1.00
2	58.07	0.91	60.33	0.86
3	61.67	0.53	55.37	0.56
4	57.11	0.76	60.19	0.84
5	56.96	0.69	63.44	0.80
6	59.89	0.93	58.52	1.02
Total	59.04	8.69	59.18	8.92

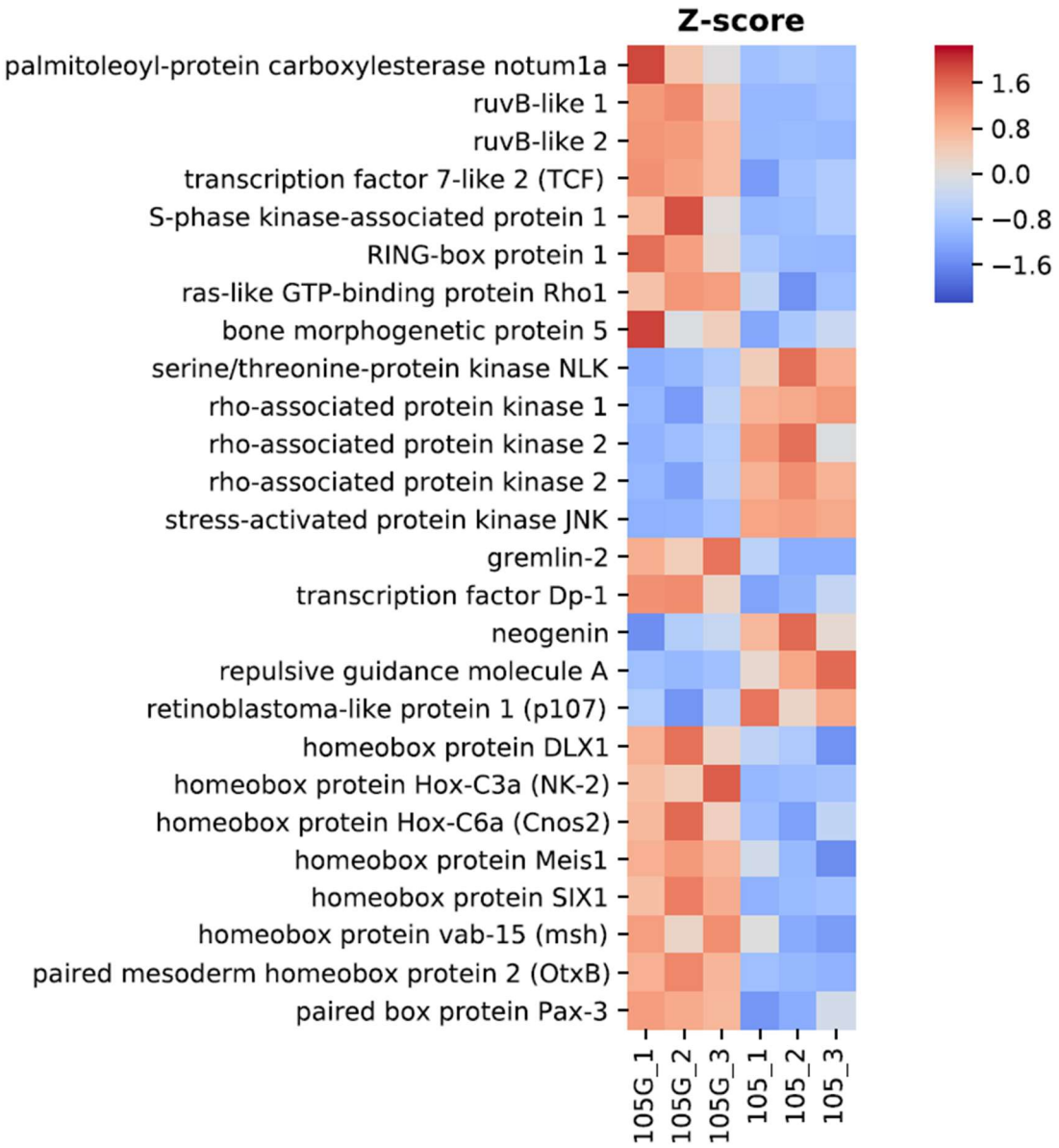

Figure 2.7 Heat map showing gene expression patterns involved in the Wnt pathway and homeobox genes in strains 105G and 105. The Z-scores are calculated from the FPKMs of each gene. The displayed expressions are selected notable genes' (FDR < 0.05).

activated in the acquired symbiotic hydra. TGF-β signaling causes retinoblastoma-like protein 1 (p107) and transcription factor Dp-1 to regulate the transcription activity of transcription factor E2F. E2F activity is inhibited by p107, and this protein is formed by the dimerization of E2F and Dp-1 (Zhu et al., 1993; Helin et al., 1993). p107 was downregulated, and Dp-1 was upregulated, in strain 105G (Fig. 2.7). This result indicates that transcription of E2F is also activated in strain 105G. Furthermore, I investigated the upregulation of the homeobox genes, which are also transcription factors, as other factors that may alter polyp size. Dlx1 and NK-2 are homeobox genes that are expressed in the foot in *Hydra*. Dlx1 is upregulated during foot formation in ectodermal cells (Wenger et al., 2016; Wenger et al., 2019). NK-2 is expressed in endodermal epithelial cells before foot formation (Grens et al., 1996). These homeobox genes are activated by Wnt/β-catenin signaling, as well as TCF/LEF, and regulate targeted genes (Reddy et al., 2019). Wnt signaling might activate the initiation and development of budding via these transcription factors. Paired mesoderm homeobox protein 2 (OtxB) is another homeobox gene that was observed to be upregulated in strain 105G (Fig. 2.7) and expressed in endodermal cells according to single-cell RNA-seq data from *Hydra* (Siebert et al., 2019). OtxB is a close homolog to three Otx genes in *Nematostella vectensis*. The Otx genes in *N. vectensis* are expressed in the endoderm of the foot and pharynx and the ectoderm of the tentacle and are involved in endodermal development and patterning (Mazza et al., 2007). OtxB might be involved in endodermal development according to the function of homologous genes. The upregulation of the transcription factors TCF/LEF, Dlx1, and NK-2 suggests that the horizontal transmission of chlorococci to hydra activates transcription by TCF/LEF and homeobox genes, and the decrease in polyp sizes and the increase in asexual reproduction rates in the acquired symbiotic strain 105G may depend on these expression changes. However, it remains unclear how these transcription factors control bud development by Wnt signaling.

I looked for common DEGs in the symbiotic strains 105G and J7. The genes encoding lysosomal enzymes were commonly upregulated in the symbiotic strains 105G and J7 (Fig. 2.4b). In *H. viridissima*, most of the symbiotic algae are digested in host lysosomes during

infection (McNeil and McAuley, 1984), and the symbiotic algae are digested in the host cells to maintain the number of algal cells (Dunn, 1987). These algal cells can be digested inside enveloped vacuoles by lysosomal enzymes. Similarly, the upregulation of the lysosomal enzymes in the symbiotic *H. vulgaris* could be responsible for the digestion of the symbiotic chlorococci, suggesting that symbiotic *H. vulgaris* may have the potential to employ their lysosomes to digest the symbionts as a resource and/or to maintain a constant cell density of the symbionts in the host cells. I found gene expression changes in strain 105G in the endocytosis and phagocytosis pathways in the KEGG pathway (Fig. 2.8). The neural Wiskott-Aldrich syndrome protein (N-WASP) and the actin-related protein 2/3 complex (Arp2/3) complex play essential roles in the polymerization of actin filament in clathrin-coated endocytosis and phagocytosis (May et al., 2000; Merrifield et al., 2004). Rab7 induces fusion of late endosomes and phagosomes with lysosomes in the presence of damaged symbionts in *Aiptasia* (Chen et al., 2003). The upregulation of N-WASP, Arp2/3, and Rab7 may be involved in the uptake of symbionts by phagocytosis and the maintenance of the number of symbionts in host cells.

The two RBL family genes were also largely upregulated in common in the symbiotic strains 105G and J7 (Table 2.5). RBLs play a role in innate immune recognition to bind L-rhamnose and D-galactose resides in polysaccharides and induce an increase in phagocytic activity (Watanabe et al., 2009; Ogawa et al., 2011). In the stony coral *Pocillopora damicornis*, RBL recognizes both pathogenic bacteria and symbiotic algae to bind polysaccharides on cell wall surfaces (Zhou et al., 2017). Galactose is among the major components of cell walls in *Chlorococcum*, and the cell walls also contain some rhamnose (Miller, 1978), and the symbiotic *Chlorococcum* is agglutinated under the influence of a galactose binding lectin (Reich and Greenblatt, 1992). If RBLs can bind to polysaccharides on cell surfaces of the symbiotic chlorococci and be related to the recognition and uptake of the endosymbionts in *H. vulgaris*, it is possible that the upregulation of the genes in the pathway from phagocytosis to lysosome reflects host reactions to the presence of the symbionts.

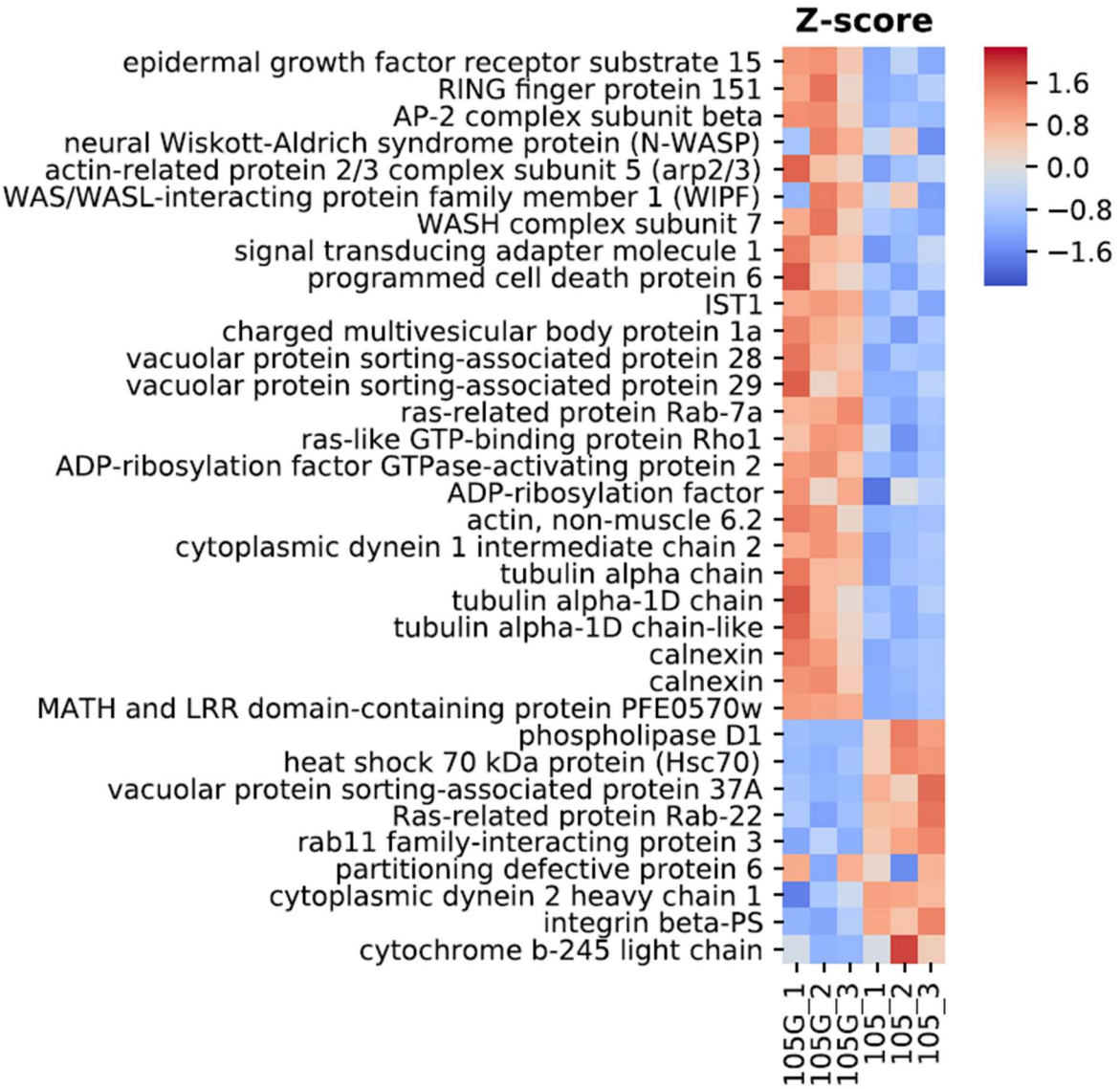

Figure 2.8 Heat map showing gene expression patterns involved in endocytosis and phagocytosis pathways in strains 105G and 105. The Z-scores are calculated from the FPKMs of each gene. The displayed expressions are selected notable genes' (FDR < 0.05).

Next, I found commonly downregulated genes in the symbiotic strains 105G and J7. Polycystic kidney disease proteins (PKDLs) and voltage-dependent calcium channels (VDCCs) were observed to be commonly downregulated in the 105G and J7 strains (Fig. 2.4c). PKDLs are non-selective cation channels that have permeability to Ca^{2+} (Chen et al., 1999), while VDCCs are voltage-gated ion channels with selective permeability to Ca^{2+} (Catterall, 2011), and these products are localized in the plasma membrane according to the Uniprot annotation. PKDLs belong to the polycystin cation channel family and have sequences similar to those of other polycystins. Ishikawa et al. (2016b) proposed the hypothesis of Ca^{2+} homeostasis disruption due to the inhibition of genes related to polycystin in endodermal cells with symbionts. However, most DEGs coding VDCCs and related to polycystins, such as PKDLs, are expressed in nematocytes according to single-cell RNA-seq data from *Hydra* (Siebert et al., 2019). Polycystins and VDCCs were confirmed to be involved in nematocyst discharge (McLaughlim, 2017; Gitter et al., 1994). The downregulation of these calcium ion channel genes in symbiotic states is probably due to changes in nematocytes, rather than disruption of calcium homeostasis, in endodermal cells containing symbionts. In fact, the stenoteles, which are the largest types of nematocysts, in strain 105G are smaller than the stenoteles in the original non-symbiotic strain 105, and the number of stenoteles per tentacle and the length of tentacles were decreased in strain 105G (Miyokawa et al., 2018). In addition, myosins and nematogalectins were downregulated in the 105G and J7 strains (Fig. 2.4c). These myosins and nematogalectins were mainly expressed in nematocytes and battery cells and nematoblasts, respectively, according to the single-cell RNA-seq data of *Hydra* (Siebert et al., 2019). These proteins play important roles in nematocyst maturation (Beckmann and Özbek, 2012; Beckmann, 2013). The downregulation of the genes expressed in nematoblasts and nematocytes in the 105G strain is consistent with Miyokawa et al. (2018), which reported the reduction in stenotele size and count in this strain. This inhibition of nematocyte development and the reduction in stenotele size and count may cause a decrease in prey capture ability in the 105G strain. The report comparing the asexual reproduction rate and the polyp size between strain 105G and 105 in Miyokawa et al. (2018) says that the 105G strain showed an increase

in the asexual reproduction rate under the high-light condition and that the polyp size of strain 105G was observed to be reduced compared to that of strain 105. The increase in the asexual reproduction rate suggests that the photosynthetic products of symbionts are transported to host endodermal cells and are used as nutrients. The photosynthetic products may make up for the decrease in the ability to catch prey. As the reduction of the polyp size, however, it has not been determined whether the symbiotic chlorococcum could supply sufficient nutrients to their host.

Ishikawa et al. (2016b) proposed that the instability of the symbiosis in strain J7 was derived from the downregulation of gene expression related to cell adhesion molecules. In this study, coadhesin, zonadhesin, protocadherin (Fat cadherin), and protocadherin-like proteins (Fat-like cadherin) were downregulated in the symbiotic strains 105G and J7 (Fig. 2.9). Fat and Fat-like cadherin are transmembrane proteins with structures that are evolutionarily conserved from cnidarians to mammals and are involved in tissue growth and planar cell polarity in the adherens junctions (Magie and Martindale, 2008; Hulpiau and Van Roy, 2011). These cadherin genes were mainly expressed in the battery cells according to the single-cell RNA-seq data of *Hydra* (Siebert et al., 2019). Battery cells surround such nematocytes as stenoteles and play a role in docking sites of nematocyst vesicles to anchor the nematocytes to the basement membrane on tentacles (Hufnagel et al., 1985; Hobmayer et al., 1990). Nematocytes are bound to battery cells by adherens junctions (Campbell, 1987b), where Fat and Fat-like cadherin are located. The downregulation of Fat and Fat-like cadherin might reflect the reduction of adherens junctions as a reduction in stenotele size and count due to symbiosis.

2.4.3 Difference in adaptation to symbiosis between 105G strain and J7 strain

In the differential gene expression analysis for 105G/105, the genes assigned to the GO terms translation, mitochondrion, and oxidation-reduction process were upregulated. This result was different from that of another symbiotic organism in the previous study. In host organisms that have green algae as endosymbionts, namely, *H. viridissima* and *Paramecium bursaria*, translation is the enriched GO term in downregulated genes in the symbiotic state

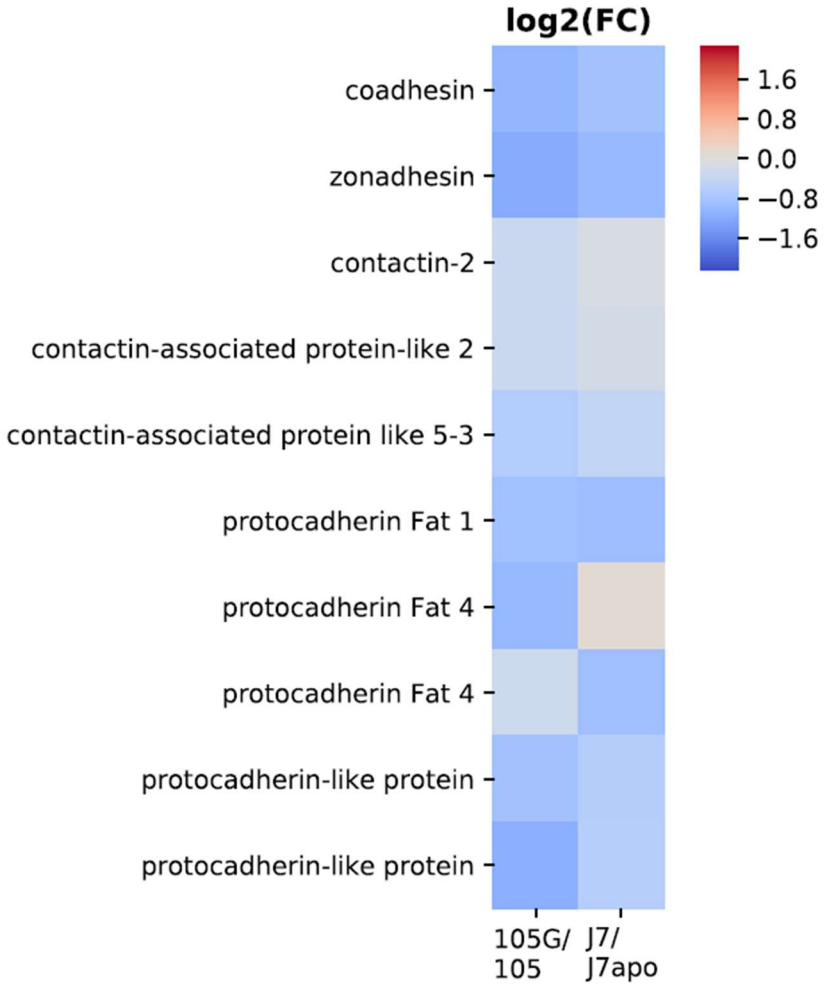

Figure 2.9. Heat map showing fold changes of genes involved in cell adhesion in 105G/105 and J7/J7apo pairs. The fold changes are calculated from the FPKMs of each strain pair. The displayed expressions are selected notable genes' (FDR < 0.05).

(Kodama et al., 2014; Ishikawa et al., 2016b). Ishikawa et al. (2016b) interpreted that the respiratory chain process in *H. viridissima* cells is inactivated to suppress the generation of harmful reactive oxygen species (ROS). Furthermore, Kodama et al. (2014) demonstrated that protein biosynthesis in *P. bursaria* cells is controlled by substance exchange between the hosts and the symbionts. In these well-established symbioses, it is suggested that cooperative biosynthesis and/or substance exchange between the host cells and the symbiont algae have been established. The increase in metabolic activity may be a physiological phenomenon due to increased oxygen and/or nutrient supply by the symbionts, and the cooperative and adaptive responses to the symbionts may not have yet occurred in the newly formed symbiotic strain 105G.

Translation and mitochondrial activity reciprocally interact and control energy balance in cells through ATP production and consumption (Morita et al., 2013). The difference in the patterns of expression changes of translation and respiratory chain complexes between the 105G and J7 strains may reflect different levels of cellular energy production and the changes in substance exchanges between the hosts and the symbionts. Nutritional signals activate TOR complex 1 (TORC1) via the TOR pathway, which is a pathway that is conserved from yeast to mammals (Panchaud et al., 2013). In the 105G strain, some genes in the TOR pathway, such as ras-related GTP-binding proteins (rag GTPases: ragA/B, ragC/D) and LAMTOR2, were upregulated (Fig. 2.10). LAMTOR2 is a part of the regulator complex and composes a binding platform to the rag GTPase (Su et al., 2017), and Rag GTPases bind to the regulator complex and activate TORC1 in response to the amino acid signal from lysosomes (Bar-Peled et al., 2012; Kim et al., 2008). TORC1 activation induces translation activity, including ribosome biogenesis, and inhibits autophagy (Hay and Sonenberg, 2004). In the symbiotic sea anemone *Aiptasia*, amino acids synthesized by symbiotic algae from photosynthetic products are translocated to host cells (Wang and Douglas, 1999), and Voss et al. (2019) reported that nutrients from symbionts activate TORC1 signaling and that signaling prompts translation and metabolism in the host cell. However, the authors reported that genes related to lysosomes and

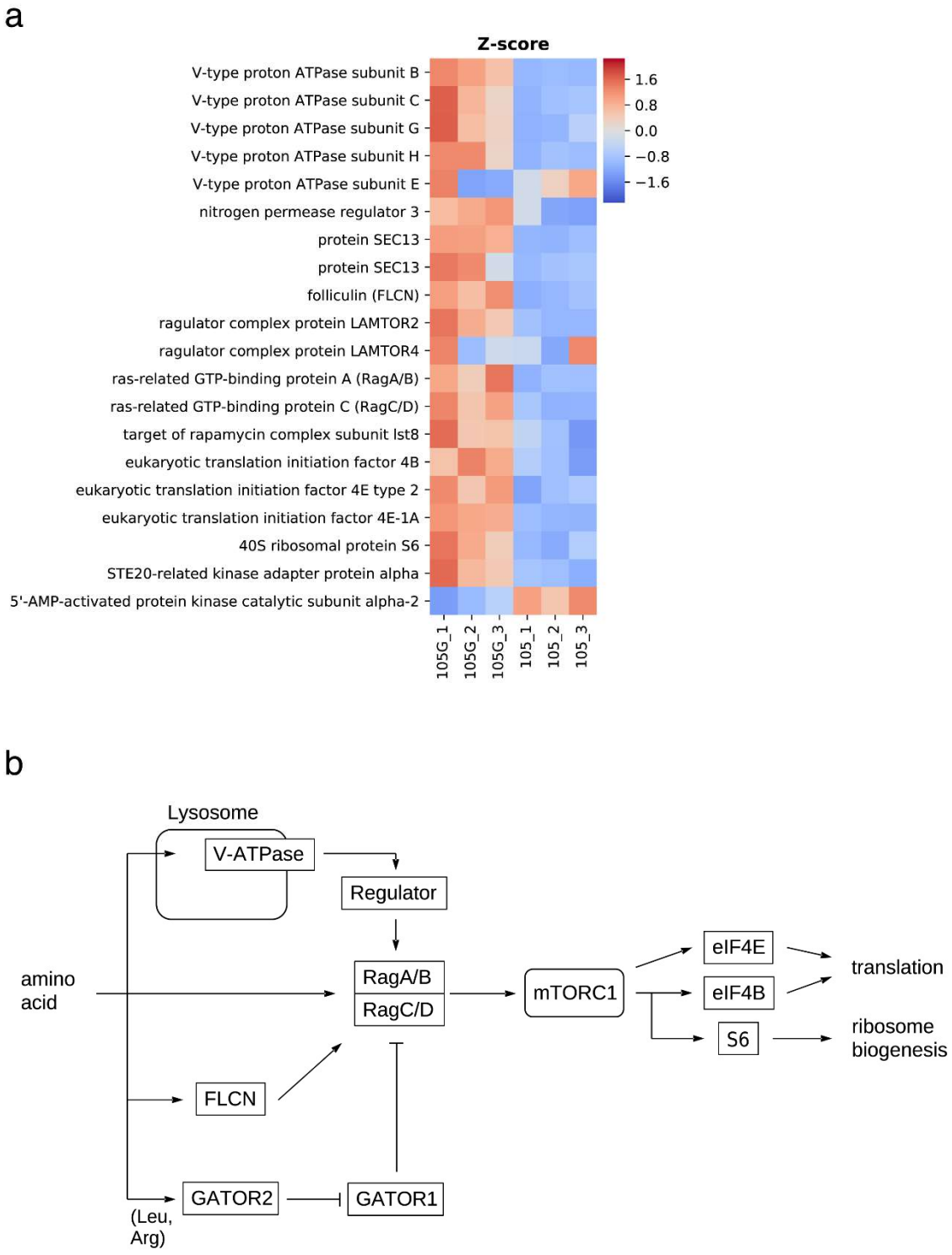

Figure 2.10. Gene expression changes involved in the TOR pathway. (**a**) Heat map showing the expression patterns of the genes in strains 105G and 105. The Z-scores are calculated from the FPKMs of each gene. The displayed expressions are selected notable genes' (FDR < 0.05). (**b**) Overview of the TOR pathway based on DEGs in strain 105G. Genes enclosed in squares represent upregulated genes in strain 105G.

translation are downregulated in symbiotic *Aiptasia*, similar to the symbiotic organisms mentioned above, (*H. viridissima*: Ishikawa et al., 2016b; *P. bursaria*: Kodama et al., 2014). This finding implies that there are other systems to inhibit translation and cellular metabolism in stable symbiotic organisms, while *H. vulgaris* may not have these systems. Alternatively, the symbiotic *H. vulgaris* might have a reason not to inhibit translation activity to maintain the symbiosis. *Chlorococcum* can use peptone, which is an enzyme digest of animal protein containing amino acids, as a nitrogen source, as well as other general nitrogen sources (Liu et al., 2000). If the symbiotic chlorococci take up amino acids from the host cells, ignoring the metabolic needs of the host, the host will have to pay the cost of synthesizing additional amino acids. Several enzymes synthesizing amino acids and involved in the TCA cycle, which generates precursors of amino acids, were upregulated in the 105G strain (Fig. 2.11). Thus, the effect on cellular metabolism caused by endosymbiosis would be different between the 105G and J7 strains and stable symbiotic organisms.

I conducted the rapamycin experiment to elucidate the upregulations of the genes related to translation and metabolism were necessary to maintain the symbiotic system in the 105G strain. This result is shown in Fig. 2.12. About half of the symbiotic polyps degenerated in 3 μM rapamycin, and it indicates that 3 μM rapamycin was more harmful to the symbiotic strains (105G, J7) than the non-symbiotic strain (105, J7apo). The treatment with 1 μM rapamycin showed that the threshold concentrations of rapamycin for definite mortality increase were lower in the 105G strain than in the J7 strain. The results showed that symbiosis with chlorococci alters the sensitivity to inhibitors of translation in the host cell. In addition, the degree of sensitivity was greater in the 105G strain than in the J7 strain. These results suggested that the J7 strain has an adaptive mechanism to balance the cellular metabolism of hosts and chlorococci, which does not exist in the 105G strain. Indeed, the J7 strain did not show significant expression changes in the genes related to translation between the non-symbiotic and symbiotic strains, despite drastic changes in the host cell environment. The difference in the sensitivity to rapamycin treatment between the acquired symbiotic strain 105G and the

native symbiotic strain J7 may imply that the evolution of the ability to balance cellular metabolism between the host and the symbiont is a key requirement for adaptation to endosymbiosis with chlorococci.

This study provided an overview of the symbiotic system in *H. vulgaris* from the changes in the gene expression patterns. In the symbiotic strains 105G and J7, similar gene expression patterns were found in genes related to uptake and maintenance of the symbionts, nematocyte differentiation, and development (Fig. 2.12a). These expression patterns indicate that these processes are likely to be essential mechanisms of brown hydra-chlorococcum symbiosis. On the other hand, the genes involved in translation and respiration were determined to be upregulated only in the acquired symbiotic strain 105G (Fig. 2.12b). I also observed a difference between the non-symbiotic strain and the symbiotic strains regarding mortality caused by translation inhibition through rapamycin treatment. The difference in mortality between the acquired symbiotic strain and the native symbiotic strain suggested that the native symbiotic strain was more adapted to endosymbiosis with *Chlorococcum* than the symbiotic strain acquired by horizontal transmission. Clarifying the unstable symbiotic mechanism may provide a better understanding of the evolution of symbiosis.

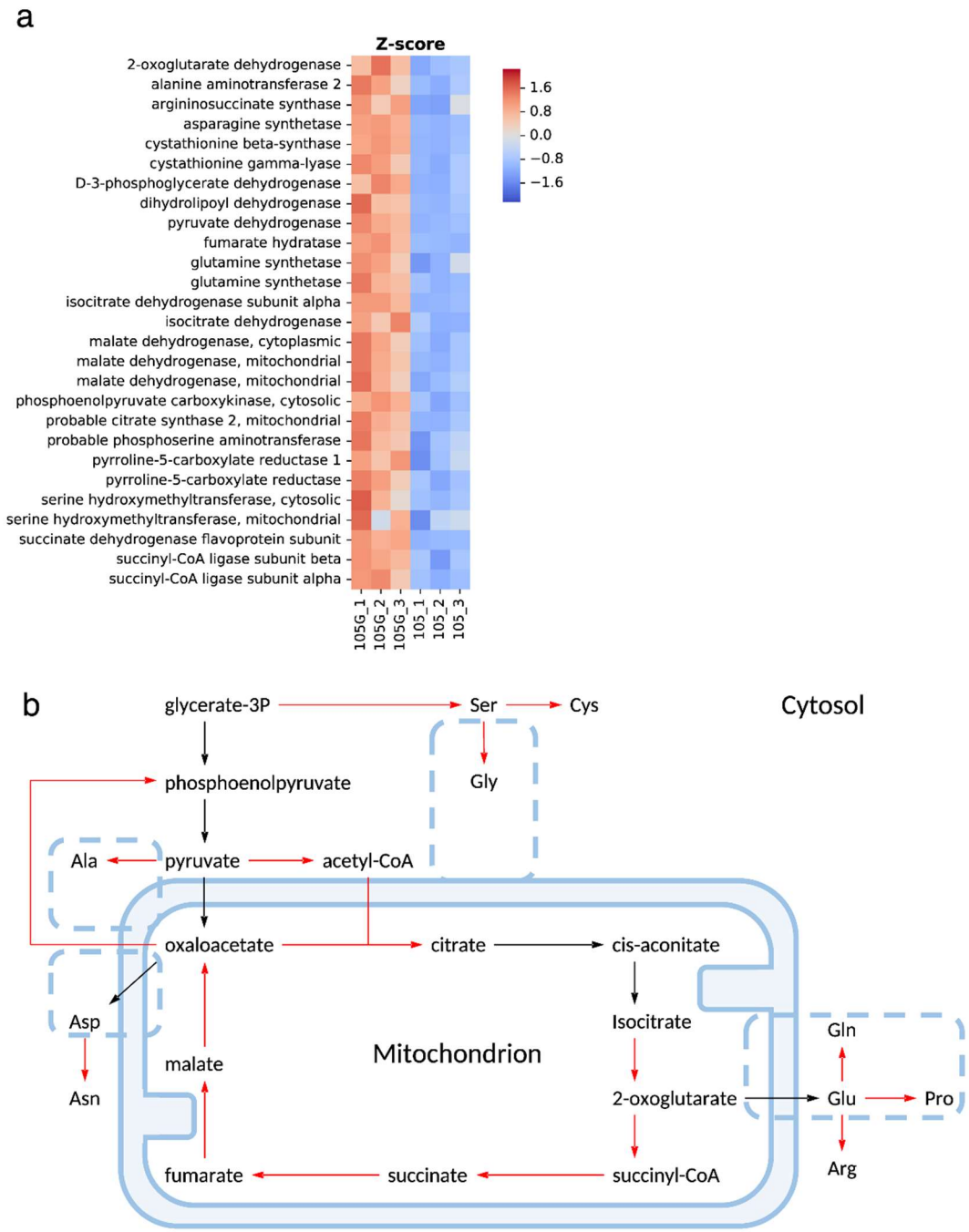

Figure 2.11. Expression changes in genes encoding enzymes that synthesize amino acids and are involved in the TCA cycle. (**a**) Heat map showing fold changes of the genes in strains 105G and 105. The Z-scores are calculated from the FPKMs of each gene (FDR < 0.05). (**b**) Overview of the TCA cycle and the pathway of amino acid synthesis based on DEGs in strain 105G. Red arrows represent enzymes coded in upregulated genes in strain 105G, and black arrows represent enzymes coded in genes not showing significant differences in strain 105G. Rounded rectangles with dashed lines show that amino acids inside the rectangles are synthesized in both mitochondria and cytosol.

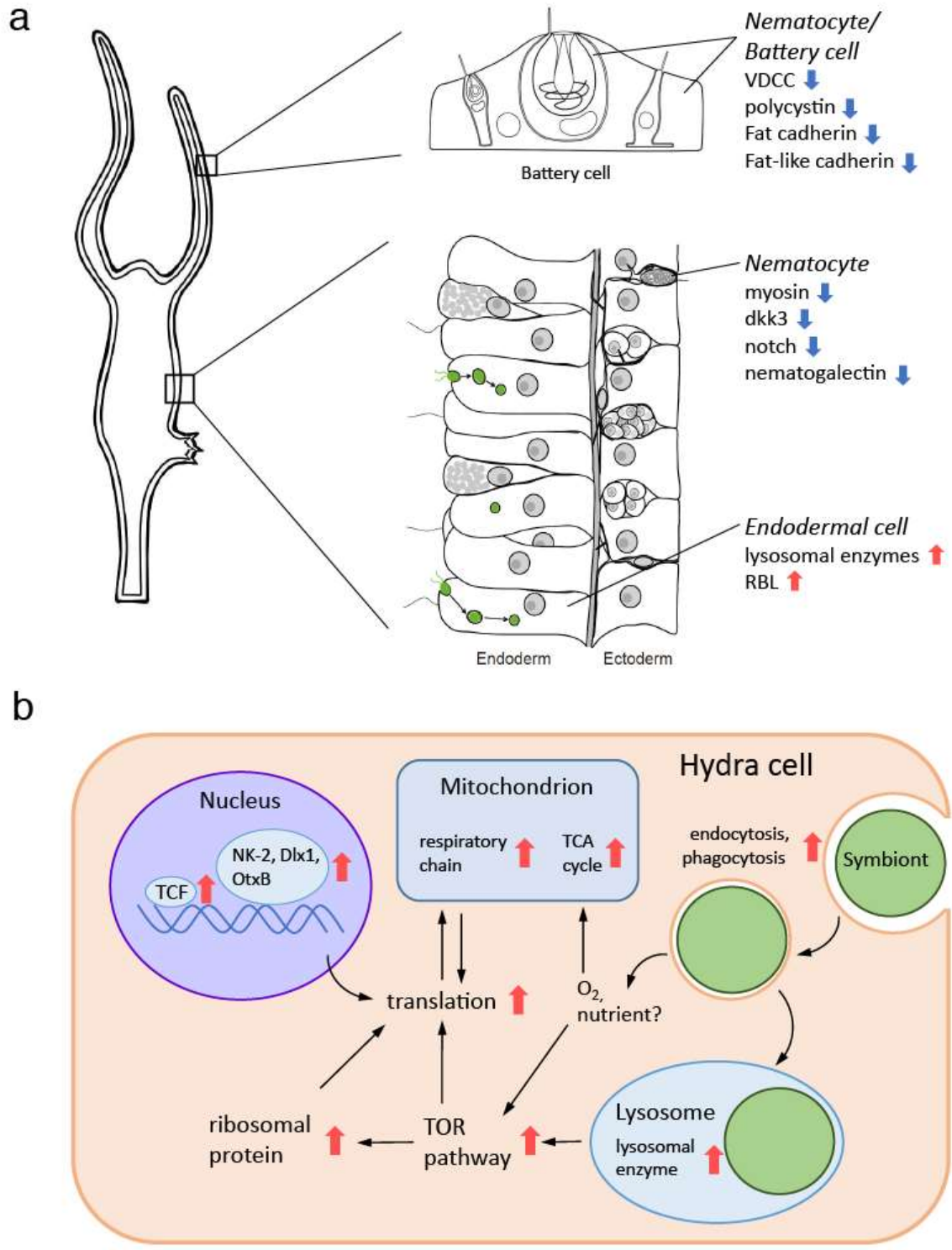

Figure 2.12. Summary of probable changes in the symbiotic hydra cells. The red arrows show the related genes that were upregulated, and the blue arrows show the related genes that were downregulated. (**a**) Common gene expression changes in symbiotic polyps in strains 105G and J7. (**b**) Cellular metabolism changes in strain 105G cells. The black arrows represent signaling and substance transmission.

CHAPTER 3

Gene expression patterns reveal specificity between green hydra and symbiotic chlorella

3.1 Introduction

Symbiosis is a long-term, close, and reciprocal biological interaction between multiple organisms (Douglas, 2015). Symbiosis enables organisms to adapt to new niches and diversify their lifestyle (Moran, 2007; Lengyel et al., 2009; Joy, 2013). Animal-plant symbiosis is a particular case of symbiosis: photosymbiosis. Photosymbiosis in animals is widespread across multiple taxa. In the photosymbiosis, hosts protect their symbionts from the symbionts' predators and environmental fluctuation, and the symbionts provide the hosts with nutrients derived from photosynthetic products (Melo Clavijo et al., 2018). Among the photosymbiotic systems in cnidaria (corals, sea anemones, and hydras) have been widely known to establish symbiotic relationships with zooxanthellae or green algae, and their symbioses have profound effects on their lifecycle and ecology (Muscatine and Lenhoff, 1963; Muscatine 1971; Muscatine and Porter, 1977). Among these symbiotic organisms, green hydra (*Hydra viridissima*) has an endosymbiotic relationship with green algae*, Chlorella,* and it is one of the best-studied symbiotic systems (Kovacevic 2012). *Hydra-Chlorella* symbiosis has been used as a suitable experimental organism for a long time because of its rapid reproduction time by budding and regeneration potential. Recently whole-genome sequences of the green hydra and its symbiotic chlorella have been determined (Hamada et al., 2018; Hamada et al., 2020). It enables us to perform functional genomic analysis. Green hydras bear the symbiotic chlorellae enveloped in membranes called symbiosome in the endodermal cells and provide the symbiotic chlorellae with carbon and nitrogen sources for photosynthesis and receive maltose produced by photosynthetic reactions (Muscatine and Lenhoff, 1963; Roffman and Lenhoff, 1969; Huss et al., 1994). This symbiotic interaction allows the host hydra to increase the proliferation rate by budding and tolerance to starvation (Ishikawa et al., 2016b). The symbiotic chlorella cannot survive outside the host cell for a long time and is transmitted vertically to a hydra offspring

by algal migration to a budding polyp and an egg (Habetha and Bosch, 2005; Kawaida et al., 2013). The molecular phylogenetic analysis of the hydra species indicated that the green hydra is a basal clade that diverged from other hydra species groups over 100 million years ago (Schwentner and Bosch, 2015). The green hydra seems to have acquired symbiosis with the chlorellae at the early stage of its evolution because all green hydras have symbiotic relationships with the chlorellae (Kawaida et al., 2013). On the other hand, the molecular phylogenetic analysis of the chlorella species suggested that the establishment of symbiotic relationships between free-living chlorellae and the green hydras have occurred multiple times (Rajević et al., 2015). In this respect, the evolutionary process of the symbiosis between green hydra and chlorella is still unclear.

The symbiont has a certain degree of host specificity, and the host hydra recognizes and selects symbiotic chlorellae taken into the endoderm cells. Aposymbiotic (symbiont-removed) green hydra can establish the symbiotic relationship with non-native chlorellae which are symbiotic with other green hydra strains but cannot establish the symbiotic relationship with some non-native chlorellae symbiotic with *Paramecium bursaria* and free-living chlorellae (Jolley and Smith 1980; McAuley and Smith 1982). Although the green hydra can establish the symbiotic relationship with NC64A chlorella, which is the symbiotic alga with *P. bursaria*, the symbiotic hydra harboring NC64A chlorella shows a lower proliferation rate by budding than the hydra harboring the native symbiotic chlorella (Hamada et al., 2018). It suggests that changing the combination of green hydra and chlorella causes different interactions between the host cells and the algae and affects the whole symbiotic system. Hanada (2020) conducted symbiont exchange experiments using two green hydra strains, K10 and M9. The K10 and M9 strains belong to phylogenetically distinct clades, respectively (Fig. 3.1). In both strains, the aposymbiotic strains (K10apo, M9apo) have lower proliferation rates by budding than the symbiotic strains. Interestingly, the M9 strain harboring non-native symbionts (M9 polyps with K10 chlorella, M9exc) does not change much with its proliferation rate from that of the original M9, although the K10 strain with non-native symbionts (K10 polyps with M9 chlorella,

K10exc) showed a lower proliferation rate than the original K10 strain. Furthermore, the numbers of tentacles and stenoteles, a form of nematocyte, per tentacle have decreased in the K10 hydras harboring the non-native symbionts.

This study aims to elucidate the difference in the symbiotic schemes of the green hydra strains and identify what affects their symbiont specificity. I obtained transcriptome of the green hydras, K10, M9, K10apo, M9apo, K10exc, and M9exc, with RNA-seq, and examined the changes in the cellular metabolic system by differential gene expression analysis and Gene Ontology enrichment analysis. The different gene expression patterns were found in translation, respiratory chain, and nitrogen metabolism when the symbionts were removed and replaced. Different gene expression patterns of the strains harboring non-native symbionts suggested the strain-specific host-symbiont interactions that affected the cellular systems.

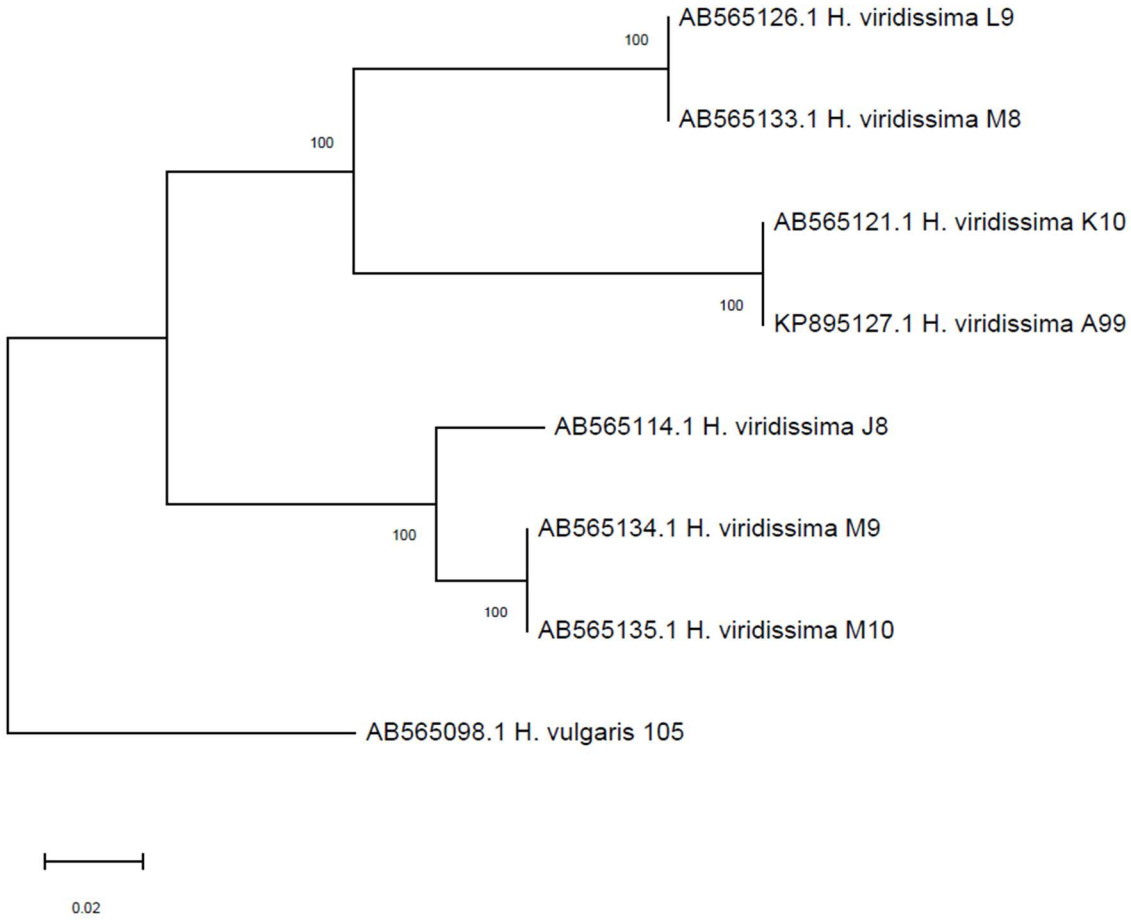

Figure 3.1 Phylogenetic relationship of *H. viridissima* strains constructed with the maximum likelihood method inferred from the nucleotide sequences of *COI*. The numbers along branches indicate the bootstrap value.

3.2 Materials and Methods

3.2.1 Materials

In this study, two strains of *H. viridissima*: K10 (the Swiss strain) and M9 (the Israel strain) were used (Fig. 3.1). Aposymbiotic hydras of these strains, K10apo and M9apo, were created by the DCMU (3-(3,4-dichlorophenyl)-1,1-dimethylurea) treatment (Pardy, 1976). The hydras harboring non-native symbionts were created by microinjection of non-native chlorellae into gastric cavities in the aposymbiotic hydras (Hanada, 2020). M9 chlorellae were injected into the K10apo polyp (K10exc), and K10 chlorellae were injected into an M9apo polyp (M9exc). All the strains were cultured in hydra culture solution (HCS; 1 mM NaCl, 1 mM $CaCl_2$, 0.1 mM KCl, 0.1 mM $MgSO_4$, 1 mM tris-(hydroxymethyl)-aminomethane; pH 7.4, adjusted with HCl) in glass vessels at 20 °C under 14 h∶10 h light/dark illumination cycles (84 μmol/m^2/s light intensity). Polyps were fed newly hatched *Artemia* nauplii two times per week. The day after feeding, the polyps were transferred into another glass vessel with fresh HCS.

3.2.2 RNA extraction and sequencing

Total RNA was extracted from 30 intact polyps starved for three days. The hydra polyps were homogenized using BioMasher II (Nippi, Tokyo), and the total RNA was extracted using the acid guanidinium thiocyanate-phenol-chloroform (AGPC) method (Chomczynski and Sacchi, 1987) and RNeasy Plus Mini Kit (QIAGEN, Hilden, Germany). The extracted RNA was treated with DNase I (Roche, Mannheim, Germany) to remove genomic DNA. The total RNA samples for a differential gene expression analysis were sent to Novogene Co., Ltd. (Beijing, China) for cDNA library construction and sequencing of 150 bp paired-end reads on Illumina HiSeq 4000. Then, I conducted sequencing of total RNA samples of 300 bp paired-end reads for de novo assembly. The mRNA was extracted from the total RNA samples using NEBNext Poly(A) mRNA Magnetic Isolation Module (New England Biolabs, Ipswich, MA). cDNA libraries were constructed using the TruSeq Stranded mRNA library prep (Illumina, San Diego, CA). The cDNA libraries were purified using AMPure XP magnetic beads (Beckman Coulter, Brea, CA).

These libraries were sequenced using Illumina MiSeq.

3.2.3 De novo assembly and annotation of *Hydra* contigs

Low-quality ends (QV < 30) and adapter sequences were trimmed, and short reads (<20 bp) were discarded for quality control using cutadapt (Martin, 2011). The remaining rRNA was filtered out using SortMeRNA 2 (Kopylova et al., 2012). De novo assembly was performed on the reads generated from HiSeq and MiSeq using Trinity (Haas et al., 2013), and shorter contigs (<200 bp) were discarded. Reads from Hiseq were mapped to the assembled contigs using salmon (Patro et al., 2017). Clustering the assembled contigs and counting the reads were performed with Corset (Davidson and Oshlack, 2014). A similarity search of the clustered contigs against UniprotKB was conducted using BLASTX with an e-value cutoff of 1e-5 to remove sequences from the symbiotic chlorellae and annotate the contigs. For each contig, I calculated e-values against homologous protein sequences of Opisthokonta and Viridiplantae in UniprotKB and those of *H. vulgaris* in TrEMBL. Contigs whose e-value of the best hits against Opisthokonta and *Hydra* sequences were smaller than those against Viridiplantae were considered hydra's contigs. These hydra's contigs were annotated with the UniProtKB Swiss-Prot, and the remaining unannotated contigs were annotated with entries of *H. vulgaris*, whose whole genome was sequenced and annotated (Chapman et al., 2010), in the UniProtKB TrEMBL to find hydra-specific genes. To find orthologs between K10 and M9, protein sequences translated from the contigs were estimated using TransDecoder (https://github.com/TransDecoder/TransDecoder), and an orthogroup, which is the set of genes that are descended from a single gene in the last common ancestor, were inferred by Orthofinder (Emms and Kelly, 2015) using protein sequences of K10 and M9 estimated by TransDecoder, and *H. vulgaris* in RefSeq database.

3.2.4 Differential gene expression analysis and GO enrichment analysis

Differential gene expression analyses were performed between the K10, K10apo, and K10exc polyps and between the M9, M9apo, and M9exc polyps using edgeR (Robinson et al., 2010),

and contigs with FDR < 0.05 were considered to be differentially expressed genes (DEGs). Gene Ontology (GO) enrichment analysis was performed using the DAVID Functional Annotation tool (Huang et al., 2009). Uniprot Accession Numbers of DEGs with any CPM were used as the inputs in the GO enrichment analysis. GO Direct was used among GO categories for the GO enrichment analysis. GO terms with Benjamini-Hochberg corrected P-value < 0.05 by Fisher's exact test were considered to be significantly enriched among the differentially expressed genes.

3.2.5 The experiment of supplying glutamine for symbiotic hydra polyps

To investigate whether glutamine is responsible for the proliferation of hydras, I measured the proliferation rates by budding of the original K10 and the K10exc polyps. Glutamine (Wako, Osaka, Japan) was dissolved in 2 mL HCS in a 12-well plastic container to make 1, 10, or 100 μM solutions. One polyp of K10 or K10exc was put in each well. These polyps were cultured at 20 °C under 14 h∶10 h light/dark illumination cycles (15 μmol/m^2/s light intensity) for 28 days. Polyps were fed newly hatched *Artemia* nauplii two times per week. The day after feeding, the polyps were transferred into another glass vessel with fresh HCS. The numbers of polyps in a well under each condition were counted per week. The differences in the average number of polyps were tested with Welch's *t*-test.

3.3 Results

3.3.1 De novo assembly, mapping, and annotation

I prepared the aposymbiotic polyps of the K10 and M9 strains, K10apo and M9apo, and the polyps with the non-native symbionts, K10exc, M9exc. Transcriptomes of the original symbiotic polyps, aposymbiotic polyps, and polyps harboring non-native symbiotic chlorellae were compared to identify the genes responsible for the symbiotic mechanisms in two strains. After the quality filtering, I obtained 144 million read pairs for the K10 strain and 138 million for the M9 strain. The average mapping rates by salmon were 89.5 % in the K10 strain and

89.2 % in the M9 strain (median K10 strain: 89.6 %; M9 strain: 89.1 %). *De novo* assembly using Trinity yielded 161896 contigs in the K10 strain and 191536 contigs in the M9 strain. Corset was used to cluster the homologous contigs and inferred the mRNA sequences. The assembled contigs were clustered into 52384 contigs in the K10 strain and 58773 contigs in the M9 strain by Corset. Then, I conducted a homology search using BLASTX to extract and annotate hydra-derived contigs. The number of contigs annotated by UniProtKB Swiss-Prot was 16202 in the K10 strain and 15430 in the M9 strain, and that annotated by *Hydra* entries in UniProtKB TrEMBL is 6370 and 19899, respectively. These annotated contigs were considered possible hydra-derived contigs, and the annotated contigs with counts per million mapped reads (CPM) > 0 were used subsequent differential gene expression analyses. In the following sections, the original symbiotic polyps were used as a control when I identified the DEGs in the aposymbiotic polyps (K10Apo or M9Apo) and the polyps harboring non-native symbionts (K10exc or M9exc).

3.3.2 Differential gene expression analysis of K10 strain

Among the annotated contigs of the K10 strain, 957 and 1293 genes were significantly differentially expressed in the K10apo polyps and the K10exc polyps compared to the original K10 polyps (Fig. 3.2a, $q < 0.05$). In these comparisons, 700 DEGs were commonly identified. In addition, the fold changes of DEGs found in the K10apo polyps and/or the K10exc polyps showed a significant positive correlation ($R = 0.84$, $p < 0.001$, Fig. 3.2b). It indicated the K10apo and K10exc polyps have similar gene expression changes from the original symbiotic ones. Next, I performed Gene Ontology enrichment analysis toward the DEGs with UniProtKB Swiss-Prot annotation. Six GO terms were enriched in the upregulated DEGs and two GO terms in the downregulated DEGs in the K10apo polyps (Table 3.1). Ten GO terms were enriched in the upregulated DEGs and six GO terms in the downregulated DEGs in the K10exc polyps (Table 3.2). Most of the enriched GOs were shared between the K10apo and the K10exc polyps. GO translation was commonly enriched in the upregulated genes and includes seven ribosomal proteins, two eukaryotic translation initiation factors, and one elongation factor (Table 3.3).

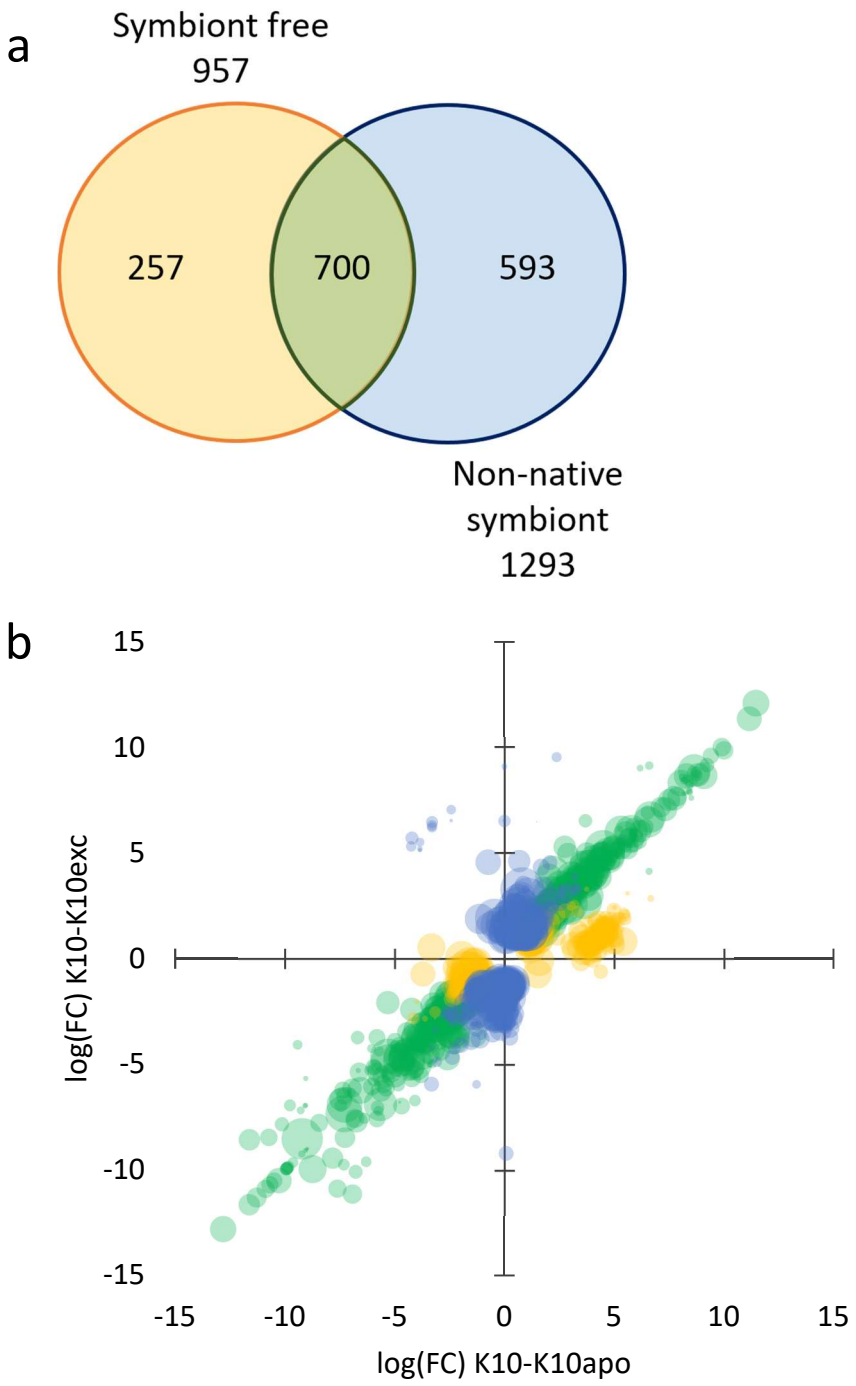

Figure 3.2 Gene expression changes of the K10 strain with no symbiont and the non-native symbiont compared to the K10 hydra with the native symbiont. **(a)** Venn diagram representing the number of DEGs between K10-K10apo (yellow) and K10-K10exc (blue). **(b)** Bubble chart of the fold changes of DEGs between K10-K10apo and K10-K10exc. The size of each bubble represents its CPM value. Green bubbles are genes differentially expressed between both K10-K10apo and K10-K10exc. Yellow bubbles are genes differentially expressed between only K10-K10apo. Blue bubbles are genes differentially expressed in only K10-K10exc.

Table 3.1 Enriched GO terms in the DEGs between K10-K10apo.

Upregulated genes in K10apo (K10apo > K10)

Category	Term	Count	Pop Hits	Fold Enrichment	q-value
MF	structural constituent of ribosome	36	285	4.26	1.31E-10
BP	translation	35	309	3.83	1.74E-08
CC	cytosolic large ribosomal subunit	17	108	5.45	1.54E-05
CC	ribosome	19	174	3.78	2.84E-04
CC	extracellular exosome	59	1135	1.80	4.49E-04
BP	cytoplasmic translation	11	68	5.47	0.012697

Downregulated genes in K10apo (K10apo > K10)

Category	Term	Count	Pop Hits	Fold Enrichment	q-value
MF	cytochrome-c oxidase activity	8	26	12.88	5.79E-04
CC	integral component of membrane	66	1962	1.52	0.035332

Table 3.2 Enriched GO terms in the DEGs between K10-K10exc.

Upregulated genes in K10exc (K10exc > K10)

Category	Term	Count	Pop Hits	Fold Enrichment	q-value
MF	structural constituent of ribosome	57	285	5.15	1.31E-22
BP	translation	56	309	4.78	4.80E-20
CC	ribosome	32	174	4.91	6.02E-11
CC	cytosolic small ribosomal subunit	20	62	8.62	6.19E-11
CC	cytosolic large ribosomal subunit	25	108	6.18	8.09E-11
CC	cytosolic ribosome	12	30	10.69	3.45E-07
BP	cytoplasmic translation	15	68	5.82	9.47E-05
CC	extracellular exosome	72	1135	1.69	2.81E-04
BP	ribosomal large subunit assembly	10	34	7.76	0.001144
BP	ribosomal small subunit assembly	7	21	8.79	0.025099

Downregulated genes in K10exc (K10exc > K10)

Category	Term	Count	Pop Hits	Fold Enrichment	q-value
CC	integral component of membrane	119	1962	1.65	4.96E-07
MF	cytochrome-c oxidase activity	12	26	11.77	5.75E-07
CC	respiratory chain	12	41	7.94	2.34E-05
CC	respiratory chain complex IV	7	10	19.00	4.17E-05
BP	homophilic cell adhesion*	11	40	7.60	0.001352
MF	calcium ion binding	32	340	2.40	0.001928

* homophilic cell adhesion via plasma membrane adhesion molecules

Table 3.3 Common upregulated genes with GO translation between K10-K10apo and K10-K10exc.

id	logFC(K10_K10apo)	logFC(K10_M9exc)	logCPM	Protein name
Cluster-20290.1	3.32	3.55	1.26	39S ribosomal protein L43,mitochondrial
Cluster-8816.10269	1.77	2.06	9.40	60S ribosomal protein L12
Cluster-16162.4	2.01	2.17	8.55	Ribosomal protein L35
Cluster-8816.558	3.92	4.02	6.89	Elongation factor 1-gamma
Cluster-8816.560	2.70	2.77	7.31	Elongation factor 1-gamma
Cluster-8816.559	1.74	1.79	8.15	Elongation factor 1-gamma
Cluster-8816.6445	2.20	2.47	8.63	Eukaryotic translation initiation factor 3 subunit D
Cluster-9766.1	2.33	2.33	3.31	Eukaryotic translation initiation factor 4 gamma 1
Cluster-4042.0	1.71	2.11	3.47	Mitochondrial carnitine/acylcarnitine carrier protein
Cluster-8816.7653	5.32	5.20	2.71	Phosphate carrier protein,mitochondrial

On the other hand, GO integral component of membrane was commonly enriched in the downregulated genes and includes five cytochrome c oxidases, three NADH-ubiquinone oxidoreductases, and one ammonium transporter (Table 3.4).

Next, I examined the DEGs found only in the K10apo (257 DEGs) or the K10exc (593 DEGs) polyps to identify changes in the symbiosis system caused by removing the symbiont and changes caused by the introduction of the non-native symbiont (Fig. 3.3). In order to exclude genes which were not determined to be the common DEGs due to the low power of a test, DEGs with the difference in those fold changes is greater than 1 were considered to be DEGs between only K10-K10apo or K10-K10exc. With this method, I filtered the DEGs only in the K10apo (248 DEGs) or the K10exc (465 DEGs) polyps. The DEGs unique to the K10apo polyps contained the genes for ribosomal proteins and products constituting the TCA cycle and the electron transport chain (Table 3.5), which were downregulated in the K10apo polyps. The DEGs unique to the K10exc polyps contained 2-oxoglutarate dehydrogenase and NADH-ubiquinone oxidoreductase, constituting the TCA cycle and the electron transport chain, respectively. Both were downregulated in the K10exc polyps. In addition, downregulation of ion channels related to nematocyte discharge and factors promoting nematocyte differentiation were found only in the K10exc polyps (Table 3.6).

3.3.3 Differential gene expression analysis of M9 strain

There were 85 significant DEGs in the M9apo polyps and 973 in the M9exc polyps in the comparison with the original symbiotic M9 polyps (Fig. 3.4a, $q < 0.05$). Only 10 common DEGs were found between the two above comparisons, and 75 DEGs were unique to the M9apo polyps; 963 DEGs were unique to the M9exc polyps. The fold changes of the DEGs in the M9apo and the M9exc polyps had no correlation ($R = -0.086$, Fig. 3.4b), suggesting that the changes in gene expression pattern from the original symbiotic polyps were quite different between the M9apo strain and the M9exc strain (cf. Fig. 3.5a,b).

Table 3.4 Common downregulated genes with GO integral component of membrane between K10-K10apo and K10-K10exc

id	logFC(K10-K10apo)	logFC(K10-K10exc)	logCPM	Protein name
Cluster-8148.1	-6.16	-5.28	0.55464	C-type lectin domain family 17, member A
Cluster-14692.10	-4.09	-5.22	1.97808	Protocadherin Fat4-like
Cluster-21630.0	-2.31	-3.79	5.30785	Cytochrome c oxidase subunit 1
Cluster-1196.0	-9.84	-9.84	0.86666	Cytochrome c oxidase subunit 1
Cluster-1209.0	-9.62	-9.62	0.66162	Cytochrome c oxidase subunit 1
Cluster-8816.7050	-2.21	-3.50	4.3592	Cytochrome c oxidase subunit 2
Cluster-8816.3900	-2.38	-3.63	4.40209	Cytochrome c oxidase subunit 3
Cluster-9479.0	-1.56	-1.82	3.2012	Galactose-3-O-sulfotransferase 3
Cluster-8816.2367	-4.70	-4.72	4.34392	Mitochondrial pyruvate carrier
Cluster-8816.2364	-4.05	-3.77	4.6733	Mitochondrial pyruvate carrier
Cluster-15272.0	-2.07	-3.71	2.8988	NADH-ubiquinone oxidoreductase chain 1
Cluster-8816.6125	-2.72	-3.61	1.71853	NADH:ubiquinone reductase
Cluster-18612.0	-2.52	-3.54	4.44252	NADH-ubiquinone oxidoreductase chain 5
Cluster-14692.5	-2.99	-3.24	2.63175	Cadherin EGF LAG seven-pass G-type receptor 2
Cluster-14692.4	-1.72	-1.59	2.97394	Cadherin EGF LAG seven-pass G-type receptor 2
Cluster-14692.7	-2.20	-2.33	2.20792	Cadherin EGF LAG seven-pass G-type receptor 2
Cluster-14692.6	-5.51	-5.92	1.9183	Cadherin protein
Cluster-14692.9	-2.26	-2.44	3.47362	Cadherin EGF LAG seven-pass G-type receptor 2
Cluster-13351.8	-3.06	-2.42	4.79247	Putative ammonium transporter 3
Cluster-13351.4	-1.84	-1.72	5.33015	Putative ammonium transporter 3
Cluster-2083.9	-2.96	-3.96	1.31145	Sodium-independent sulfate anion transporter
Cluster-18103.1	-3.09	-3.37	0.82979	Sugar phosphate exchanger 3
Cluster-8816.5206	-4.79	-4.13	1.87594	V-type proton ATPase proteolipid subunit
Cluster-6696.4	-5.71	-4.37	0.61719	V-type proton ATPase 21 kDa proteolipid subunit

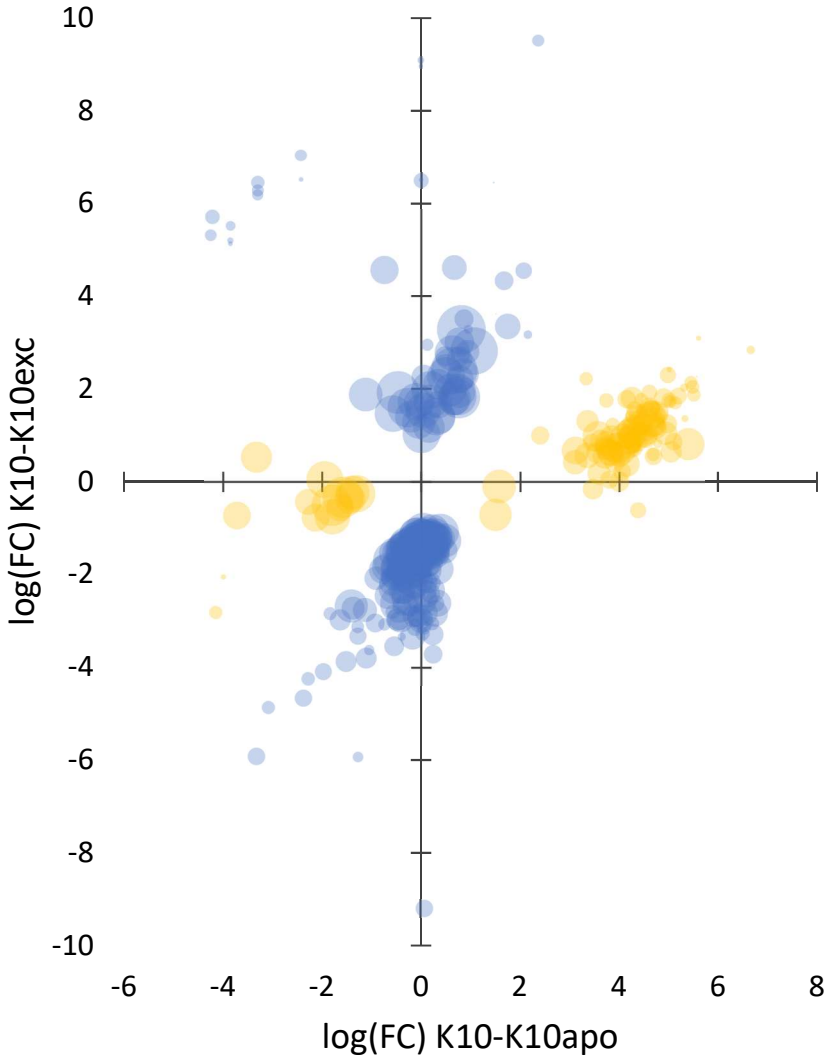

Figure 3.3 Bubble chart of the fold changes of DEGs between only K10-K10apo or K10-K10exc. Yellow: the fold changes of genes differentially expressed between only K10-K10apo. Blue: the fold changes of genes differentially expressed between only K10-K10exc. In order to exclude genes which were not determined to be the common DEGs due to low power of test, DEGs with the difference in those fold changes is greater than 1 were considered to be DEGs between only K10-K10apo or K10-K10exc.

Table 3.5a Genes differentially expressed between only K10-K10apo. **(a)** Upregulated genes in K10apo related to translation.

id	logFC(K10-K10apo)	logFC(K10-K10exc)	logCPM	Protein name
Cluster-8816.9595	4.35	0.85	0.65	40S ribosomal protein S10
Cluster-23251.17	4.43	1.30	2.70	40S ribosomal protein S12
Cluster-8816.3635	3.47	-0.16	1.95	40S ribosomal protein S14
Cluster-2768.6	4.73	1.16	2.40	40S ribosomal protein S15
Cluster-8816.5466	4.28	1.20	2.48	40S ribosomal protein S20
Cluster-8816.2933	4.02	0.64	2.21	40S ribosomal protein S23
Cluster-8816.4654	4.38	1.05	2.24	40S ribosomal protein S24
Cluster-8816.151	4.07	0.64	2.71	40S ribosomal protein S26
Cluster-20650.7	5.48	2.04	0.85	40S ribosomal protein S29
Cluster-8816.4837	3.80	0.04	1.51	40S ribosomal protein S3
Cluster-8816.5043	4.18	0.76	2.77	60S ribosomal protein L40
Cluster-8816.8433	5.51	1.87	0.86	40S ribosomal protein S5
Cluster-8816.8722	4.61	1.92	1.15	40S ribosomal protein S8
Cluster-8816.2072	3.59	0.18	2.41	40S ribosomal protein S9
Cluster-4790.4	4.22	0.81	2.18	60S ribosomal protein L10a
Cluster-8816.6247	3.73	0.86	2.27	60S ribosomal protein L11
Cluster-8816.10268	4.48	1.23	2.15	60S ribosomal protein L12
Cluster-2025.25	4.17	1.10	2.34	60S ribosomal protein L14
Cluster-16429.9	4.69	0.58	0.82	60S ribosomal protein L17
Cluster-10845.0	5.01	1.75	1.11	60S ribosomal protein L21
Cluster-8816.6834	4.45	1.76	0.88	60S ribosomal protein L22
Cluster-12445.38	3.11	0.42	2.76	60S ribosomal protein L23
Cluster-8816.2767	4.23	1.09	3.32	60S ribosomal protein L27a
Cluster-15371.1	3.36	1.30	2.27	60S ribosomal protein L28
Cluster-8816.10111	4.48	1.00	2.72	60S ribosomal protein L3
Cluster-8816.8399	3.97	0.86	1.68	60S ribosomal protein L30
Cluster-8816.8311	4.90	1.80	1.78	60S ribosomal protein L32
Cluster-8816.5556	4.34	1.41	2.14	60S ribosomal protein L35
Cluster-19710.5	4.30	1.17	2.39	60S ribosomal protein L36
Cluster-8816.1873	4.98	1.24	1.67	Ribosomal protein L37
Cluster-8816.4574	3.73	0.70	2.19	60S ribosomal protein L36a
Cluster-8816.1565	3.80	0.70	1.99	60S ribosomal protein L6
Cluster-8816.7068	3.12	0.67	3.54	60S ribosomal protein L8
Cluster-8816.4387	3.84	0.61	3.18	Elongation factor 1-alpha
Cluster-8816.5574	3.71	0.54	2.82	40S ribosomal protein S27a

Table 3.5b Genes differentially expressed between only K10-K10apo. **(b)** Upregulated genes related to respiration and others.

id	logFC(K10-K10apo)	logFC(K10-K10exc)	logCPM	Protein name
(respiration)				
Cluster-17174.1	4.78	0.82	0.41	Acyl-CoA dehydrogenase family member 10
Cluster-8816.4530	3.57	0.97	4.34	ADP/ATP translocase 3
Cluster-8816.863	4.15	1.77	1.58	Ornithine decarboxylase
Cluster-8816.1822	4.27	0.84	1.46	ATPase protein 9
Cluster-8816.1815	3.74	1.74	0.98	ATPase protein 9
Cluster-22050.0	5.20	1.84	1.32	Cytochrome c
Cluster-8546.1	5.60	3.08	0.13	NADH dehydrogenase 1 alpha subcomplex subunit 4
Cluster-8816.3904	4.62	1.59	1.89	Malate dehydrogenase
Cluster-18868.1	4.31	1.55	1.30	Malate dehydrogenase
Cluster-8816.1684	4.74	1.19	1.86	Phosphoenolpyruvate carboxykinase
Cluster-8816.1676	4.54	0.97	2.50	Phosphoenolpyruvate carboxykinase
Cluster-8816.6174	4.24	1.40	0.68	Citrate synthase
Cluster-8816.6173	3.87	1.23	0.89	Citrate synthase
(other)				
Cluster-22899.0	4.94	1.04	2.61	Acidic mammalian chitinase
Cluster-8816.5208	4.25	0.96	3.30	Antistasin
Cluster-8816.1064	5.45	2.13	0.79	Cathepsin B
Cluster-8816.2800	4.26	1.79	2.42	Cathepsin L1
Cluster-8816.6978	4.32	0.88	2.65	Chymotrypsin-like elastase family member 3A
Cluster-8816.6977	4.17	0.96	2.20	Chymotrypsin-like elastase family member 3A
Cluster-14123.3	4.79	1.32	1.12	Cathepsin D
Cluster-3829.0	4.69	0.55	1.45	Chymotrypsin-like elastase family member 2A
Cluster-8816.5266	4.98	2.29	1.22	Myosin regulatory light chain 12B
Cluster-8816.8810	5.31	2.02	0.31	Nematoblast-specific protein nb039a-sv9
Cluster-11168.1	4.63	1.61	0.34	Protocadherin Fat4-like
Cluster-3217.4	3.91	0.43	2.04	Spinalin
Cluster-11504.0	4.83	1.41	1.16	Dickkopf-like protein Dlp-1
Cluster-5581.15	4.27	0.77	1.12	VEGF

Table 3.6a Genes differentially expressed between only K10-K10exc. **(a)** Upregulated genes in K10exc

id	logFC(K10-K10apo)	logFC(K10-K10exc)	logCPM	Protein name
Cluster-363.0	0.00	6.51	0.09	40S ribosomal protein S12
Cluster-1057.0	4.24	5.30	0.64	40S ribosomal protein S2
Cluster-1113.0	3.30	6.28	0.65	40S ribosomal protein S6
Cluster-1037.0	3.85	5.12	0.10	40S ribosomal protein SA
Cluster-1096.0	3.30	6.19	0.57	Ribosomal protein L10
Cluster-1017.0	3.29	6.45	0.81	60S ribosomal protein L3
Cluster-8816.6706	-1.07	2.81	10.27	60S ribosomal protein L34
Cluster-1681.0	4.21	5.69	0.97	60S ribosomal protein L5
Cluster-136.0	2.42	7.03	0.53	60S ribosomal protein L8
Cluster-19043.0	1.68	4.32	1.62	Glutamate decarboxylase 2
Cluster-8816.4814	0.31	1.40	6.48	Glutamine--fructose-6-phosphate transaminase
Cluster-8816.6856	0.01	1.02	6.50	Glutamine--fructose-6-phosphate transaminase
Cluster-8816.4940	2.16	3.16	0.35	Histidine ammonia-lyase
Cluster-993.0	3.84	5.50	0.45	ATP synthase subunit alpha
Cluster-7536.5	0.00	6.50	0.87	Elongation factor 1-alpha
Cluster-397.0	-1.47	6.46	0.01	Elongation factor 2
Cluster-19171.0	-0.63	2.77	5.83	Acyl-CoA synthetase family member 4
Cluster-8816.8592	-0.85	2.31	4.54	Glutamine synthetase
Cluster-16467.0	0.36	1.66	3.51	Dickkopf-3 related protein
Cluster-21999.0	0.75	1.82	6.14	Facilitated glucose transporter member 8
Cluster-8816.650	0.68	1.74	3.81	Collagen alpha-6(VI) chain
Cluster-4325.0	2.07	4.54	1.26	NLR type 1
Cluster-8816.7122	-0.87	3.50	1.69	Proton-coupled folate transporter
Cluster-8816.7123	-0.78	2.63	3.02	Proton-coupled folate transporter
Cluster-7339.8	-0.51	2.42	4.09	ADP-ribosyl cyclase/cyclic ADP-ribose hydrolase
Cluster-7339.1	0.05	1.70	4.06	ADP-ribosyl cyclase/cyclic ADP-ribose hydrolase
Cluster-10150.1	-0.04	1.53	5.75	Caspase D
Cluster-8816.4451	-0.81	3.27	10.93	Dynein heavy chain 2, axonemal
Cluster-5063.0	0.74	4.55	3.69	Thrombospondin type 1 repeat-containing protein 2
Cluster-5063.1	-0.67	4.60	2.84	Thrombospondin type 1 repeat-containing protein 2
Cluster-4325.2	-0.05	2.25	2.74	NACHT, LRR and PYD domains-containing protein 12

Table 3.6b Genes differentially expressed between only K10-K10exc. **(b)** Downregulated genes in K10exc.

id	logFC(K10-K10apo)	logFC(K10-K10exc)	logCPM	Protein name
Cluster-15315.2	-1.05	-3.62	0.51	2-oxoglutarate dehydrogenase,mitochondrial
Cluster-17197.0	-0.05	-1.43	4.91	Galactose-3-O-sulfotransferase 3
Cluster-23546.0	-0.70	-1.84	3.70	Folate gamma-glutamyl hydrolase
Cluster-7258.0	-1.97	-4.09	1.34	NADH-ubiquinone oxidoreductase chain 3
Cluster-8816.1970	-2.38	-4.67	1.25	NADH-ubiquinone oxidoreductase chain 6
Cluster-15446.6	-0.12	-1.90	3.94	Pyruvate kinase
Cluster-23260.1	-0.34	-1.45	5.58	Vesicular glutamate transporter 3
Cluster-8816.6295	-0.14	-1.24	6.00	Vesicular glutamate transporter 3
Cluster-19419.4	-0.33	-1.51	3.71	Vesicular inhibitory amino acid transporter
Cluster-5392.1	0.67	-2.45	3.29	Vesicular inhibitory amino acid transporter
Cluster-8816.6708	-0.34	-1.94	3.72	Myosin regulatory light chain 12B
Cluster-18436.0	-0.02	-1.42	3.51	Nematocilin A
Cluster-9495.0	-0.27	-1.44	3.40	Polycystic kidney disease protein 1-like 2
Cluster-21183.0	-0.21	-1.86	2.59	Transcriptional activator GLI3
Cluster-21618.0	0.15	-1.32	3.68	Potassium voltage-gated channel subfamily A member 2
Cluster-8816.9413	-0.32	-1.76	4.08	Transcriptional activator GLI3
Cluster-8816.7350	-1.63	-2.97	2.07	Potassium voltage-gated channel subfamily H member 2
Cluster-8816.5487	0.00	-1.48	3.34	Voltage-dependent calcium channel subunit alpha-2/delta-4
Cluster-8816.3788	-0.52	-1.54	4.75	Minicollagen 17
Cluster-8816.8819	-1.13	-2.76	2.68	Nematoblast-specific protein nb039a-sv15
Cluster-8816.1717	-0.48	-1.48	3.08	Calcium-activated potassium channel subunit alpha-1
Cluster-8816.1719	-0.13	-1.71	4.49	Calcium-activated potassium channel subunit alpha-1
Cluster-3166.5	-0.40	-1.23	3.83	Polycystic kidney disease protein 1-like 2
Cluster-8816.3463	0.12	-2.12	5.78	Polycystin-2
Cluster-12833.0	0.28	-1.95	3.47	Transcriptional activator GLI3
Cluster-23114.9	0.17	-1.74	3.89	Voltage-dependent N-type calcium channel subunit alpha-1B
Cluster-3158.3	0.24	-1.93	5.49	Nematocilin A
Cluster-8816.3502	-0.40	-1.08	6.10	Nematocyst outer wall antigen
Cluster-14669.0	0.04	-1.41	4.66	Transcription factor jun-D
Cluster-3217.0	-0.18	-1.35	6.36	Nematoblast-specific protein nb054-sv9
Cluster-22044.0	-0.39	-2.68	1.66	Aristaless-like protein
Cluster-3837.8	-0.11	-1.29	4.94	Dynein heavy chain 10, axonemal
Cluster-8816.8222	-2.28	-4.24	0.86	Dynein heavy chain 7, axonemal
Cluster-8816.8224	-1.27	-3.32	1.37	Dynein heavy chain 7, axonemal
Cluster-8816.1158	-0.27	-1.57	3.26	Dynein intermediate chain 2,axonemal
Cluster-8816.892	-0.41	-1.66	3.10	Kinesin-like protein
Cluster-3837.5	0.07	-1.53	4.71	Dynein heavy chain 10, axonemal
Cluster-8816.8223	-0.22	-2.33	3.08	Dynein heavy chain 7, axonemal
Cluster-8816.8225	-0.10	-2.41	3.53	Dynein heavy chain 7, axonemal
Cluster-19333.0	0.14	-2.89	2.34	Dynein regulatory complex protein 10

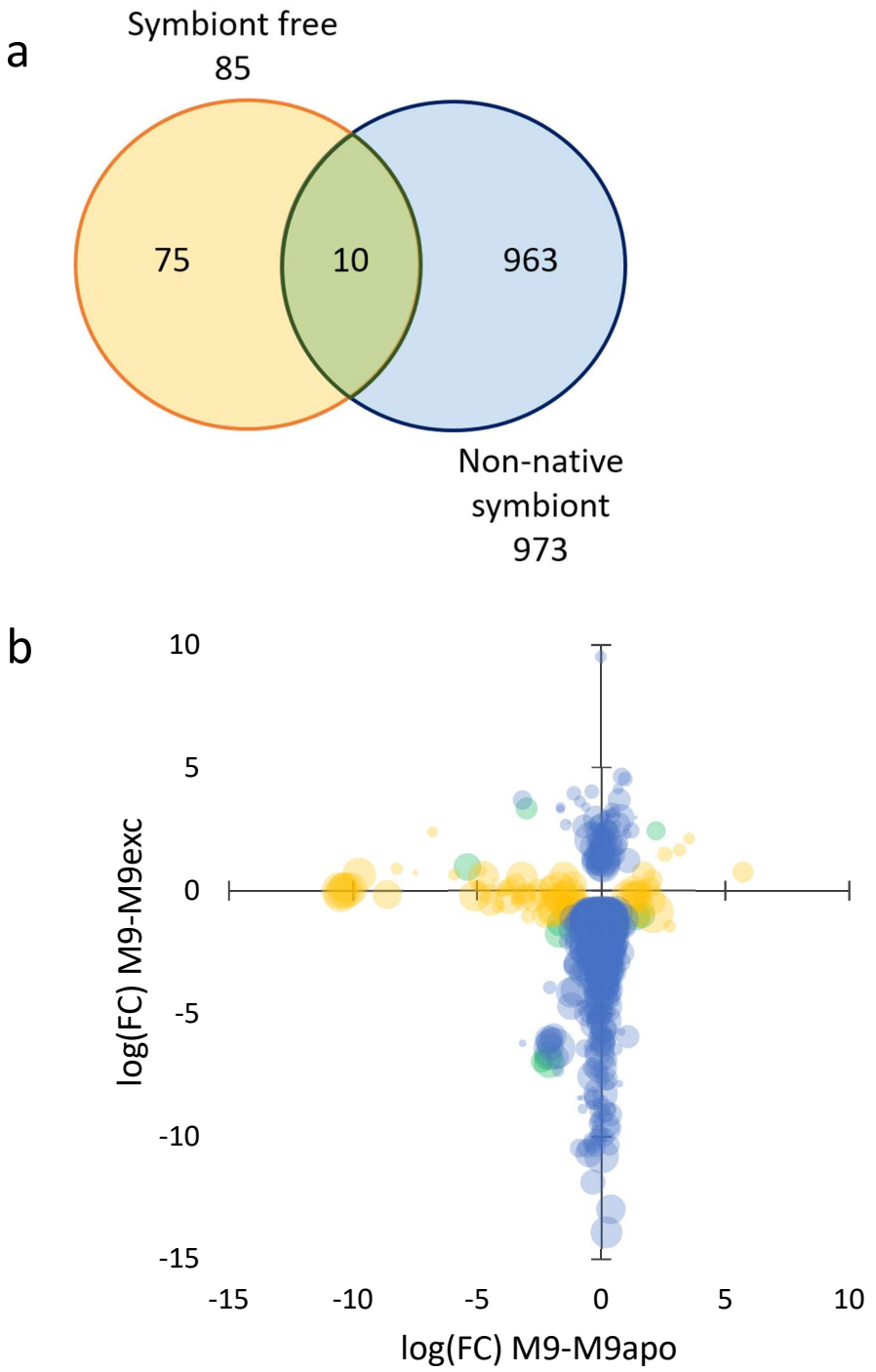

Figure 3.4 Gene expression changes of the M9 strain with no symbiont and the non-native symbiont compared to the M9 hydra with the native symbiont. **(a)** Venn diagram representing the number of DEGs between M9-M9apo (yellow) and M9-M9exc (blue). **(b)** Bubble chart of the fold changes of DEGs between M9-M9apo and M9-M9exc. The size of each bubble represents its CPM value. Green bubbles are genes differentially expressed between both M9-M9apo and M9-M9exc. Yellow bubbles are genes differentially expressed between only M9-M9apo. Blue bubbles are genes differentially expressed in only M9-M9exc.

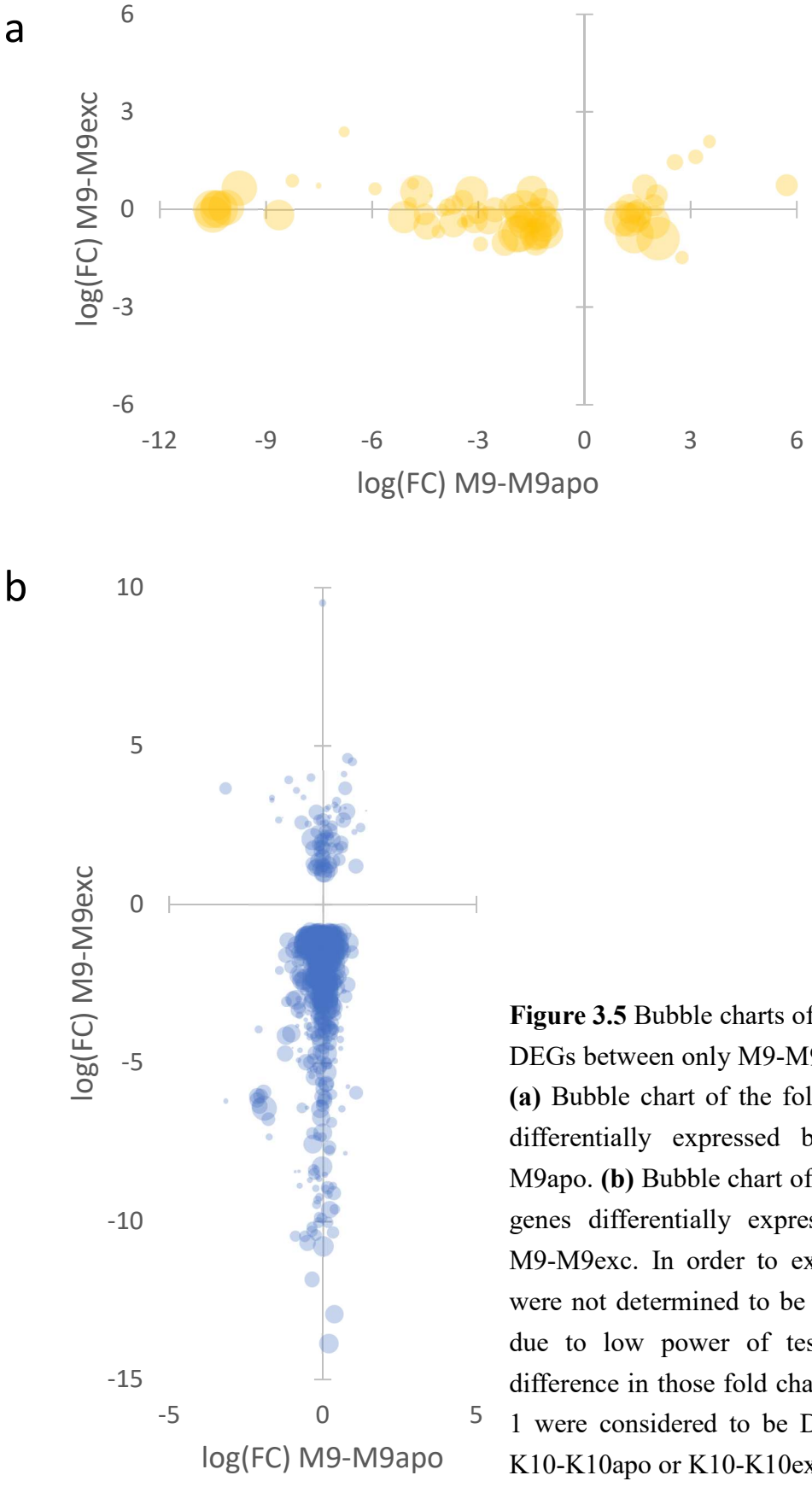

Figure 3.5 Bubble charts of the fold changes of DEGs between only M9-M9apo or M9-M9exc. **(a)** Bubble chart of the fold changes of genes differentially expressed between only M9-M9apo. **(b)** Bubble chart of the fold changes of genes differentially expressed between only M9-M9exc. In order to exclude genes which were not determined to be the common DEGs due to low power of test, DEGs with the difference in those fold changes is greater than 1 were considered to be DEGs between only K10-K10apo or K10-K10exc.

Then, I conducted a GO enrichment analysis for these DEGs. No GO terms were significantly enriched in both upregulated and downregulated DEGs in the M9apo polyps. Removal of symbionts did not significantly change the gene expression pattern in the M9 strain, but the genes encoding ammonium transporters and ascorbate peroxidases, which are related to nutrient exchange between symbiont and hosts or active oxygen scavenging, were downregulated in the M9apo polyps (Table 3.7).

When the symbionts were replaced with the non-native symbiont, GO voltage-gated calcium channel complex was only enriched in the upregulated genes, and five GO terms, e.g. extracellular matrix and calcium ion binding, were enriched in the downregulated genes (Table 3.8). The downregulated genes with the exemplified enriched GO terms contained collagens, which constitute mesoglea, and cadherins, which function in cell adhesion. The downregulations of cadherin genes in the M9apo polyps were reported in Ishikawa et al. (2016b). The upregulated genes with GO voltage-gated calcium channel complex were four calcium channels, while the downregulated genes included polycystins, which function calcium-regulated cation channel (Chen et al, 1999). Voltage-gated calcium channel and polycystin were related to nematocyte discharge (Gitter et al., 1994; McLaughlin, 2017), and these genes tend to downregulate in symbiotic hydras of *H. vulgaris* (Chapter 2). The genes for ion channels related to nematocyst discharge, factors promoting nematocyte differentiation were downregulated in the M9exc polyps (Table 3.9). These genes were also downregulated in the K10exc polyps. The genes of ribosomal proteins and those constituting the TCA cycle and the electron transport chain were downregulated in the M9exc polyps but upregulated in K10exc polyps.

Table 3.7 Genes related to symbiosis which were differentially expressed between only M9-M9apo.

M9 < M9apo

id	logFC(M9-M9apo)	logFC(M9-M9exc)	logCPM	Protein name
Cluster-15475.4977	1.94	-0.40	6.10	Acyl-CoA synthetase family member 4
Cluster-15475.11855	1.28	0.01	4.81	Succinate-semialdehyde dehydrogenase

M9 > M9apo

id	logFC(M9-M9apo)	logFC(M9-M9exc)	logCPM	Protein name
Cluster-909.0	-6.80	2.39	0.61	Elongation factor 2
Cluster-15475.10258	-3.29	-0.36	0.92	Acyl-coenzyme A thioesterase 1
Cluster-25226.0	-2.94	-1.06	1.24	Acyl-coenzyme A thioesterase 1
Cluster-15475.7057	-1.73	0.00	8.16	Glutamine synthetase
Cluster-7111.0	-5.90	0.64	0.85	Vesicular inhibitory amino acid transporter
Cluster-9863.5	-4.74	0.54	5.93	Putative ammonium transporter 3
Cluster-9863.3	-3.19	0.51	6.04	Putative ammonium transporter 3
Cluster-15475.8989	-3.70	-0.42	4.45	Putative ascorbate peroxidase
Cluster-7581.0	-1.85	-0.29	4.27	Putative ascorbate peroxidase
Cluster-4626.26	-9.76	0.64	6.74	Hydralysin
Cluster-3438.0	-10.40	0.12	4.99	Periculin 2b

Table 3.8 Enriched GO terms in the DEGs between M9-M9exc.

Upregulated genes in K10C (M9exc > M9)

Category	Term	Count	Pop Hits	Fold Enrichment	q-value
CC	voltage-gated calcium channel complex	4	23	26.92	0.039995

Downregulated genes in K10C (M9exc< M9)

Category	Term	Count	Pop Hits	Fold Enrichment	q-value
CC	extracellular matrix	18	93	3.69	0.001915
CC	extracellular exosome	84	1024	1.56	0.003694
MF	calcium ion binding	40	343	2.12	0.005426
CC	proteinaceous extracellular matrix	16	93	3.28	0.010482
CC	extracellular region	30	275	2.08	0.021195

Table 3.9a Genes differentially expressed between only M9-M9exc. **(a)** DEGs related to translation

id	logFC(M9-M9apo)	logFC(M9-M9exc)	logCPM	Protein name
Cluster-23815.1	-0.17	-2.90	2.82	28S ribosomal protein S16,mitochondrial
Cluster-7018.11	0.04	-1.18	5.31	28S ribosomal protein S5,mitochondrial
Cluster-22278.1	0.05	-1.07	4.43	39S ribosomal protein L27,mitochondrial
Cluster-4672.4	-0.07	-1.04	5.21	39S ribosomal protein L43,mitochondrial
Cluster-15475.3990	0.08	-1.25	7.71	39S ribosomal protein L9, mitochondrial
Cluster-15475.3947	-0.14	-1.20	4.86	40S ribosomal protein S10
Cluster-15475.1662	0.07	-3.04	4.67	40S ribosomal protein S11
Cluster-15475.535	-0.02	-1.13	6.34	40S ribosomal protein S14
Cluster-15475.3772	0.10	-1.21	4.20	40S ribosomal protein S15a
Cluster-15475.2191	-0.09	-1.38	3.56	40S ribosomal protein S17
Cluster-15475.2193	-0.10	-1.54	3.00	40S ribosomal protein S17
Cluster-15475.7002	-0.13	-1.14	7.17	40S ribosomal protein S4
Cluster-15475.4285	-0.07	-1.45	7.20	40S ribosomal protein S5
Cluster-15475.4234	-0.24	-1.15	7.43	40S ribosomal protein S7
Cluster-15475.4235	-0.19	-1.26	6.61	40S ribosomal protein S7
Cluster-15475.5758	-0.08	-1.22	4.83	60S ribosomal protein L13
Cluster-15475.5930	0.19	-3.91	4.83	60S ribosomal protein L21
Cluster-15475.6366	-0.26	-1.27	5.99	60S ribosomal protein L23
Cluster-15475.8599	0.10	-5.29	7.47	60S ribosomal protein L36
Cluster-15475.8598	0.05	-6.21	4.13	60S ribosomal protein L36
Cluster-15475.7173	-0.09	-1.15	5.13	60S ribosomal protein L6
Cluster-4626.20	-0.26	-2.78	3.61	60S ribosomal protein L7a
Cluster-15475.6385	-0.01	-1.10	6.13	Eukaryotic translation initiation factor 3 subunit G
Cluster-15475.5624	0.09	-2.24	5.95	Eukaryotic translation initiation factor 3 subunit G

Table 3.9b Genes differentially expressed between only M9-M9exc. **(b)** DEGs related to respiration.

id	logFC(M9-M9apo)	logFC(M9-M9exc)	logCPM	Protein name
Cluster-15475.1712	0.00	-1.08	7.95	2-oxoglutarate dehydrogenase
Cluster-21127.0	-1.91	-5.92	3.98	ATP synthase subunit a
Cluster-15475.6328	-0.29	-1.90	2.51	ATP synthase subunit O
Cluster-15475.1008	-0.55	-1.34	4.33	Cytochrome b(558) alpha chain
Cluster-26097.0	-1.73	-7.33	0.85	Cytochrome c oxidase subunit 1
Cluster-16888.0	-2.04	-6.35	4.36	Cytochrome c oxidase subunit 2
Cluster-9174.0	-2.11	-6.05	4.43	Cytochrome c oxidase subunit 3
Cluster-20893.1	-0.28	-2.30	5.97	Glutamate decarboxylase 2
Cluster-22564.0	0.05	-1.48	2.85	Glutamine--fructose-6-phosphate transaminase
Cluster-13923.1	0.01	-1.40	5.78	NADH dehydrogenase [ubiquinone] iron-sulfur protein 7
Cluster-15475.2847	-1.89	-6.43	10.43	NADH-ubiquinone oxidoreductase chain 1
Cluster-15475.6268	-2.12	-6.17	3.96	NADH-ubiquinone oxidoreductase chain 4
Cluster-15475.7345	-2.01	-6.04	3.72	NADH-ubiquinone oxidoreductase chain 5
Cluster-15475.92	-0.39	-1.04	6.88	Succinate--CoA ligase [ADP/GDP-forming] subunit alpha
Cluster-19524.1	-0.16	-1.09	4.52	Succinate-CoA ligase subunit beta
Cluster-19524.2	-0.06	-1.22	5.78	Succinate-C+B199:M213oA ligase subunit beta

Table 3.9c Genes differentially expressed between only M9-M9exc. **(c)** DEGs related to nematocyte.

id	logFC(M9-M9apo)	logFC(M9-M9exc)	logCPM	Protein name
Cluster-15475.3603	0.07	-2.89	4.23	Minicollagen 10
Cluster-15475.3600	0.03	-2.21	7.33	Minicollagen 10
Cluster-15475.3599	0.03	-2.45	7.67	Minicollagen 10
Cluster-15475.3602	0.02	-2.47	6.42	Minicollagen 10
Cluster-15475.4750	-0.06	-2.09	3.23	Minicollagen 12
Cluster-25387.1	0.07	-2.63	7.40	Minicollagen 16
Cluster-25387.2	0.23	-2.45	7.64	Minicollagen 17
Cluster-25387.0	-0.04	-2.42	1.58	Minicollagen 17
Cluster-15475.5466	0.10	-3.31	8.43	Minicollagen 5
Cluster-15475.6228	0.21	-3.29	7.35	Minicollagen 6
Cluster-15475.5060	0.15	-2.99	7.95	Minicollagen 6
Cluster-15475.5045	0.14	-2.36	7.30	Minicollagen 8
Cluster-15475.5048	0.03	-2.06	8.03	Minicollagen 8
Cluster-15475.5509	-0.14	-2.21	6.69	Minicollagen 9
Cluster-15475.5515	-0.06	-2.00	5.63	Minicollagen 9
Cluster-15475.8089	0.37	-1.56	7.78	Nematoblast specific protein
Cluster-15475.8090	0.35	-1.46	8.61	Nematoblast specific protein
Cluster-15475.7543	0.01	-1.50	4.85	Nematoblast specific protein
Cluster-15475.8091	0.30	-1.23	7.77	Nematoblast-specific protein nb035-sv2
Cluster-15475.10129	0.18	-2.73	6.65	Nematoblast-specific protein nb039a-sv15
Cluster-15475.6565	-0.03	-1.77	4.39	Nematoblast-specific protein nb039a-sv15
Cluster-15475.10131	0.13	-2.45	8.63	Nematoblast-specific protein nb039a-sv9
Cluster-15475.10137	0.11	-2.52	6.57	Nematoblast-specific protein nb039a-sv9
Cluster-15475.10136	0.09	-1.52	5.46	Nematoblast-specific protein nb039a-sv9
Cluster-15475.10135	0.08	-2.12	7.14	Nematoblast-specific protein nb039a-sv9
Cluster-15475.2189	-0.20	-1.26	8.41	Nematocilin B
Cluster-16736.3	0.34	-1.29	7.59	Nematocyst outer wall antigen
Cluster-18736.2	0.01	-1.48	6.76	Nematocyst outer wall antigen
Cluster-15475.6764	-0.59	-0.98	5.47	Polycystic kidney disease protein 1-like 2
Cluster-15475.5452	-0.53	-1.18	5.38	Polycystic kidney disease protein 1-like 2
Cluster-15475.5450	-0.26	-1.48	5.39	Polycystic kidney disease protein 1-like 2
Cluster-715.0	-0.19	-1.27	4.57	Polycystic kidney disease protein 1-like 2
Cluster-8616.3	-0.29	-2.12	3.02	Polycystic kidney disease protein 1-like 2
Cluster-15475.5454	-0.21	-1.07	4.40	Polycystic kidney disease protein 1-like 2
Cluster-15475.6949	-0.16	-1.71	5.55	Polycystic kidney disease protein 1-like 2
Cluster-15475.5451	-0.16	-1.15	5.17	Polycystic kidney disease protein 1-like 2
Cluster-8616.6	-0.11	-2.06	2.48	Polycystic kidney disease protein 1-like 2

(Table 3.9c continued on next page)

(Table 3.9c continued)

id	logFC(M9-M9apo)	logFC(M9-M9exc)	logCPM	Protein name
Cluster-8616.1	0.13	-3.95	1.76	Polycystic kidney disease protein 1-like 2
Cluster-15475.5456	-0.06	-2.55	5.11	Polycystic kidney disease protein 1-like 2
Cluster-7195.4	-0.63	-1.28	5.98	K+ voltage-gated channel subfamily A member 2
Cluster-13889.2	-0.19	-3.87	0.74	Protocadherin Fat 1
Cluster-7986.3	-0.08	-2.48	2.80	Protocadherin Fat4-like
Cluster-7986.1	-0.05	-2.14	4.74	Protocadherin Fat4-like

3.3.4 Comparison of the proliferation rates of symbiotic hydra polyps in providing glutamine

I examined whether the proliferation rates changed in the original symbiotic K10 polyps and the K10exc polyps when glutamine was supplied to the HCS (1, 10, or 100 μM). The number of polyps 28 days after the start of glutamine supplementation were shown in Fig. 3.6. In the original symbiotic polyps, the number of polyps was 12.7 ± 3.6 (mean ± SD, control), 6.5 ± 2.8 (1μM), 7.8 ± 1.8 (10 μM), 12.2 ± 2.4 (100 μM). In the K10exc polyps, the number of polyps was 2.5 ± 0.67 (mean ± SD, control), 3.0 ± 1.0 (1 μM), 4.2 ± 1.5 (10 μM), 2.0 ± 0.58 (100 μM). The proliferation rates between K10 and K10exc in control and 100 μM were significantly different (P = 0.036, 0.0067). However, the proliferation of the polyps was not dependent on the concentration of glutamine.

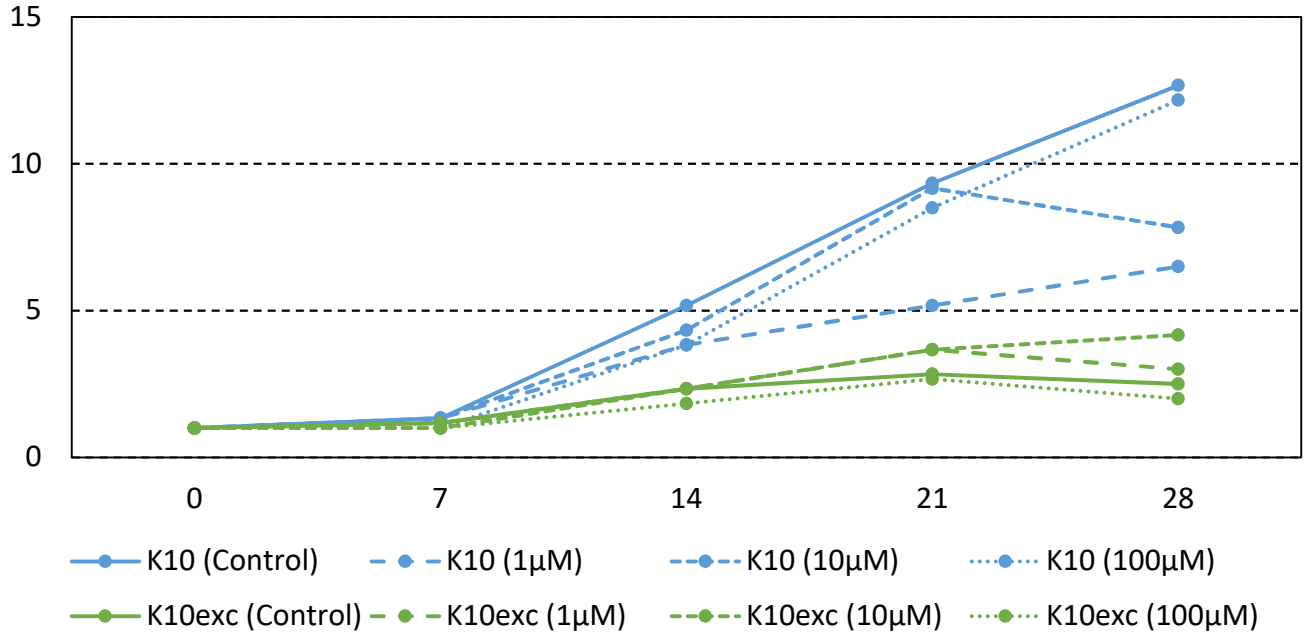

Figure 3.6 Proliferation rate of K10 (blue) and K10exc (green) polyps with glutamine (1, 10, 100 μM) in the HCS. The number of polyps in each of K10 and K10exc was counted every seven days (n = 6).

3.4 Discussion

3.4.1 Cellular energy balance in *H. viridissima* K10, M9, and other host organisms having endosymbiotic relationships with algae

In the K10apo and K10exc strain, the upregulation of genes with GO translation and the downregulation of genes of electron transport chain complexes were commonly observed. Translation is one of the most ATP-consuming cellular processes (Buttgereit and Brand, 1995; Rolfe and Brown, 1997) and is energy-balanced with the ATP-producing system, electron transport chain (Vander Heiden et al., 2009). In marine invertebrates, the activity of the electron transport chain is regulated by oxygen partial pressure in the cell (Abele et al., 2007). The removal and replacement of symbionts caused the loss of oxygen production by photosynthesis, which can result in suppression of the function of the electron transport chain, and change in the energy balance. If the hydras which replaced the symbiont caused the same thing, it might suppress the function of the electron transport chain too. ATP production by the respiratory chain and photosynthesis generates ROS (Reactive oxygen species) (Lee et al., 2011; Mittler et al., 2004). When the host is supplied with photosynthetic products from the symbiont, ROS from photosynthesis damage the host cells. In coral-*Symbiodinium* symbiosis, ROS generated by the symbiont at a high temperature can cause coral bleaching, which expels symbiont necessary for coral survival from the coral cells, due to cellular damage by ROS (Weis, 2008; Plass-Johnson et al., 2015). Among the enzymes which degrade ROS, ascorbate peroxidase (APX) was downregulated in the K10 strain when the symbionts were removed and replaced, while, in the M9 strain, the ascorbate peroxidase was downregulated only in the hydras whose symbionts were removed (Fig. 3.7). Ascorbate peroxidase is an enzyme degrading H_2O_2, which is a kind of ROS, to H_2O in plants (Caverzan et al., 2012). The green hydra also possesses the ascorbate peroxidase, but it has not been found in other animals (Habetha and Bosch, 2005). These ascorbate peroxidase genes did not belong to the same orthogroup and therefore did not be considered as orthologs. The production of ROS and its degradation by the peroxidase can be balanced in the symbiotic hydra cells with the native chlorella. When the removal and

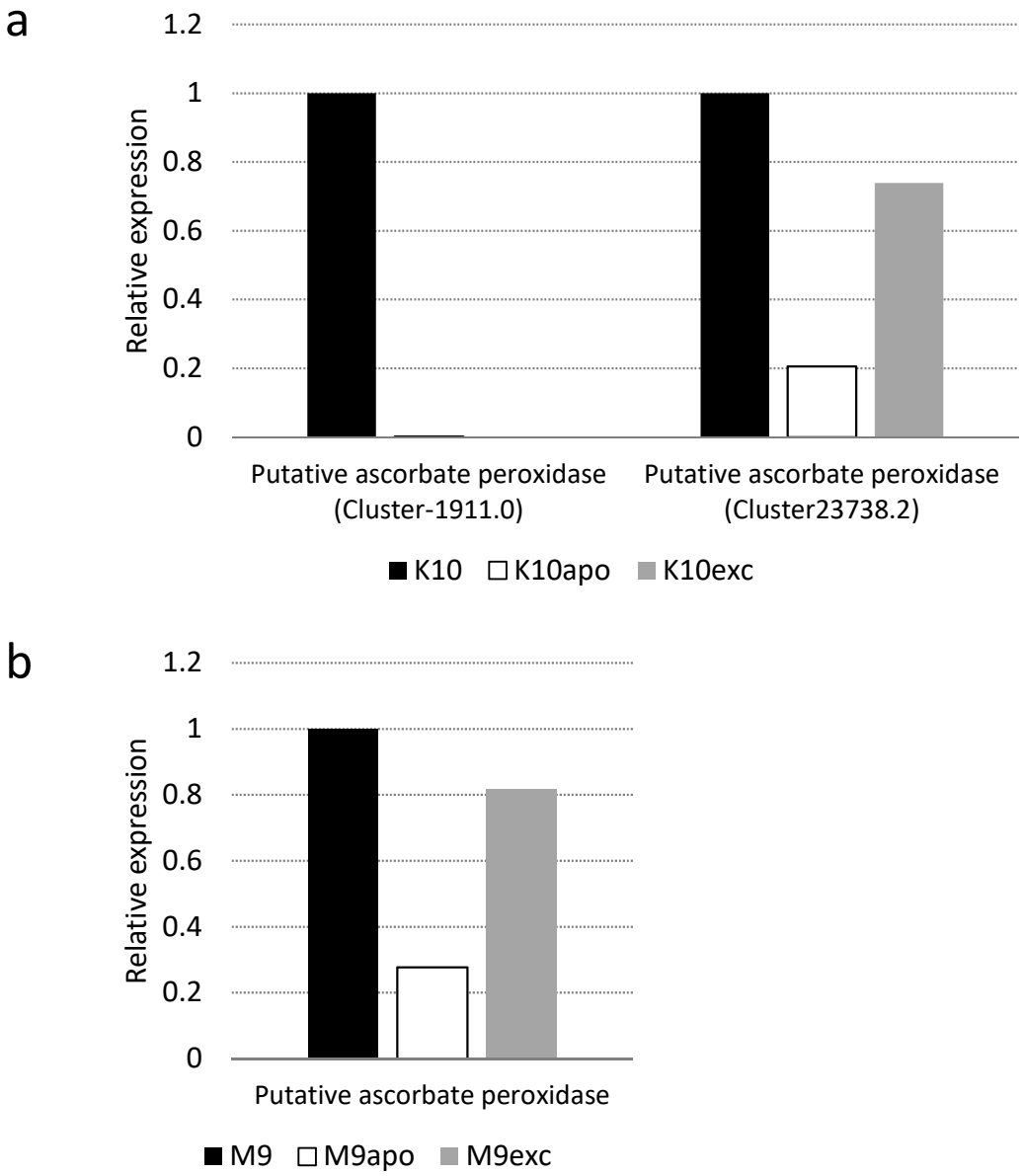

Figure 3.7 Relative gene expression amount of ascorbate peroxidases calculated from their fold changes. **(a)** Ascorbate peroxidases differentially expressed between K10-K10apo and K10-K10exc. **(b)** An ascorbate peroxidase differentially expressed between M9-M9apo.

replacement of the symbionts in the K10 strain, the production of ROS by the electron transport chain was reduced, but the expression of ascorbate peroxidase (Cluster-1911.0) was also reduced. It implied the downregulation of the ascorbate peroxidase damaged to the host cells. In the hydras which replaced the symbiont in the M9 strain, the expression of the ascorbate peroxidase did not reduce, although the function of the electron transport chain was suppressed. Those changes in the intracellular energy balance and the gene expression changes of the ascorbate peroxidase may represent effects in the hydra cells from the host specificity of the symbiotic chlorellae and influence the changes of the hydras in proliferation and morphology during symbiosis with the non-native symbionts.

Table 3.10 shows trends of the expression changes of genes related to translation and electron transport chain compared to other endosymbiotic hosts with algae. Ishikawa et al. (2016b) analyzed GO enrichment in *H. viridissima* M9 strain between the symbiotic and aposymbiotic hydras. The authors report GO terms such as translation and respiratory chain were enriched in the upregulated genes in M9apo. Unlike the enrichment in the M9 strain in Ishikawa et al. (2016b), regulation of genes related to translation and respiratory chain in the K10 strain did not correspond to each other (Table 3.1). When the symbionts were removed in the M9 strain, the enrichment of GO translation and GO respiratory chain was not observed in this study. It may be because few replicates in RNA-seq brought little statistical power in the analyses. Hamada et al. (2018) conducted an experiment replacing the symbiont of *H. viridissima* A99 with *Chlorella variabilis* NC64A. In the experiment, the aposymbiotic A99 hydras and the A99 hydras whose symbiont was replaced to NC64A are decreased in the proliferation rates like K10apo and K10exc in this study. However, the number of genes commonly differentially expressed in the aposymbiotic A99 hydras and the A99 hydras which were replaced the symbiont is as low as 1.7% of all the DEGs, and there are few DEGs related to translation and electron transport chain in these common DEGs (Hamada et al., 2018). Yuyama et al. (2018) infected sea anemone *Aiptasia tenuis* with zooxanthella *Symbiodinium trenchii* and observed the expression changes of the anemones after 10, 20 days. In the non-

Table 3.10 Expression patterns of genes with GO translation and electron transport chain (respiratory chain) in host organisms having endosymbiotic relationships with algae. Columns Translation and Electron transport chain show whether each GO term was enriched in upregulated or downregulated genes (UP: enriched in upregulated genes, DOWN: enriched in downregulated genes, NONE: not enriched).

Host organism	Translation	Electron transport chain	Reference
Hydra vulgaris 105G	UP	UP	Chapter 2
H. viridissima K10	DOWN	UP	This study
H. viridissima M9	DOWN	DOWN	Ishikawa et al., (2016b)
H. viridissima A99	NONE	NONE	Hamada et al., (2018)
Aiptasia tenuis	DOWN	UP	Yuyama et al., (2018)
Paramecium bursaria	DOWN	DOWN*	Kodama et al., (2014)

*oxidation-reduction process

symbiotic anemone, the genes with GO translation are upregulated compared with the symbiotic one after 10 days, and the genes with GO electron transport chain are downregulated compared with the symbiotic one after 10, 20 days. In *P. bursaria*, which is a symbiotic protist, the genes with GO translation and GO oxidation-reduction process, which includes electron transport chain, are upregulated in the aposymbiotic host (Kodama et al., 2014). The gene expression patterns in this study were compared with those of the previous studies (Table 3.10). The expression patterns in the aposymbiotic hydras and the hydras which replaced the symbiont in the K10 strain coincided with those in the non-symbiotic *A. tenuis*, and it suggests that similar cellular processes worked in these symbiotic hydras and anemones. On the other hand, in the M9 strain, ribosomal proteins and genes involved in the electron transport chain were downregulated in the hydras which replaced the symbiont, but the proliferation rate of the hydras did not change. It might be affected by the following two factors. The efficiency of photosynthesis depends on the combination of hosts and *Chlorella* (Sørensen et al., 2020), and the amount of maltose released by symbiotic chlorellae varies with strains (Mews and Smith, 1982; Rees, 1989). The expression changes of the genes related to translationand electron transport chain in the K10 hydra were different from other *H. viridissima* strains and *P. bursaria*, and it implies that irregular cellular metabolism occurred in the aposymbiotic hydras and the hydras which replaced the symbiont.

3.4.2 Effects of specificity between the host and the symbiont on nitrogen metabolism

The substances exchanged between hosts and symbiotic algae are nitrogen sources required by the symbionts and photosynthetic products provided by the symbionts. Nitrogen sources used by symbionts are different between symbiotic systems. For example, the coral symbiont zooxanthellae utilize NO_3^- and NH_4^+ taken up by the host from seawater as a nitrogen source (Lipschultz and Cook, 2002; Grover et al., 2003; Tanaka et al., 2006), while *P. bursaria* has a low ability to utilize NH_4^+ due to low activity of glutamine synthetase and glutamate dehydrogenase and is dependent on host amino acid synthesis (Kato et al., 2006). The chlorella symbiotic with the green hydra has lost the ability to utilize NO_3^- and NH_4^+ as nitrogen sources,

and the host hydra needs to convert these substances into glutamine (Hamada et al., 2018). Nitrogen assimilation in the host is shown in Fig. 3.8. Ammonium is the source of glutamine which the host synthesizes as a nitrogen source for the symbiont, and glutamine is synthesized from glutamate by glutamine synthetase (McAuley, 1995; Hamada et al., 2018). The expression changes in the genes involved in the metabolic pathway of glutamine are shown in Table 3.11. In the aposymbiotic K10 hydra, glutamine synthetase, glutamate dehydrogenase, which synthesizes glutamate in cnidarians, and ammonium transporter were downregulated. When the symbiont was replaced in the K10 strain, one glutamine synthetase, glutamate dehydrogenase, and ammonium transporter were commonly downregulated, and glutamate decarboxylase and glutamine--fructose-6-phosphate transaminase, which degrades glutamate, were upregulated. In the aposymbiotic M9 hydra, glutamine synthetase and ammonium transporter were also downregulated, but glutamate decarboxylase and glutamine--fructose-6-phosphate transaminase were downregulated in the hydra which replaced the symbiont. Symbiotic polyps of the green hydra release little ammonium in the light, while aposymbiotic polyps release ammonium, and it indicates that ammonium is assimilated by glutamine synthetase and glutamate dehydrogenase in the symbiotic hydra (Rees, 1986). In both K10 and M9 aposymbiotic hydras, glutamine synthetase and ammonium transporter were downregulated, and it suggests that the absence of the symbionts inhibits the synthesis of glutamine and ammonium, the nitrogen source of the symbiotic chlorellae. The K10 hydra which replaced the symbiont restrained glutamine synthesis due to reduction in glutamate supply by decreases in ammonium transport and glutamate degradation. There were no such gene expression changes which suppress the glutamate supply in the M9 hydra which replaced the symbiont. These expression patterns made me suspect that the supply of glutamine to the symbiotic chlorella was suppressed and that it was involved in the reduction of the proliferation rate in the K10 hydra which replaced the symbiont. However, there were no changes in the proliferation rates depending on the concentration when I provided glutamine directly to the symbiotic polyps (Fig. 3.6). It indicates that glutamine taken up by the hydra cell was not directly utilized by the symbiotic chlorella and that the supply of glutamine was not a

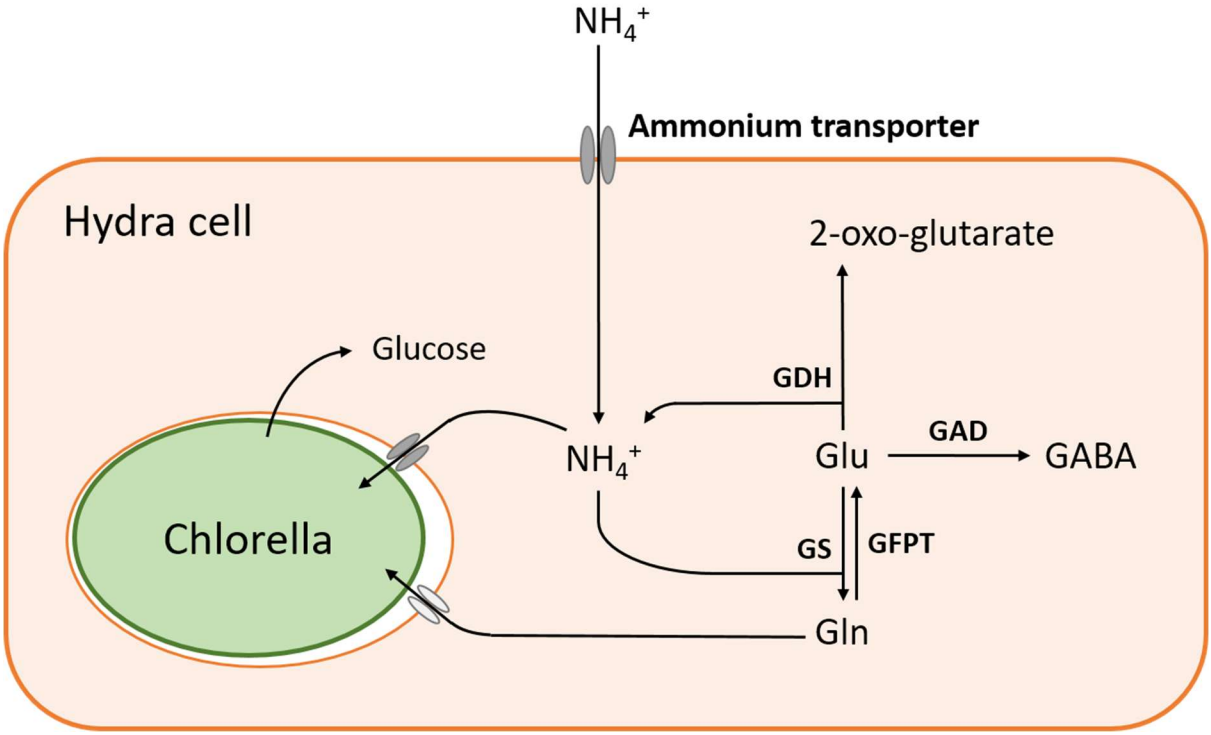

Figure 3.8 Schematic overview of the metabolite exchange between the green hydra and the symbiotic chlorella. The ammonium is taken up by the hydra cells and utilized for glutamine synthesis. GDH, Glutamate dehydrogenase; GAD, Glutamate decarboxylase; GS, Glutamine synthetase; GFPT, Glutamine--fructose-6-phosphate transaminase.

Table 3.11 DEGs related to glutamine and glutamate metabolism in K10 and M9 strains.

K10 strain

	K10-K10apo		K10-K10exc				
id	logFC	UP/DOWN	logFC	UP/DOWN	logCPM	Protein name	Function
Cluster-1117.10	-7.60	DOWN	-10.86	DOWN	1.86	Glutamate dehydrogenase	(+/-)glutamate
Cluster-11916.1	-2.16	DOWN	-1.58	DOWN	5.18	Glutamine synthetase	(+)glutamine
Cluster-11916.2	-1.31	DOWN	-0.83	NONE	5.74	Glutamine synthetase	(+)glutamine
Cluster-11916.3	-1.09	DOWN	-0.70	NONE	6.09	Glutamine synthetase	(+)glutamine
Cluster-19043.0	1.68	NONE	4.32	UP	1.62	Glutamate decarboxylase 2	(-)glutamate
Cluster-8816.8592	0.85	NONE	2.31	UP	4.54	Glutamine synthetase	(+)glutamine
Cluster-8816.6856	0.01	NONE	1.02	UP	6.50	Glutamine--fructose-6-phosphate transaminase	(-)glutamine
Cluster-8816.4814	0.31	NONE	1.40	UP	6.48	Glutamine--fructose-6-phosphate transaminase	(-)glutamine
Cluster-22230.1	0.07	NONE	-1.36	DOWN	5.24	Amino acid transporter	Glu transporter
Cluster-23260.1	-0.34	NONE	-1.45	DOWN	5.58	Vesicular glutamate transporter 3	Glu transporter
Cluster-8816.6295	0.14	NONE	-1.24	DOWN	6.00	Vesicular glutamate transporter 3	Glu transporter
Cluster-13351.8	-3.06	DOWN	-2.42	DOWN	4.79	Putative ammonium transporter 3	NH4+ transporter
Cluster-13351.4	-1.84	DOWN	-1.72	DOWN	5.33	Putative ammonium transporter 3	NH4+ transporter

M9 strain

	M9-M9apo		M9-M9exc			
id	logFC	UP/DOWN	logFC	UP/DOWN	logCPM	Protein name	
Cluster-15475.7057	-1.73	DOWN	0.00	NONE	8.16	Glutamine synthetase	(+)glutamine
Cluster-20893.1	-0.28	NONE	-2.30	DOWN	5.97	Glutamate decarboxylase 2	(-)glutamate
Cluster-22564.0	0.05	NONE	-1.48	DOWN	2.85	Glutamine--fructose-6-phosphate transaminase	(-)glutamine
Cluster-9863.6	-5.37	DOWN	0.94	UP	4.51	Putative ammonium transporter 3	NH4+ transporter
Cluster-9863.5	-4.74	DOWN	0.54	NONE	5.93	Putative ammonium transporter 3	NH4+ transporter
Cluster-9863.3	-3.19	DOWN	0.51	NONE	6.04	Putative ammonium transporter 3	NH4+ transporter

In Function, (+) means the synthesis of glutamine or glutamate, and (-) means the degradation of glutamine or glutamate.

bottleneck as a nitrogen source in the photosynthesis of the symbiont. There are some previous researches on green hydras which replaced the symbiotic chlorellae with *Chlorella* NC64A. *Chlorella* NC64A is a symbiotic alga with *P. bursaria* and has less ability to release maltose than the symbiotic chlorella with green hydra (Mews and Smith, 1982; Rees, 1989). The activity of glutamine synthetase is decreased, and the activity of glutamate dehydrogenase is increased in the aposymbiotic green hydra and the hydra which replace the symbiont with NC64A (Rees, 1986). When the H. viridissima A99 aposymbiotic hydras are introduced with NC64A, the proliferation rate of the hydras is decreased such as that of K10exc (Hamada et al., 2018). Considering these reports, the gene expression patterns in nitrogen assimilation were linked to the supply of photosynthetic products from the symbiotic chlorella and probably affected the proliferation rate.

3.4.3 Cellular differentiation by Wnt signaling in the hydra with the non-symbiotic algae

In K10exc, the number of stenoteles per tentacle and the number of Artemia which can be preyed upon at one time are decreased (Hanada, 2020). In the differential gene expression analysis, I found downregulation of the genes promoting differentiation into nematocyte and coding products constituting nematocyst (Table 3.6b, Fig. 3.9). Wnt signaling is a factor in the differentiation of interstitial cells such as nematoblast, a precursor of nematocyte. The Wnt signaling is known to be a pathway regulating head development and budding in *Hydra* (Hobmayer et al., 2000; Mortzfeld et al., 2019) and also activated in nematoblasts and interacts with nematoblast-specific proteins to differentiate nematoblasts (Khalturin et al., 2007). Wnt protein was downregulated in K10exc (Fig. 3.9a). It suggests that the Wnt signal, the upstream differentiation factor, was suppressed and that it causes the downregulation of the downstream genes differentiating nematoblast and constituting nematocyst. These gene expression changes could inhibit nematoblast differentiation and reduce the number of stenoteles. In M9exc, there were also downregulations of the genes promoting differentiation into nematocyte and coding products constituting nematocyst (Fig 3.9a). The reductions in the number of the stenoteles and predatory ability are not observed in M9exc unlike K10exc (Hanada, 2020). GSK-3β was

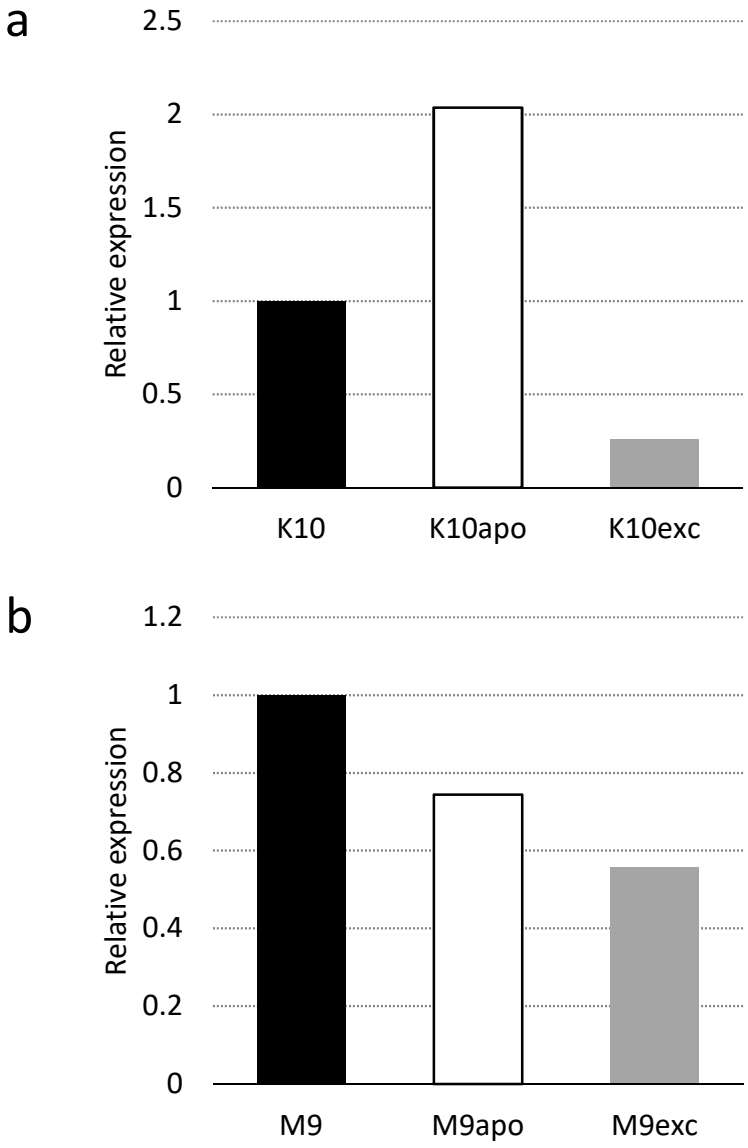

Figure 3.9 Relative gene expression amounts of genes related to Wnt signaling calculated from their fold changes. **(a)** Wnt gene was downregulated in K10exc compared with K10 and K10apo. **(b)** GSK-3β gene was downregulated in M9exc compared with M9.

downregulated in M9exc (Fig 3.9b). GSK-3β represses β-catenin in the Wnt pathway, and thus the downregulation of GSK-3β promotes differentiation of interstitial cells (Bosch, 2009). It is possible that the downregulation of GSK-3β was balanced with the downregulation of other genes related to nematoblast and nematocyte and did not decrease the number of stenoteles. However, Wnt signaling also controls the growth of hydra polyps (Mortzfeld et al., 2019), so it is necessary to examine what these gene expression changes directly affect.

The symbiont removal and replacement experiments and the differential gene expression analyses in the K10 and M9 strains provided insight into the effects of the symbiont existence and their host specificity. In the K10 strain, the general trend was similar between removal and replacement of the symbionts, while no such trend was observed in the M9 strain. It was linked to the proliferation rate changes (Hanada, 2020). The expression changes in the genes related to translation and electron transport chain also coincided between the removal and replacement of the symbionts in the K10 strain. It suggests that changes in cellular metabolism and energy balance in the aposymbiotic K10 hydra did not recover in the hydra introduced with the non-native symbiont. The expression changes of the genes involved in glutamine synthesis reveal the changes in nitrogen assimilation in the host when the symbionts were removed and were replaced. Comparison of the gene expression patterns by symbiont removal and exchange experiments has made it possible to figure out how the host specificity of the symbiont functions at the cellular level. It will provide an insight into the evolutionary process and origins of symbiosis.

CHAPTER 4

General Discussion

There are two types of symbiosis with green algae in *Hydra*: the stable symbiosis with a long evolutionary history in *H. viridissima*, the immature symbiosis developed recently in *H. vulgaris*. It seems that different symbiotic mechanisms act between *H. viridissima* and *H. vulgaris*, and so a hydra is a suitable organism to study evolutionary processes of symbiosis. In this study, newly established combinations of host-symbiont systems by conducting two different procedures, horizontal transmission of symbionts into non-symbiotic brown hydras and artificial introduction of non-native symbionts into aposymbiotic green hydras, were used to compare the changes in cellular metabolisms and symbiotic mechanisms through gene expression.

In Chapter 2, I demonstrated the horizontal transmission of the symbiotic chlorococcum in *H. vulgaris* and compared the changes in gene expressions of the brown hydras whose symbionts acquired by the horizontal transmission with those of the native symbiotic hydra. I collected the symbiotic chlorococcum in host cells and the chlorococcum in HCS, and *rbcL* and 18S rDNA sequences were determined to identify the algae in HCS as the symbiont. The sequences of *Chlorococcum* in hydra cells and HCS were the same, and these algae were found to be identical. It indicated that the symbiotic chlorococcum had escaped from the hydra cells and transferred to the non-symbiotic hydra via the surrounding water. From the phylogenetic analysis, it was found that the symbiotic chlorococcum belonged to Stephanosphaerinia, which contains some algae in the genera *Chlorococcum* and *Oophila*, the salamander symbiont.

In order to investigate the changes in the cellular metabolism when the hydra acquires a symbiont by horizontal transmission, I conducted a differential gene expression analysis by RNA-seq. In the 105G strain, which had been obtained as a symbiont by horizontal propagation, 3803 genes were upregulated and 3476 genes were downregulated compared to the original non-symbiotic strain, 105 strain. Strain 105G was decreased in the polyp size and increased in

the proliferation rate, and TCF/LEF and Dp-1, which are transcription factors promoting budding, were upregulated in the symbiotic strain. These suggest that faster budding decreased the polyp size in 105G strain. In Gene Ontology enrichment analysis, 31 GO terms were enriched in the upregulated genes, and 8 GO terms were enriched in the downregulated genes. The GO terms enriched in the upregulated genes included translation and respiratory chain complex. Compared with the aposymbiotic hydra, 484 genes were upregulated, and 1303 genes were downregulated in the native symbiotic strain J7. GO term: lysosome was enriched in the upregulated genes, and the lysosomal enzymes such as cathepsin were also upregulated in the 105G strain. It suggests that symbiotic algae were digested in the host cell. GO terms: integral component of membrane and calcium ion binding were enriched in the downregulated genes, and it was consistent with the 105G strain. Polycystin and protocadherin have these GO terms and were expressed in nematocyte and battery cells. These expressions coordinated with the reduction of the stenotele size and number in the 105G strain. In the 105G strain, genes constituting the TOR pathway, which regulates energy balance between translation and respiration in response to amino acids, were upregulated, but the expressions of these genes did not change in the J7 strain. Then, I performed the rapamycin treatment experiments, which inhibited the TOR pathway. Rapamycin treatments prevented polyps in all the strains budding and degenerated polyps in the symbiotic hydra (105G, J7). The effect of rapamycin was stronger in the 105G strain than in the J7 strain. This suggests that the native symbiotic hydra has already obtained the ability to adapt even if its energy balance is affected by the symbiotic algae or external factors, but that the hydra which acquired the symbiont through horizontal transmission does not yet have such ability. Adaptation of the symbiosis in *H. vulgaris* may have been evolving in stages.

In Chapter 3, I mentioned the changes in host-symbiont interaction by differential gene expression analysis with RNA-seq when the symbiont was removed from *H. viridissima* and replaced with the non-native symbiont. Comparing the gene expression with the original symbiotic hydra K10, I found 957 DEGs when the symbiont was removed and 1293 DEGs

when the symbiont was replaced with the non-native one. GO enrichment analysis showed that six GO terms, including translation, were enriched in the upregulated genes in the K10 hydra from which the symbiont was removed, while cytochrome-c oxidase activity and integral component of membrane were enriched in the downregulated genes. These GO terms were commonly enriched in the hydra whose symbiont was replaced. There are 700 common DEGs between the hydras whose symbionts were removed and replaced, and these fold changes showed a strong correlation. These gene expression changes in the K10 strain indicate that the translation and electron transfer systems, which are major components of the cellular energy balance, were regulated conversely by removing the symbiont and are not restored by the introduction of the non-native symbiont. In the M9 strain, 75 genes were differentially expressed when the symbiont was removed, and 65 of those 75 genes were not differentially expressed when the symbiont was replaced. When the symbiont was replaced, 756 genes were differentially expressed, and 746 of those 756 genes were not differentially expressed when the symbiont was removed. The genes related to the differentiation of nematoblasts and the structure of nematocyte were downregulated in the symbiont-replaced M9 strain. Genes having these functions were also downregulated in the hydra whose symbiont was replaced in the K10 strains, but a clear morphological change in nematocyte (decreased number of stenoteles) was found only in the K10 strain. This could be explained by balanced regulation of genes in the Wnt signaling pathway, which regulates the differentiation of nematoblasts upstream, during symbiont replacement. Ammonium transporter and glutamate synthetase were downregulated in both K10 and M9 strains upon removal of the symbiont. The downregulations of these genes were observed only in the K10 strain when the symbiont was replaced. The downregulations coordinated with the decrease in the asexual proliferation rate. It suggests that the absence and replacement of the symbionts affected nitrogen assimilation in the host cells and that the effects of symbiont replacement on nitrogen assimilation differed between the strains.

Summarizing the above, I investigated the evolutionary processes from symbiosis in the early stage to stable symbiosis based on gene expression changes between the symbiotic hydras

and the non-symbiotic hydras in *H. vulgaris* and *H. viridissima*. In *H. vulgaris*, which is likely to be at the early stage of symbiosis evolution, the results suggested that a balanced cellular metabolic system would be a key factor for stabilizing and adapting to symbiosis (Chapter 2). Ishikawa et al. (2016a) proposed the two-step evolutionary process: *H. vulgaris* evolved the capability for symbiosis with the chlorococcum from the non-symbiotic hydras (the first step), and then the native symbiotic strains have established the relatively stable symbiosis (the second step). From the viewpoint of gene expression patterns, my results seem to trace the second step symbiosis evolution of *H. vulgaris* from these non-symbiotic hydras to a relatively stable symbiotic system in the native symbiotic strain. The other symbiotic hydra, *H. viridissima*, has established an advanced and stable symbiotic relationship with the chlorella and co-evolved with the symbiont (Kawaida et al., 2013). My results suggested that an incompatible combination between a host and a symbiont in *H. viridissima* leads to a reversion to an unstable state of the symbiont relationship due to an unbalanced cellular metabolic system (chapter 3). The evolution of stabilization of symbiotic systems may be followed by the lineage-specific co-evolution of host and symbiont interactions that would be adaptive to various environments. Further comparative analysis with omics techniques (proteome, metabolome) between 105G and J7 strains in *H. vulgaris* and between K10 and M9 strains in *H. viridissima* will provide an overview of the evolution of the symbiotic system.

The differential gene expression pattern in *H. vulgaris* during symbiosis is different from those of hosts which have stable symbiotic relationships with their symbiotic algae, including *H. viridissima* (Ishikawa et al, 2016b). It indicates that there may be a similar symbiotic association with their symbionts across taxonomic groups and that the host in the early stage of symbiosis has a different symbiotic association with the symbiotic algae. The evolution toward stable symbiosis with algae may acquire analogous symbiotic mechanisms which exhibit a common pattern of gene expression changes during symbiosis. The expression changes of *H. vulgaris* and *H. viridissima* during symbiosis were compared with those of other host organisms which have endosymbiosis with algae. GO enrichment analysis showed that

during symbiosis, genes with GO translation and electron transport system were upregulated in *H. vulgaris* 105G strain, while the genes having GO translation were downregulated and ones with GO electron transport chain were upregulated in *H. viridissima* K10 strain. In the previous studies, genes in translation and electron transport chain tended to be downregulated during symbiosis in *P. bursaria* (Kodama et al., 2014) and *H. viridissima* M9 (Ishikawa et al., 2016b). In *A. tenuis* (Yuyama et al., 2018), genes related to translation were downregulated during symbiosis, and ones related to the electron transport chain were upregulated as well as in *H. viridissima* K10. Unlike *P. bursaria*, which has a stable one-to-one symbiotic relationship, *H. vulgaris* 105G and *A. tenuis*, which acquired the symbiont by horizontal transmission, showed the upregulation of genes related to the electron transport chain. In the 105G strain, which is the natively non-symbiotic strain, genes related to translation were also upregulated. Cellular metabolism in the hosts during symbiosis may be adjusted depending on the process for the symbiont transmission and adaptation to symbiosis.

This study provided new insights into the establishment and evolution of symbiotic relationships between the cnidarian and green algae. Comparison of gene expression changes between two symbiotic strains of *H. vulgaris*, the strain acquired the symbiont by horizontal transmission (105G) and native symbiotic one (J7) revealed how differences in the ability to adapt to the symbiotic relationship affect the host-symbiont interaction in the early stage of symbiosis. Furthermore, I investigated the differences in the symbiosis mechanism of *H. viridissima* strains with different host-symbiont specificity when the symbionts were replaced and found differences in the metabolism of glutamine, a nitrogen source for photosynthesis of the symbionts, between the host strains. Further research focusing on the photosynthetic metabolism of the symbionts is required to identify the properties of the symbionts which affect the host.

REFERENCES

Abele, D., Philipp, E., Gonzalez, P., & Puntarulo, S. (2007). Marine invertebrate mitochondria and oxidative stress. *Frontiers in Bioscience* **12**, 933-946. https://doi.org/10.2741/2115

Baker, D. M., Freeman, C. J., Wong, J. C., Fogel, M. L., & Knowlton, N. (2018). Climate change promotes parasitism in a coral symbiosis. *The ISME journal* **12**, 921-930. https://doi.org/10.1038/s41396-018-0046-8

Bar-Peled, L., Schweitzer, L. D., Zoncu, R. & Sabatini, D. M. (2012). Ragulator is a GEF for the rag GTPases that signal amino acid levels to mTORC1. *Cell* **150**, 1196-1208. https://doi.org/10.1016/j.cell.2012.07.032

Bates, A. E., McLean, L., Laing, P., Raeburn, L. A. & Hare, C. (2010). Distribution patterns of zoochlorellae and zooxanthellae hosted by two pacific northeast anemones, *Anthopleura elegantissima* and *A. xanthogrammica*. *The Biological Bulletin.* **218,** 237-247. https://doi.org/10.1086/BBLv218n3p237

Beckmann, A. & Özbek, S. (2012). The nematocyst: a molecular map of the cnidarian stinging organelle. *International Journal of Developmental Biology* **56**, 577-582. https://doi.org/10.1387/ijdb.113472ab

Beckmann, A. (2013). Molecular factors of nematocyst morphogenesis and discharge in the freshwater polyp hydra. Doctor's thesis, University of Heidelberg.

Bosch, T. C. (2009). Hydra and the evolution of stem cells. *Bioessays* **31**, 478-486. https://doi.org/10.1002/bies.200800183

Buttgereit, F., & Brand, M. D. (1995). A hierarchy of ATP-consuming processes in mammalian cells. *Biochemical Journal* **312**, 163-167. https://doi.org/10.1042/bj3120163

Buzgariu, W., Chera, S., & Galliot, B. (2008). Chapter Twenty-Six Methods to Investigate Autophagy During Starvation and Regeneration in *Hydra*. *Methods in enzymology* **451**, 409-437. https://doi.org/10.1016/S0076-6879(08)03226-6

Campbell, R. D. (1987a). A new species of *Hydra* (Cnidaria: Hydrozoa) from North America with comments on species clusters within the genus. *Zoological Journal of the Linnean Society* **91**, 253-263. https://doi.org/10.1111/j.1096-3642.1987.tb01510a.x

Campbell, R. D. (1987b) Organization of the nematocyst battery in the tentacle of *Hydra*: arrangement of the complex anchoring junctions between nematocytes, epithelial cells, and basement membrane. *Cell Tissue Research* **249**, 647-655. https://doi.org/10.1007/BF00217337

Cates, N., & McLaughlin, J. J. (1976). Differences of ammonia metabolism in symbiotic and aposymbiotic *Condylactus* and *Cassiopea* spp. *Journal of Experimental Marine Biology and Ecology*, **21**, 1-5. https://doi.org/10.1016/0022-0981(76)90065-4

Catterall, W. A. (2011). Voltage-gated calcium channels. *Cold Spring Harbor Perspectives in Biology* **3**, a003947. https://doi.org/10.1101/cshperspect.a003947

Caverzan, A., Passaia, G., Rosa, S. B., Ribeiro, C. W., Lazzarotto, F., & Margis-Pinheiro, M. (2012). Plant responses to stresses: role of ascorbate peroxidase in the antioxidant protection. *Genetics and molecular biology* **35**, 1011-1019. https://doi.org/10.1590/s1415-47572012000600016

Chapman, J. A. et al. (2010). The dynamic genome of *Hydra*. *Nature* **464**, 592-596. https://doi.org/10.1038/nature08830

Chen, M. C., Cheng, Y. M., Sung, P. J., Kuo, C. E., & Fang, L. S. (2003). Molecular identification of Rab7 (ApRab7) in *Aiptasia pulchella* and its exclusion from phagosomes harboring zooxanthellae. *Biochemical and biophysical research communications* **308**, 586-595. https://doi.org/10.1016/S0006-291X(03)01428-1

Chen, X. Z. et al. (1999). Polycystin-L is a calcium-regulated cation channel permeable to calcium ions. *Nature* **401**, 383-386. https://doi.org/10.1038/43907

Chomczynski, P., & Sacchi, N. (1987). Single-step method of RNA isolation by acid guanidinium thiocyanate-phenol-chloroform extraction. *Analytical biochemistry* **162**, 156-159. https://doi.org/10.1016/0003-2697(87)90021-2

Cook, C. B., D'Elia, C. F., & Muller-Parker, G. (1988). Host feeding and nutrient sufficiency for zooxanthellae in the sea anemone *Aiptasia pallida*. *Marine Biology* **98**, 253-262. https://doi.org/10.1007/BF00391203

Cui, G., Liew, Y. J., Li, Y., Kharbatia, N., Zahran, N. I., Emwas, A. H., Eguiluz, V. M., & Aranda, M. (2019). Host-dependent nitrogen recycling as a mechanism of symbiont control in *Aiptasia*. *PLoS Genetics* **15**, e1008189. https://doi.org/10.1371/journal.pgen.1008189

Davidson, N. M., & Oshlack, A. (2014). Corset: enabling differential gene expression analysis for de novo assembled transcriptomes. *Genome biology* **15**, 1-14. https://doi.org/10.1186/s13059-014-0410-6

de Bary, A (1879) Die Erscheinung der Symbiose. Verlag von Karl J, Trübner, Strassburg.

Douglas, A. E., & Smith, D. C. (1984). The green hydra symbiosis. VIII. Mechanisms in symbiont regulation. *Proceedings of the Royal Society of London. Series B. Biological Sciences* **221**, 291-319. https://doi.org/10.1098/rspb.1984.0035

Douglas, A. E. (1998). Host benefit and the evolution of specialization in symbiosis. *Heredity* **81**, 599-603. https://doi.org/10.1046/j.1365-2540.1998.00455.x

Douglas, A. E. (2015). The special case of symbioses: mutualisms with persistent contact. In *Mutualism* (pp. 20-34). Oxford University Press, Oxford.

Dunn, K. (1987). Growth of endosymbiotic algae in the green hydra, *Hydra viridissima*. *Journal of Cell Scienc*, **88**, 571-578. https://doi.org/10.1242/jcs.88.5.571

Emms, D. M., & Kelly, S. (2015). OrthoFinder: solving fundamental biases in whole genome comparisons dramatically improves orthogroup inference accuracy. *Genome biology* **16**, 1-14. https://doi.org/10.1186/s13059-015-0721-2

Fishman, Y., Zlotkin, E., & Sher, D. (2008). Expulsion of symbiotic algae during feeding by the green hydra–a mechanism for regulating symbiont density? *PLoS ONE* **3**, e2603. https://doi.org/10.1371/journal.pone.0002603

Galliot, B. (2012). *Hydra*, a fruitful model system for 270 years. *International Journal of Developmental Biology* **56**, 411-423. https://doi.org/10.1387/ijdb.120086bg

Gee, L., Hartig, J., Law, L., Wittlieb, J., Khalturin, K., Bosch, T. C., & Bode, H. R. (2010). β-catenin plays a central role in setting up the head organizer in hydra. *Developmental biology*, **340**, 116-124. https://doi.org/10.1016/j.ydbio.2009.12.036

Gitter, A. H., Oliver, D., & Thurm, U. (1994). Calcium-and voltage-dependence of nematocyst discharge in *Hydra vulgaris*. *Journal of Comparative Physiology A* **175**, 115-122. https://doi.org/10.1007/BF00217442

Grens, A., Gee, L., Fisher, D. A. & Bode, H. R. (1996). *CnNK-2*, an NK-2 homeobox gene, has a role in patterning the basal end of the axis in *Hydra*. *Developmental Biology* **180**, 473-488. https://doi.org/10.1006/dbio.1996.0321

Grover, R., Maguer, J. F., Allemand, D., & Ferrier-Pages, C. (2003). Nitrate uptake in the scleractinian coral *Stylophora pistillata*. *Limnology and Oceanography* **48**, 2266-2274. https://doi.org/10.4319/lo.2003.48.6.2266

Haas, B. J. et al. (2013). *De novo* transcript sequence reconstruction from RNA-seq using the Trinity platform for reference generation and analysis. *Nature protocols* **8**, 1494-1512. https://doi.org/10.1038/nprot.2013.084

Habetha, M., & Bosch, T. C. (2005). Symbiotic *Hydra* express a plant-like peroxidase gene during oogenesis. *Journal of Experimental Biology* **208**, 2157-2165. https://doi.org/10.1242/jeb.01571

Hamada, M., Schröder, K., Bathia, J., Kürn, U., Fraune, S., Khalturina, M., Khalturin, K., Shinzato, C., Satoh, N., & Bosch, T. C. (2018). Metabolic co-dependence drives the evolutionarily ancient *Hydra–Chlorella* symbiosis. *eLife* **7**, e35122. https://doi.org/10.7554/eLife.35122

Hamada, M., Satoh, N., & Khalturin, K. (2020). A Reference Genome from the symbiotic hydrozoan, *Hydra viridissima*. *G3: Genes, Genomes, Genetics* **10**, 3883-3895. https://doi.org/10.1534/g3.120.401411

Hanada, M. (2020). Specificity of the combination between host and symbiont in green hydra, viridissima species group *Hydra*. Master's thesis, Kyushu University.

Hay, N. & Sonenberg, N. (2004). Upstream and downstream of mTOR. *Genes & Development* **18**, 1926-1945. https://doi.org/10.1101/gad.1212704

Helin, K., Wu, C. L., Fattaey, A. R., Lees, J. A., Dynlacht, B. D., Ngwu, C., & Harlow, E. (1993). Heterodimerization of the transcription factors E2F-1 and DP-1 leads to cooperative trans-activation. *Genes & development*, **7**, 1850-1861. https://doi.org/10.1101/gad.7.10.1850

Hemmrich, G., Anokhin, B., Zacharias, H., & Bosch, T. C. (2007). Molecular phylogenetics in *Hydra*, a classical model in evolutionary developmental biology. *Molecular phylogenetics and evolution* **44**, 281-290. https://doi.org/10.1016/j.ympev.2006.10.031

Hobmayer, B., Rentzsch, F., Kuhn, K., Happel, C. M., von Laue, C. C., Snyder, P., Rothbächer, U., & Holstein, T. W. (2000). WNT signalling molecules act in axis formation in the diploblastic metazoan *Hydra*. *Nature* **407**, 186-189. https://doi.org/10.1038/35025063

Hobmayer, E., Holstein, T. W., & David, C. N. (1990). Tentacle morphogenesis in hydra. II. Formation of a complex between a sensory nerve cell and a battery cell. *Development* **109**, 897-904. https://doi.org/10.1242/dev.109.4.897

Hoegh-Guldberg, O. (2011). Coral reef ecosystems and anthropogenic climate change. *Regional Environmental Change* **11**, 215-227. https://doi.org/10.1007/s10113-010-0189-2

Huang, D. W., Sherman, B. T. & Lempicki, R. A. (2009). Systematic and integrative analysis of large gene lists using DAVID bioinformatics resources. *Nature Protocols* **4**, 44-57. https://doi.org/10.1038/nprot.2008.211

Hufnagel, L. A., Kass-Simon, G., & Lyon, M. K. (1985). Functional organization of battery cell complexes in tentacles of *Hydra attenuata*. *Journal of morphology* **184**, 323-341. https://doi.org/10.1002/jmor.1051840307

Hulpiau, P. & Van Roy, F. (2011). New insights into the evolution of metazoan cadherins. *Molecular Biology and Evolution* **28**, 647-657. https://doi.org/10.1093/molbev/msq233

Huss, V. A., Holweg, C., Seidel, B., Reich, V., Rahat, M., & Kessler, E. (1994). There is an Ecological Basis for Host/Symbiont Specificity in *Chlorella*/*Hydra* Symbioses. *Endocytobiosis and Cell Research* **10**, 35-35.

Ishikawa, M., Shimizu, H., Nozawa, M., Ikeo, K., & Gojobori, T. (2016a). Two-step evolution of endosymbiosis between hydra and algae. *Molecular phylogenetics and evolution* **103**, 19-25. https://doi.org/10.1016/j.ympev.2016.07.010

Ishikawa, M., Yuyama, I., Shimizu, H., Nozawa, M., Ikeo, K., & Gojobori, T. (2016b). Different endosymbiotic interactions in two hydra species reflect the evolutionary history of endosymbiosis. *Genome Biology and Evolution* **8**, 2155-2163. https://doi.org/10.1093/gbe/evw142

Ishitani, T. et al. (1999). The TAK1-NLK-MAPK-related pathway antagonizes signalling between β-catenin and transcription factor TCF. *Nature* **399,** 798-802. https://doi.org/10.1038/21674

Ito, T. (1947a). A new fresh-water polyp, *Hydra magnipapillata*, n. sp. from Japan. *Science reports of The Tohoku Univ: 4th Ser. (Biology)* **18**, 6–10.

Ito, T. (1947b). Two new species of fresh-water polyp from Japan. *Science reports of The Tohoku Univ: 4th Ser. (Biology)* **18**, 17–23.

Jankowski, T., Collins, A. G., & Campbell, R. (2008). Global diversity of inland water cnidarians. In *Freshwater Animal Diversity Assessment* (pp. 35-40). Springer, Dordrecht. https://doi.org/10.1007/978-1-4020-8259-7_4

Jolley, E., & Smith, D. C. (1980). The green hydra symbiosis. II. The biology of the establishment of the association. *Proceedings of the Royal Society of London. Series B. Biological Sciences* **207**, 311-333. https://doi.org/10.1098/rspb.1980.0026

Joy, J. B. (2013). Symbiosis catalyses niche expansion and diversification. *Proceedings of the Royal Society B: Biological Sciences* **280**, 20122820. https://doi.org/10.1098/rspb.2012.2820

Kato, Y., Ueno, S., & Imamura, N. (2006). Studies on the nitrogen utilization of endosymbiotic algae isolated from Japanese *Paramecium bursaria*. *Plant science* **170**, 481-486. https://doi.org/10.1016/j.plantsci.2005.09.018

Kawaida, H., Shimizu, H., Fujisawa, T., Tachida, H., & Kobayakawa, Y. (2010). Molecular phylogenetic study in genus *Hydra*. *Gene* **468**, 30-40. https://doi.org/10.1016/j.gene.2010.08.002

Kawaida, H., Ohba, K., Koutake, Y., Shimizu, H., Tachida, H., & Kobayakawa, Y. (2013). Symbiosis between hydra and chlorella: molecular phylogenetic analysis and experimental study provide insight into its origin and evolution. *Molecular Phylogenetics and Evolution* **66,** 906-914. https://doi.org/10.1016/j.ympev.2012.11.018

Kawasaki, Y., Nakada, T., & Tomita, M. (2015). Taxonomic revision of oil-producing green algae, *Chlorococcum oleofaciens* (Volvocales, Chlorophyceae), and its relatives. *Journal of Phycology* **51**, 1000-1016. https://doi.org/10.1111/jpy.12343

Kerney, R., Kim, E., Hangarter, R. P., Heiss, A. A., Bishop, C. D., & Hall, B. K. (2011). Intracellular invasion of green algae in a salamander host. *Proceedings of the National Academy of Sciences* **108**, 6497-6502. https://doi.org/10.1073/pnas.1018259108

Khalturin, K., Anton-Erxleben, F., Milde, S., Plötz, C., Wittlieb, J., Hemmrich, G., & Bosch, T. C. (2007). Transgenic stem cells in *Hydra* reveal an early evolutionary origin for key elements controlling self-renewal and differentiation. *Developmental biology* **309**, 32-44. https://doi.org/10.1016/j.ydbio.2007.06.013

Kim, D., Pertea, G., Trapnell, C., Pimentel, H., Kelley, R., & Salzberg, S. L. (2013). TopHat2: accurate alignment of transcriptomes in the presence of insertions, deletions and gene fusions. *Genome biology* **14**, 1-13. https://doi.org/10.1186/gb-2013-14-4-r36

Kim, E., Goraksha-Hicks, P., Li, L., Neufeld, T. P. & Guan, K. L. (2008). Regulation of TORC1 by Rag GTPases in nutrient response. *Nature Cell Biology* **10**, 935-945. https://doi.org/10.1038/ncb1753

Kodama, Y., Suzuki, H., Dohra, H., Sugii, M., Kitazume, T., Yamaguchi, K., Shigenobu, S., & Fujishima, M. (2014). Comparison of gene expression of *Paramecium bursaria* with and without *Chlorella variabilis* symbionts. *BMC genomics* **15**, 1-8. https://doi.org/10.1186/1471-2164-15-183

Kopylova, E., Noé, L., & Touzet, H. (2012). SortMeRNA: fast and accurate filtering of ribosomal RNAs in metatranscriptomic data. *Bioinformatics* **28**, 3211-3217. https://doi.org/10.1093/bioinformatics/bts611

Kovacevic, G. (2012). Value of the *Hydra* model system for studying symbiosis. *International Journal of Developmental Biology* **56**, 627-635. https://doi.org/10.1387/ijdb.123510gk

Lee, S., Tak, E., Lee, J., Rashid, M. A., Murphy, M. P., Ha, J., & Kim, S. S. (2011). Mitochondrial H_2O_2 generated from electron transport chain complex I stimulates muscle differentiation. *Cell research* **21**, 817-834. https://doi.org/10.1038/cr.2011.55

Lengyel, S., Gove, A. D., Latimer, A. M., Majer, J. D., & Dunn, R. R. (2009). Ants sow the seeds of global diversification in flowering plants. *PLoS ONE* **4**, e5480. https://doi.org/10.1371/journal.pone.0005480

Lesser, M. P., Stat, M. & Gates, R. D. (2013). The endosymbiotic dinoflagellates (*Symbiodinium* sp.) of corals are parasites and mutualists. *Coral Reefs* **32**, 603-611. https://doi.org/10.1007/s00338-013-1051-z

Lipschultz, F., & Cook, C. (2002). Uptake and assimilation of ^{15}N-ammonium by the symbiotic sea anemones *Bartholomea annulata* and *Aiptasia pallida*: conservation versus recycling of nitrogen. *Marine Biology*, **140**, 489-502. https://doi.org/10.1007/s00227-001-0717-1

Liu, B. H., Zhang, D. H. & Lee, Y. K. (2000). Effects of nutrient levels on cell growth and secondary carotenoids formation in the freshwater green alga, *Chlorococcum* sp. *Journal of Microbiology and Biotechnology* **10**, 201-207.

Loewith, R., Jacinto, E., Wullschleger, S., Lorberg, A., Crespo, J. L., Bonenfant, D., Oppliger, O., Jenoe, P., & Hall, M. N. (2002). Two TOR complexes, only one of which is rapamycin sensitive, have distinct roles in cell growth control. *Molecular cell*, **10**, 457-468. https://doi.org/10.1016/S1097-2765(02)00636-6

Loomis, W. F. (1955). Glutathione control of the specific feeding reactions of hydra. *Annals of the New York Academy of Science* **62**, 211-227. https://doi.org/10.1111/j.1749-6632.1955.tb35372.x

Luo, W. & Brouwer, C. (2013). Pathview: an R/Bioconductor package for pathway-based data integration and visualization. *Bioinformatics* **29**, 1830-1831. https://doi.org/10.1093/bioinformatics/btt285

Ma, M., Gong, Y., & Hu, Q. (2018). Identification and feeding characteristics of the mixotrophic flagellate *Poterioochromonas malhamensis*, a microalgal predator isolated from outdoor massive *Chlorella* culture. *Algal research* **29**, 142-153. https://doi.org/10.1016/j.algal.2017.11.024

Maeda, Y., Nojima, D., Sakurai, M., Nomaguchi, T., Ichikawa, M., Ishizuka, Y., & Tanaka, T. (2019). Genome analysis and genetic transformation of a water surface-floating microalga *Chlorococcum* sp. FFG039. *Scientific reports* **9**, 1-7. https://doi.org/10.1038/s41598-019-47612-8

Magie, C. R. & Martindale, M. Q. (2008). Cell-cell adhesion in the Cnidaria: insights into the evolution of tissue morphogenesis. *The Biological Bulletin* **214**, 218-232. https://doi.org/10.2307/25470665

Martin, M. (2011). Cutadapt removes adapter sequences from high-throughput sequencing reads. *EMBnet. journal* **17**, 10-12. https://doi.org/10.14806/ej.17.1.200

Martínez, D. E., Iñiguez, A. R., Percell, K. M., Willner, J. B., Signorovitch, J., & Campbell, R. D. (2010). Phylogeny and biogeography of *Hydra* (Cnidaria: Hydridae) using mitochondrial and nuclear DNA sequences. *Molecular Phylogenetics and Evolution* **57**, 403-410. https://doi.org/10.1016/j.ympev.2010.06.016

May, R. C., Caron, E., Hall, A. & Machesky, L. M. (2000). Involvement of the Arp2/3 complex in phagocytosis mediated by FcγR or CR3. *Nature Cell Biology.* **2**, 246-248. https://doi.org/10.1038/35008673

Mazza, M. E., Pang, K., Martindale, M. Q. & Finnerty, J. R. (2007). Genomic organization, gene structure, and developmental expression of three Clustered *otx* genes in the sea anemone *Nematostella vectensis*. *Journal of Experimental Zoology Part B: Molecular and Developmental Evolution* **308**, 494-506. https://doi.org/10.1002/jez.b.21158

McAuley, P. J., & Smith, D. C. (1982). The green hydra symbiosis. V. Stages in the intracellular recognition of algal symbionts by digestive cells. *Proceedings of the Royal Society of London. Series B. Biological Sciences* **216**, 7-23. https://doi.org/10.1098/rspb.1982.0058

McAuley, P. J. (1995). Ammonium metabolism in the green hydra symbiosis. *The Biological Bulletin* **188**, 210-218. https://doi.org/10.2307/1542086

McLaughlin, S. (2017). Evidence that polycystins are involved in *Hydra* cnidocyte discharge. *Invertebrate Neuroscience* **17**, 1-14. https://doi.org/10.1007/s10158-016-0194-3

McNeil, P. L. & McAuley, P. J. (1984). Lysosomes fuse with one half of alga-bearing phagosomes during the reestablishment of the European green hydra symbiosis. *Journal of Experimental Zoology* **230**, 377-385. https://doi.org/10.1002/jez.1402300306

Melo Clavijo, J., Donath, A., Serôdio, J., & Christa, G. (2018). Polymorphic adaptations in metazoans to establish and maintain photosymbioses. *Biological Reviews* **93**, 2006-2020. https://doi.org/10.1111/brv.12430

Merrifield, C. J., Qualmann, B., Kessels, M. M. & Almers, W. (2004). Neural wiskott aldrich syndrome protein (N-WASP) and the Arp2/3 complex are recruited to sites of clathrin-mediated endocytosis in cultured fibroblasts. *European Journal of Cell Biology* **83**, 13-18. https://doi.org/10.1078/0171-9335-00356

Mews, L. K., & Smith, D. C. (1982). The green hydra symbiosis. VI. What is the role of maltose transfer from alga to animal? *Proceedings of the Royal Society of London. Series B. Biological Sciences* **216**, 397-413. https://doi.org/10.1098/rspb.1982.0083

Meyer, E. & Weis, V. M. (2012). Study of cnidarian-algal symbiosis in the 'omics' age. *The Biological Bulletin* **223**, 44-65. https://doi.org/10.1086/BBLv223n1p44

Miller, D. H. (1978). Cell wall chemistry and ultrastructure of *Chlorococcum oleofaciens* (Chlorophyceae). *Journal of Phycology* **14**, 189-194. https://doi.org/10.1111/j.1529-8817.1978.tb02447.x

Mittler, R., Vanderauwera, S., Gollery, M., & Van Breusegem, F. (2004). Reactive oxygen gene network of plants. *Trends in plant science* **9**, 490-498. https://doi.org/10.1016/j.tplants.2004.08.009

Miyokawa, R., Tsuda, T., Kanaya, H. J., Kusumi, J., Tachida, H., & Kobayakawa, Y. (2018). Horizontal transmission of symbiotic green algae between hydra strains. *The Biological Bulletin* **235**, 113-122. https://doi.org/10.1086/699705

Molenaar, M., van de Wetering, M., Oosterwegel, M., Peterson-Maduro, J., Godsave, S., Korinek, V., Roose, J., Destrée, O., & Clevers, H. (1996). XTcf-3 transcription factor mediates β-catenin-induced axis formation in xenopus embryos. *Cell* **86,** 391-399. https://doi.org/10.1016/S0092-8674(00)80112-9

Moran, N. A. (2007). Symbiosis as an adaptive process and source of phenotypic complexity. *Proceedings of the National Academy of Sciences* **104**, 8627-8633. https://doi.org/10.1073/pnas.0611659104

Morita, M. et al. (2013). mTORC1 controls mitochondrial activity and biogenesis through 4E-BP-dependent translational regulation. *Cell Metabolism* **18**, 698-711. https://doi.org/10.1016/j.cmet.2013.10.001

Mortzfeld, B. M., Taubenheim, J., Klimovich, A. V., Fraune, S., Rosenstiel, P., & Bosch, T. C. (2019). Temperature and insulin signaling regulate body size in *Hydra* by the Wnt and TGF-beta pathways. *Nature communications* **10**, 1-13. https://doi.org/10.1038/s41467-019-11136-6

Muscatine, L., & Lenhoff, H. M. (1963). Symbiosis: on the role of algae symbiotic with Hydra. *Science* **142**, 956-958. https://doi.org/10.1126/science.142.3594.956

Muscatine, L. (1965). Symbiosis of hydra and algae—III. Extracellular products of the algae. *Comparative Biochemistry and Physiology* **16**, 77-92. https://doi.org/10.1016/0010-406X(65)90165-9

Muscatine, L., & Lenhoff, H. M. (1965). Symbiosis of hydra and algae. I. Effects of some environmental cations on growth of symbiotic and aposymbiotic hydra. *The Biological Bulletin* **128**, 415-424. https://doi.org/10.2307/1539903

Muscatine, L. (1971). Experiments on green algae coexistent with zooxanthellae in sea anemones. *Pacific Science* **25**, 13-21.

Muscatine, L., & Porter, J. W. (1977). Reef corals: mutualistic symbioses adapted to nutrient-poor environments. *Bioscience* **27**, 454-460. https://doi.org/10.2307/1297526

Muscatine, L., & Marian, R. E. (1982). Dissolved inorganic nitrogen flux in symbiotic and nonsymbiotic medusae. *Limnology and Oceanography* **27**, 910-917. https://doi.org/10.4319/lo.1982.27.5.0910

Neckelmann, N., & Muscatine, L. (1983). Regulatory mechanisms maintaining the *Hydra-Chlorella* symbiosis. *Proceedings of the Royal society of London. Series B. Biological sciences* **219**, 193-210. https://doi.org/10.1098/rspb.1983.0067

Nema, M., Hanson, M. L., & Müller, K. M. (2019). Phylogeny of the egg-loving green alga *Oophila amblystomatis* (Chlamydomonadales) and its response to the herbicides atrazine and 2, 4-D. *Symbiosis* **77**, 23-39. https://doi.org/10.1007/s13199-018-0564-1

Ogawa, T., Watanabe, M., Naganuma, T. & Muramoto, K. (2011). Diversified carbohydrate-binding lectins from marine resources. *Journal of Amino Acids* **2011**, 1-20. https://doi.org/10.4061/2011/838914

Panchaud, N., Péli-Gulli, M. P. & De Virgilio, C. (2013). Amino acid deprivation inhibits TORC1 through a GTPase-activating protein complex for the Rag family GTPase Gtr1. *Science Signaling* **6**, 6-11. https://doi.org/10.1126/scisignal.2004112

Pardy, R. L. (1976). The production of aposymbiotic hydra by the photodestruction of green hydra zoochlorellae. *The Biological Bulletin* **151**, 225-235. https://doi.org/10.2307/1540716

Park, H. D., Greenblatt, C. L., Mattern, C. F., & Merril, C. R. (1967). Some relationships between *Chlorohydra*, its symbionts and some other chlorophyllous forms. *Journal of Experimental Zoology* **164**, 141-161. https://doi.org/10.1002/jez.1401640203

Patro, R., Duggal, G., Love, M. I., Irizarry, R. A., & Kingsford, C. (2017). Salmon provides fast and bias-aware quantification of transcript expression. *Nature methods* **14**, 417-419. https://doi.org/10.1038/nmeth.4197

Plass-Johnson, J. G., Cardini, U., Van Hoytema, N., Bayraktarov, E., Burghardt, I., Naumann, M. S., & Wild, C. (2015). Coral bleaching. In *Environmental Indicators* (pp. 117-146). Springer, Dordrecht. https://doi.org/10.1007/978-94-017-9499-2_9

Pröschold, T., Darienko, T., Silva, P. C., Reisser, W., & Krienitz, L. (2011). The systematics of *Zoochlorella* revisited employing an integrative approach. *Environmental Microbiology* **13**, 350-364. https://doi.org/10.1111/j.1462-2920.2010.02333.x

Rahat, M., & Reich, V. (1985a). A new alga/hydra symbiosis: *Hydra magnipapillata* of the" nonsymbiotic" vulgaris group hosts a *Chlorococcum*-like alga. *Symbiosis* 1, 177-184.

Rahat, M., & Reich, V. (1985b). Correlations between characteristics of some free-living *Chlorella* sp. and their ability to form stable symbioses with *Hydra viridis*. *Journal of Cell Science* **74**, 257-266.

Rahat, M., & Reich, V. (1986). Algal endosymbiosis in brown hydra: host/symbiont specificity. *Journal of cell science* **86**, 273-286.

Rahat, M., & Reich, V. (1989). *Symbiococcum hydrae* gen. et sp. nov. (Chlorosarcinales, Chlorophyta): an endosymbiotic green alga from cells of the Japanese *Hydra magnipapillata* (Coelenterata). *Phycologia* **28**, 181-187. https://doi.org/10.2216/i0031-8884-28-2-181.1

Rahat, M., & Reich, V. (1991). Zoospore formation by *Symbiococcum hydrae* (Chlorosarcinales, Chlorophyta), an alga endosymbiotic in *Hydra magnipapillata* (Coelenterata). *Phycologia* **30**, 226-230. https://doi.org/10.2216/i0031-8884-30-2-226.1

Rahat, M., & Sugiyama., T. (1993). The endodermal cells of some “brown” hydra are autonomous in their ability “to host or not to host” symbiotic algae: analysis of chimera. *Endocytobiosis Cell Research* **9**, 223– 231.

Rajević, N., Kovačević, G., Kalafatić, M., Gould, S. B., Martin, W. F., & Franjević, D. (2015). Algal endosymbionts in European *Hydra* strains reflect multiple origins of the zoochlorella symbiosis. *Molecular phylogenetics and evolution* **93**, 55-62. https://doi.org/10.1016/j.ympev.2015.07.014

Reddy, P. C., Gungi, A., Ubhe, S., Pradhan, S. J., Kolte, A., & Galande, S. (2019). Molecular signature of an ancient organizer regulated by Wnt/β-catenin signalling during primary body axis patterning in *Hydra*. *Communications biology*, **2**, 1-11. https://doi.org/10.1038/s42003-019-0680-3

Rees, T. A. V. (1986). The green hydra symbiosis and ammonium. I. The role of the host in ammonium assimilation and its possible regulatory significance. *Proceedings of the Royal society of London. Series B. Biological sciences* **229**, 299-314. https://doi.org/10.1098/rspb.1986.0087

Rees, T. A. V. (1989). The green hydra symbiosis and ammonium. II. Ammonium assimilation and release by freshly isolated symbionts and cultured algae. *Proceedings of the Royal society of London. Series B. Biological sciences* **235**, 365-382. https://doi.org/10.1098/rspb.1989.0005

Reich, V. & Greenblatt, C. L. (1992). Lectin-agglutination properties of symbiotic and non-symbiotic algae and hydra cells. *Symbiosis* **12**, 57-74.

Roberts, A., Trapnell, C., Donaghey, J., Rinn, J. L. & Pachter, L. (2011). Improving RNA-Seq expression estimates by correcting for fragment bias. *Genome Biology* **12**, R22. https://doi.org/10.1186/gb-2011-12-3-r22

Robinson, M. D., McCarthy, D. J., & Smyth, G. K. (2010). edgeR: a Bioconductor package for differential expression analysis of digital gene expression data. *Bioinformatics* **26**, 139-140. https://doi.org/10.1093/bioinformatics/btp616

Roffman, B., & Lenhoff, H. M. (1969). Formation of polysaccharides by *Hydra* from substrates produced by their endosymbiotic algae. *Nature* **221**, 381-382. https://doi.org/10.1038/221381a0

Rolfe, D. F., & Brown, G. C. (1997). Cellular energy utilization and molecular origin of standard metabolic rate in mammals. *Physiological reviews* **77**, 731-758. https://doi.org/10.1152/physrev.1997.77.3.731

Roth, M. S. (2014). The engine of the reef: photobiology of the coral–algal symbiosis. *Frontiers in microbiology* **5**, 422. https://doi.org/10.3389/fmicb.2014.00422

Schultz, N. (2016). The symbiotic green algae, *Oophila* (Chlamydomonadales, Chlorophyceae): a heterotrophic growth study and taxonomic history. Master's thesis, University of Connecticut.

Schwentner, M., & Bosch, T. C. (2015). Revisiting the age, evolutionary history and species level diversity of the genus *Hydra* (Cnidaria: Hydrozoa). *Molecular Phylogenetics and Evolution* **91**, 41-55. https://doi.org/10.1016/j.ympev.2015.05.013

Siebert, S., Farrell, J. A., Cazet, J. F., Abeykoon, Y., Primack, A. S., Schnitzler, C. E., & Juliano, C. E. (2019). Stem cell differentiation trajectories in *Hydra* resolved at single-cell resolution. *Science* **365**, eaav9314. https://doi.org/10.1126/science.aav9314

Slobodkin, L. B., Bossert, P., Matessi, C., & Gatto, M. (1991). A review of some physiological and evolutionary aspects of body size and bud size of *Hydra*. *Hydrobiologia* **216**/**217**, 377-382. https://doi.org/10.1007/978-94-011-3240-4_54

Sørensen, M. E., Wood, A. J., Minter, E. J., Lowe, C. D., Cameron, D. D., & Brockhurst, M. A. (2020). Comparison of independent evolutionary origins reveals both convergence and divergence in the metabolic mechanisms of symbiosis. *Current Biology* **30**, 328-334. https://doi.org/10.1016/j.cub.2019.11.053

Su, M. Y., Morris, K. L., Fu, Y., Lawrence, R., Stjepanovic, G., Zoncu, R., & Hurley, J. H. (2017). Hybrid structure of the RagA/C-Ragulator mTORC1 activation complex. *Molecular cell* **68**, 835-846. https://doi.org/10.1016/j.molcel.2017.10.016

Tamura, K., Stecher, G., & Kumar, S. (2021). MEGA11: molecular evolutionary genetics analysis version 11. *Molecular Biology and Evolution* **38**, 3022-3027. https://doi.org/10.1093/molbev/msab120

Tanaka, Y., Miyajima, T., Koike, I., Hayashibara, T., & Ogawa, H. (2006). Translocation and conservation of organic nitrogen within the coral-zooxanthella symbiotic system of *Acropora pulchra*, as demonstrated by dual isotope-labeling techniques. *Journal of Experimental Marine Biology and Ecology* **336**, 110-119. https://doi.org/10.1016/j.jembe.2006.04.011

Tanaka, Y., Suzuki, A., & Sakai, K. (2018). The stoichiometry of coral-dinoflagellate symbiosis: carbon and nitrogen cycles are balanced in the recycling and double translocation system. *The ISME journal* **12**, 860-868. https://doi.org/10.1038/s41396-017-0019-3

Tomczyk, S. et al. (2020). Deficient autophagy in epithelial stem cells drives aging in the freshwater cnidarian *Hydra*. *Development* **147**, dev.177840. https://doi.org/10.1242/dev.177840

Thompson, J. D., Higgins, D. G., & Gibson, T. J. (1994). CLUSTAL W: improving the sensitivity of progressive multiple sequence alignment through sequence weighting, position-specific gap penalties and weight matrix choice. *Nucleic acids research* **22**, 4673-4680. https://doi.org/10.1093/nar/22.22.4673

Trapnell, C. et al. (2012). Differential gene and transcript expression analysis of RNA-seq experiments with TopHat and Cufflinks. *Nature Protocols* **7**, 562-578. https://doi.org/10.1038/nprot.2012.016

Trench, R. K. (1971). The physiology and biochemistry of zooxanthellae symbiotic with marine coelenterates I. The assimilation of photosynthetic products of zooxanthellae by two marine coelenterates. *Proceedings of the Royal Society of London. Series B. Biological Sciences* **177**, 225-235. https://doi.org/10.1098/rspb.1971.0024

Vander Heiden, M. G., Cantley, L. C., & Thompson, C. B. (2009). Understanding the Warburg effect: the metabolic requirements of cell proliferation. *Science* **324**, 1029-1033. https://doi.org/10.1126/science.1160809

Voss, P. A., Gornik, S. G., Jacobovitz, M. R., Rupp, S., Dörr, M. S., Maegele, I., & Guse, A. (2019). Nutrient-dependent mTORC1 signaling in coral-algal symbiosis. *bioRxiv* 723312. https://doi.org/10.1101/723312

Walter, W., Sánchez-Cabo, F. & Ricote, M. (2015). GOplot: an R package for visually combining expression data with functional analysis. *Bioinformatics* 31, 2912-2914. https://doi.org/10.1093/bioinformatics/btv300

Wang, J. T. & Douglas, A. E. (1999). Essential amino acid synthesis and nitrogen recycling in an alga-invertebrate symbiosis. *Marine Biology* **135**, 219-222. https://doi.org/10.1007/s002270050619

Watanabe, Y. *et al.* (2009). The function of rhamnose-binding lectin in innate immunity by restricted binding to Gb3. *Developmental & Comparative Immunology* **33**, 187-197. https://doi.org/10.1016/j.dci.2008.08.008

Weiblen, G. D. & Treiber, E. L. (2015). Evolutionary origins and diversification of mutualism. in *Mutualism* (pp. 37-56). Oxford University Press, Oxford.

Weis, V. M. (2008). Cellular mechanisms of Cnidarian bleaching: stress causes the collapse of symbiosis. *Journal of Experimental Biology* **211**, 3059-3066. https://doi.org/10.1242/jeb.009597

Wenger, Y., Buzgariu, W. & Galliot, B. (2016). Loss of neurogenesis in *Hydra* leads to compensatory regulation of neurogenic and neurotransmission genes in epithelial cells. *Philosophical Transactions of The Royal Society B Biological Sciences* **371**, 20150040. https://doi.org/10.1098/rstb.2015.0040

Wenger, Y., Buzgariu, W., Perruchoud, C., Loichot, G. & Galliot, B. (2019). Generic and context-dependent gene modulations during *Hydra* whole body regeneration. *bioRxiv* 587147. https://doi.org/10.1101/587147

Whitney, D. D. (1907). Artificial removal of the green bodies of *Hydra viridis*. *The Biological Bulletin* **13**, 291-299. https://doi.org/10.2307/1535602

Ye, S., Bhattacharjee, M., & Siemann, E. (2019). Thermal tolerance in green hydra: identifying the roles of algal endosymbionts and hosts in a freshwater holobiont under stress. *Microbial ecology* **77**, 537-545. https://doi.org/10.1007/s00248-018-01315-1

Yellowlees, D., Rees, T. A. V., & Leggat, W. (2008). Metabolic interactions between algal symbionts and invertebrate hosts. *Plant, cell & environment* **31**, 679-694. https://doi.org/10.1111/j.1365-3040.2008.01802.x

Yuyama, I., Ishikawa, M., Nozawa, M., Yoshida, M. A., & Ikeo, K. (2018). Transcriptomic changes with increasing algal symbiont reveal the detailed process underlying establishment of coral-algal symbiosis. *Scientific reports* **8**, 1-11. https://doi.org/10.1038/s41598-018-34575-5

Zhu, L., van den Heuvel, S., Helin, K., Fattaey, A., Ewen, M., Livingston, D., Dyson, N., & Harlow, E. (1993). Inhibition of cell proliferation by p107, a relative of the retinoblastoma protein. *Genes & development*, **7**, 1111-1125. https://doi.org/10.1101/gad.7.7a.1111

Zhou, Z., Yu, X., Tang, J., Zhu, Y., Chen, G., Guo, L., & Huang, B. (2017). Dual recognition activity of a rhamnose-binding lectin to pathogenic bacteria and zooxanthellae in stony coral *Pocillopora damicornis*. *Developmental & Comparative Immunology* **70**, 88-93. https://doi.org/10.1016/j.dci.2017.01.009

Acknowledgements

I would like to express my sincere appreciation to the Chairman of the Supervisory Committee, Associate Professor Dr. Junko Kusumi, Faculty of Social and Cultural Studies for her continuous support of my graduate studies, thoughtful guidance, instruction in past researches, laboratory experiments, biological analysis in silico, and writing this thesis.

I would like to express special gratitude to the members of the Supervisory Committee: Professor Dr. Kunio Araya, Associate Professor Dr. Takuji Tachi, Visiting Professor Dr. Isao Nishiumi, Faculty of Social and Cultural Studies, and Professor Emeritus Dr. Yoshitaka Kobayakawa, Faculty of Arts and Science for their constructive suggestion and precious guidance in preparation of this thesis.

I am grateful to my advisors: Professor Dr. Yoshihisa Abe, Assistant Professor Dr. Kota Ogawa, and Dr. Kazunori Matsuo, Faculty of Social and Cultural Studies for their valuable advice and cheering me up.

I would like to thank Assistant Professor Taichi Ito, Faculty of Arts and Science for helpful advice and his encouragement.

I would also like to express my special thanks to the professor in my initial laboratory: Professor Emeritus Dr. Hidenori Tachida, Faculty of Science for his professional guidance of genetics and support for this study.

I would like to thank the researchers in my laboratory: Dr. Etsuko Moritsuka for her valuable guidance of laboratory experiments and phylogenetic analysis until my initial laboratory, Dr. Kenichi Odagiri, and Dr. Tatsuya Mishima for their support and inspiration in my study.

I would like to express thanks to National Institute of Genetics for providing the hydra strains for my study.

I gratefully acknowledge the funding provided by Japan Society for the Promotion of Science (JSPS), KAKENHI (20J12445). My study is supported by Grant-in-Aid for JSPS Fellows.

I am also grateful to the students in my laboratory: especially Shin Komagata, Huang Yu-Zen, Wu yajiao, Hiroto Ueno, Fukuda Yuto, Yukihiro Uchimi, Naoya Ito, Koki Mihara, and the students of the embryology laboratory in Faculty of Arts and Science: Takuya Tsuda, Hiroyuki Kanaya, Maki Hanada for their help and encouragement in my student life.

Finally, I would thank my parents, brother, and best friend for their support and kindness in my student life in Kyushu University.